# *Self-Assembly*

*The **spontaneous and reversible** association of molecular species to form larger, more complex supramolecular entities according to the **intrinsic information** contained in the components.*

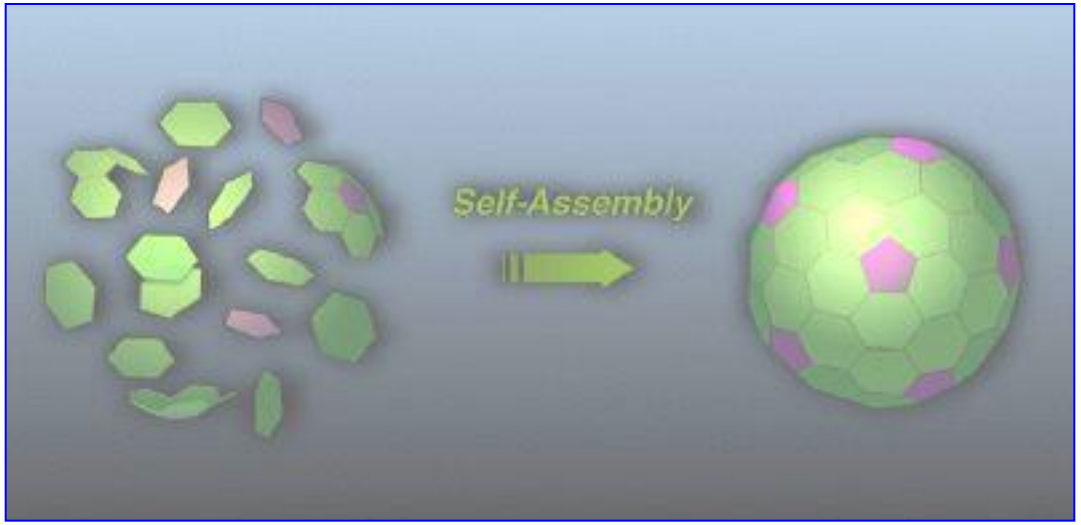

# Metal-Ligand Interaction

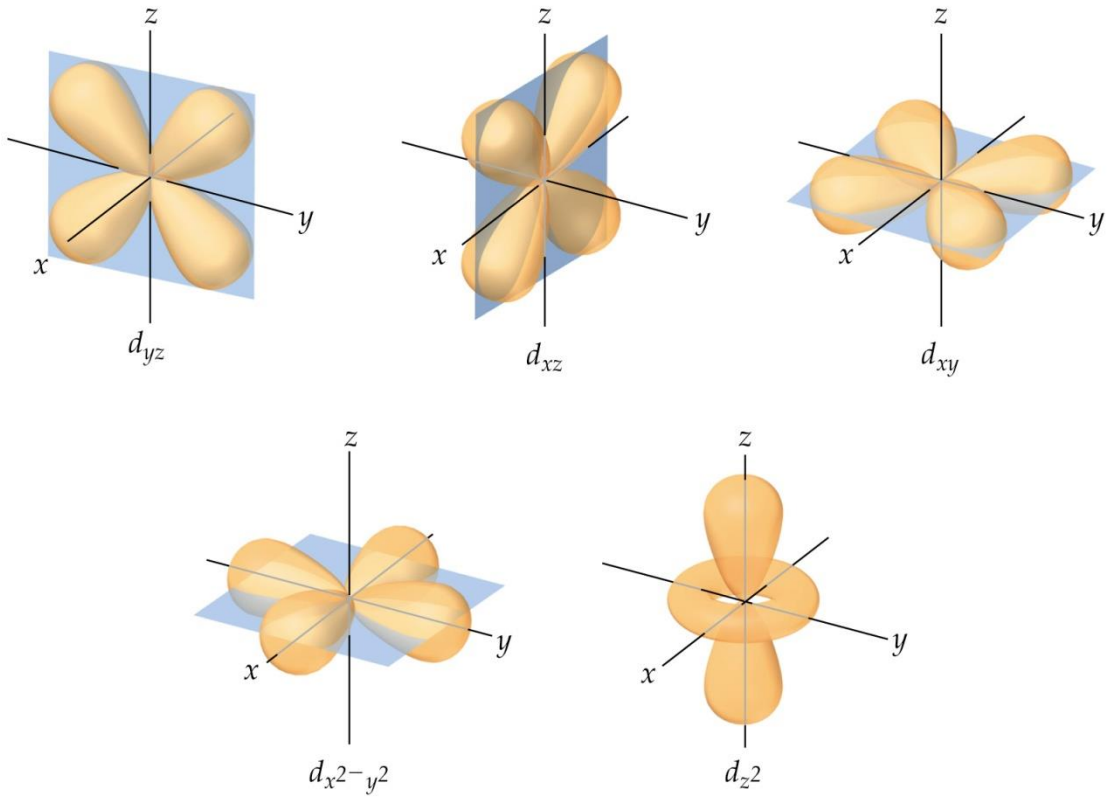

Metal as **connector** :

- labile M-L interaction (kinetic)
- stable compound (thermodynamic)
- highly directional with many geometries available

Metal as **functional group** :

- redox active (electron transfer)
- UV-vis active (color)
- photo active (phosphorescence)
- magnetic properties

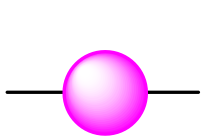

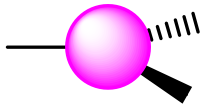

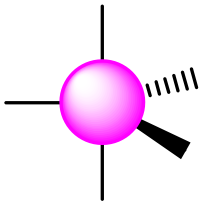

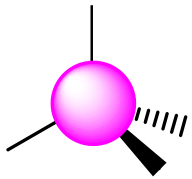

*cis*

Classical metals used:

Pd(II), Pt(II), Cu(I), Cu(II), Re(I), Co(II), Fe(II), Ag(I), Zn(II), Ru(II)…

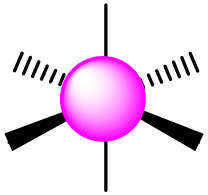

*cis*

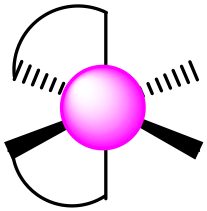

*trans*

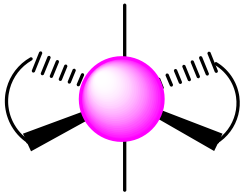



*mer-*

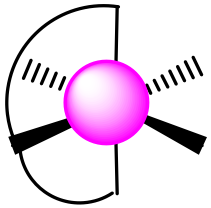

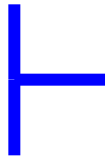

*fac-*

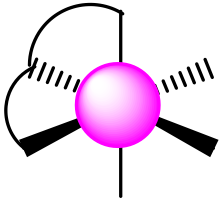

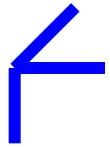

# Supramolecular Coordination Chemistry

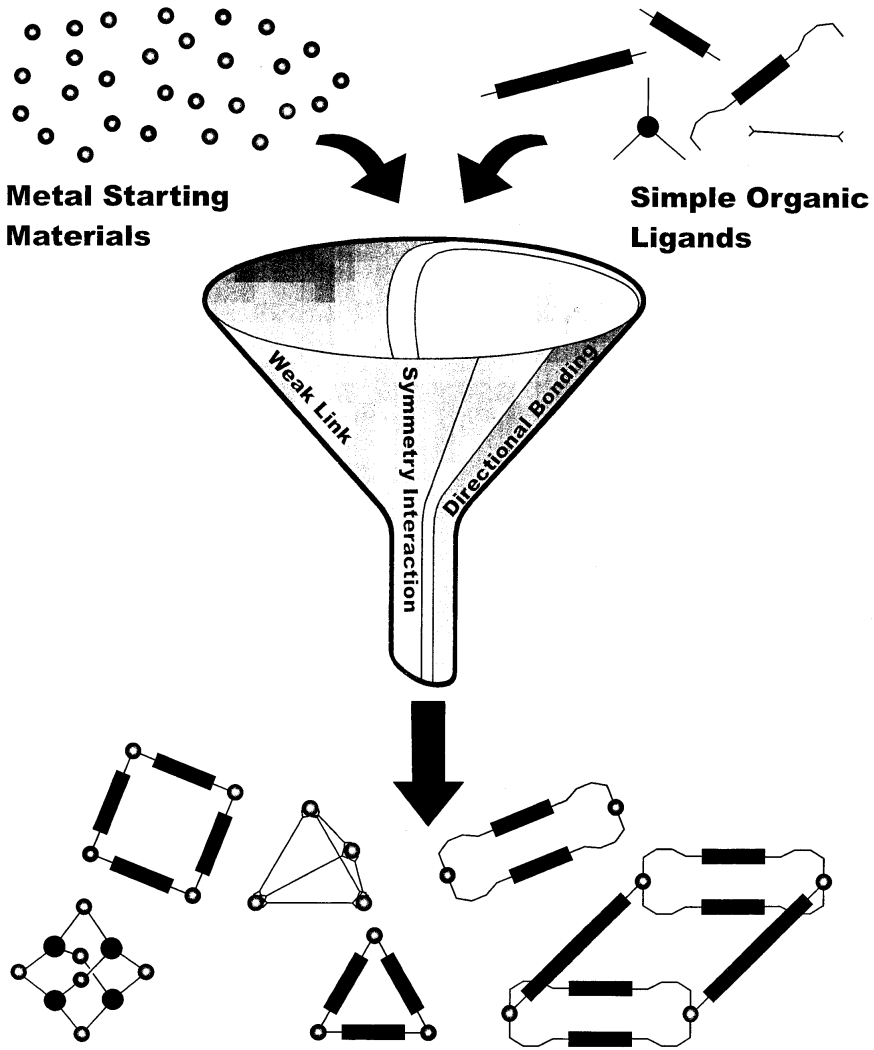

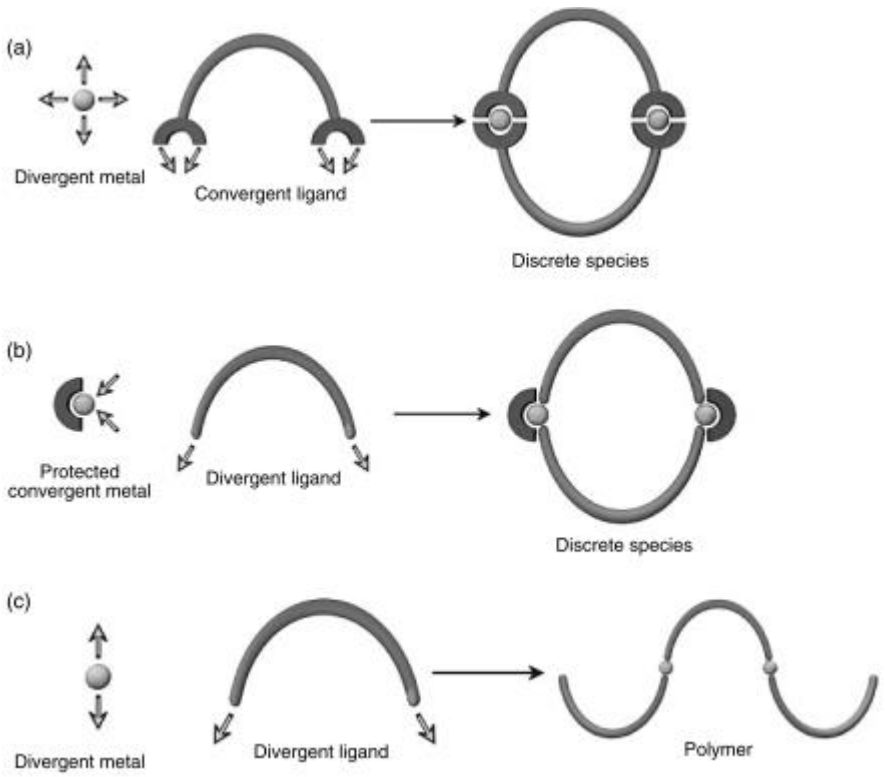
(a)
Divergent metal
Convergent ligand
Discrete species
(b)
Protected
convergent metal
Divergent ligand
Discrete species
(c)
Divergent metal
Divergent ligand
Polymer

# Directonal Bonding Approach

**M** = bb acido, **L** = bb basico, definiti secondo il numero e geometria relativa dei siti acidi e basici

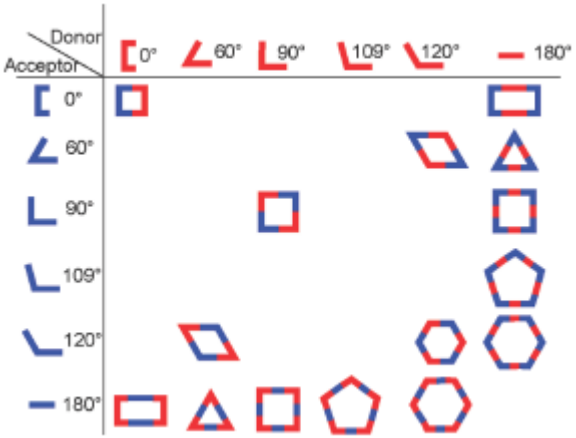


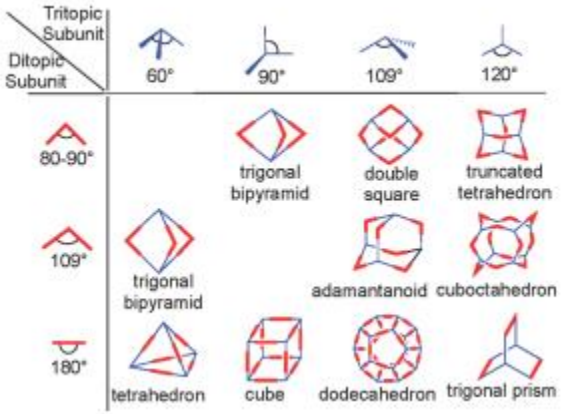

# Directonal Bonding Approach

**M** = bb acido, **L** = bb basico, definiti secondo il numero e geometria relativa dei siti acidi e basici

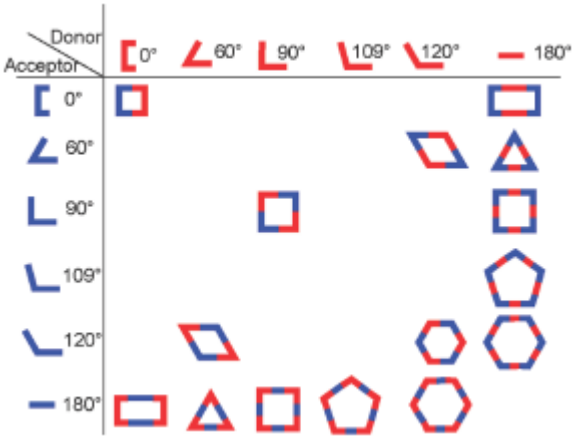

# Specie poligonali 2D

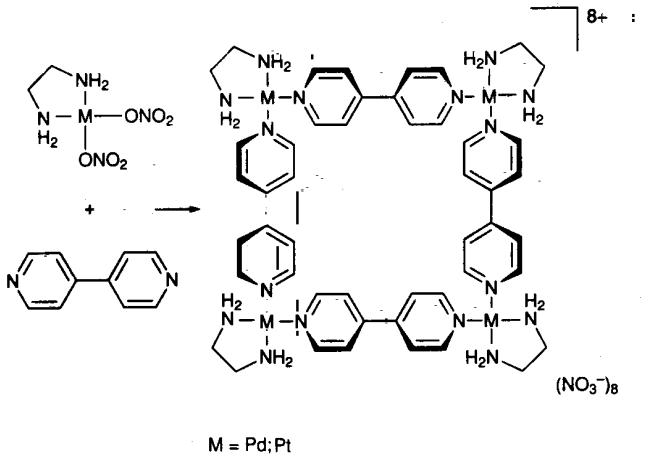


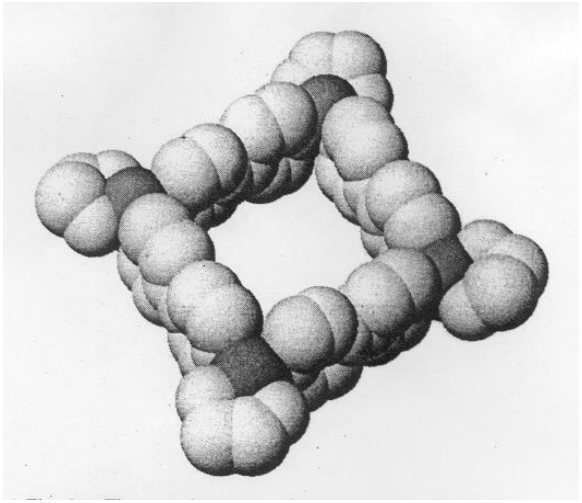

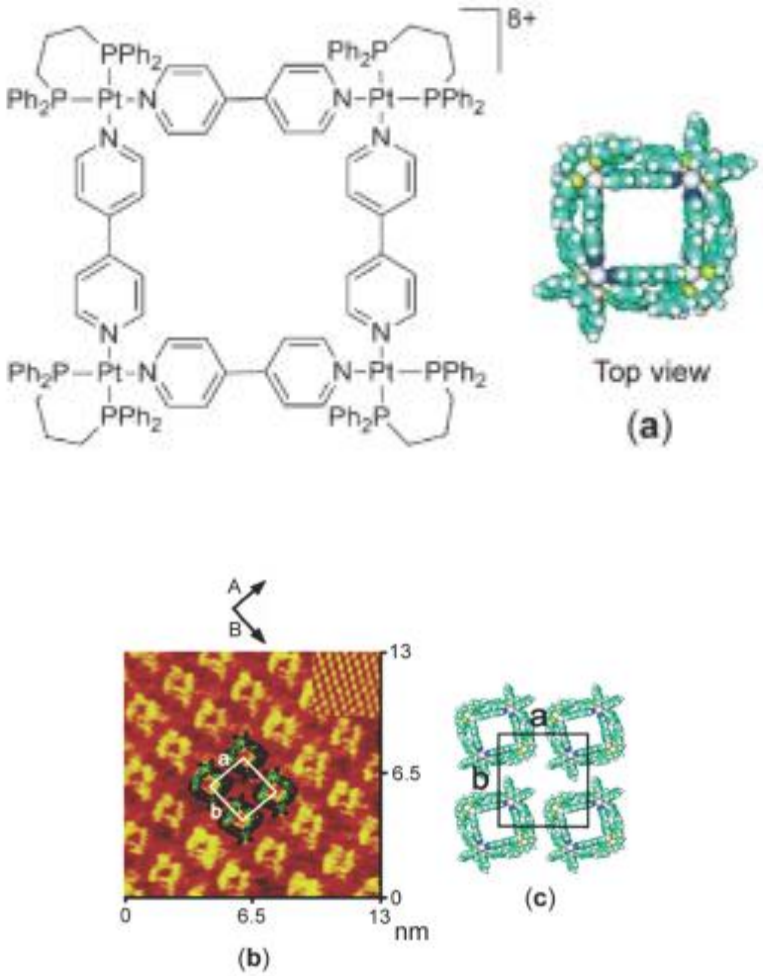


**Figure 41.** (a) Space-filling model of molecular square [Pt(dppp)(4,4′-bipyridine)]$_4$(PF$_6$)$_8$, (b) high-resolution STM images of the adlayer of square on Au(111), and (c) structural model of the adlayer.

# Triangoli Molecolari

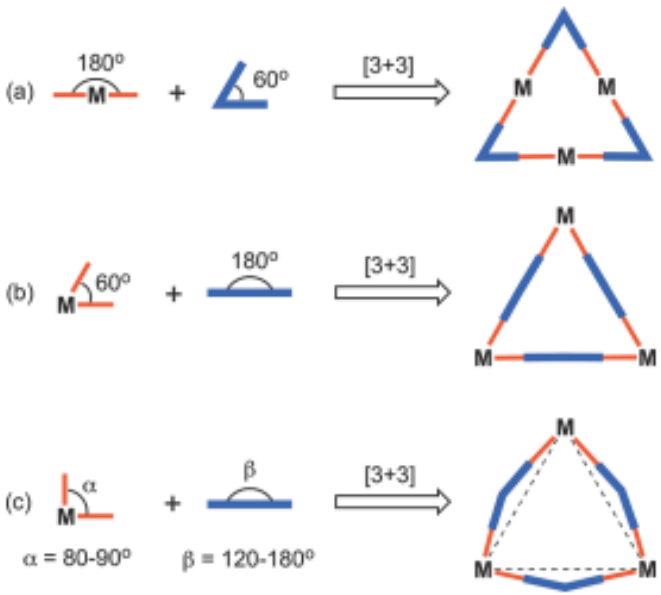

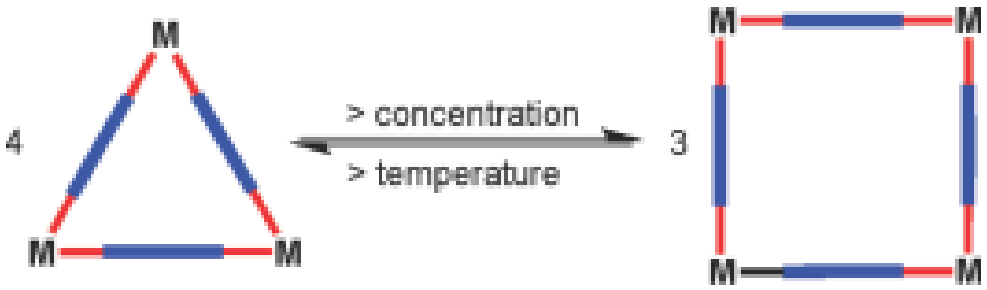


Square = Triangle endothermic $\Delta H < 0$

$\Delta S$ $< \Delta S$ $< 0$

Solvent

Concentration

Temperature

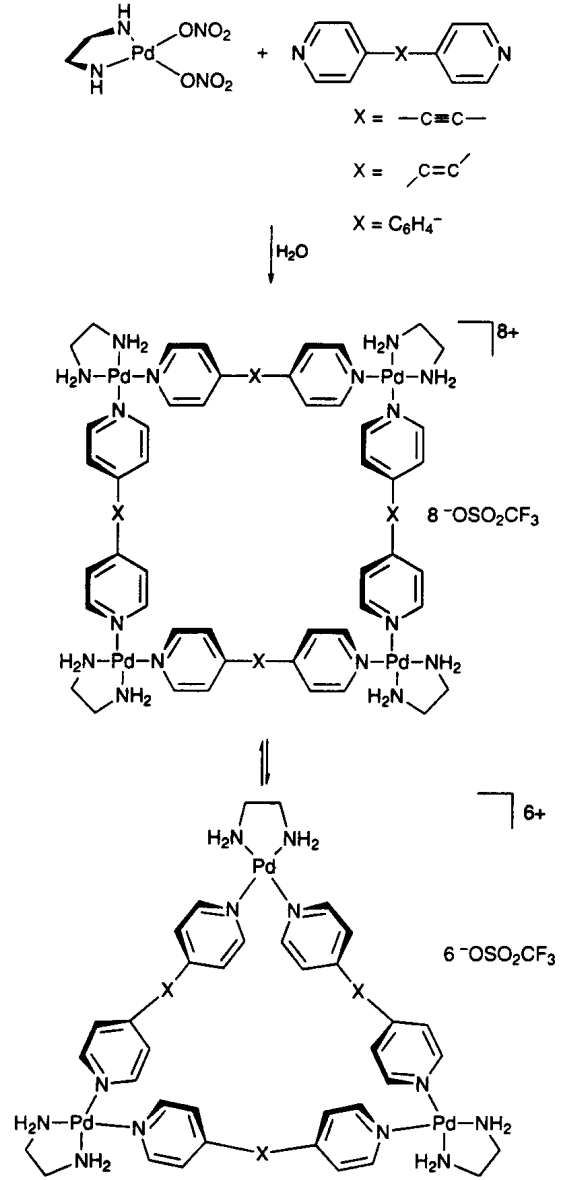
ONO2
ONO2
X = —C≡C—
X = C6H4
H2O
8+
8 −OSO2CF3
6+
6 −OSO2CF3

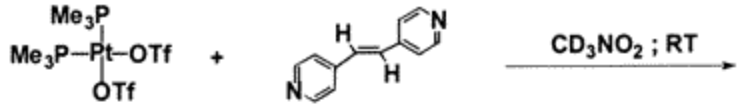


1 2

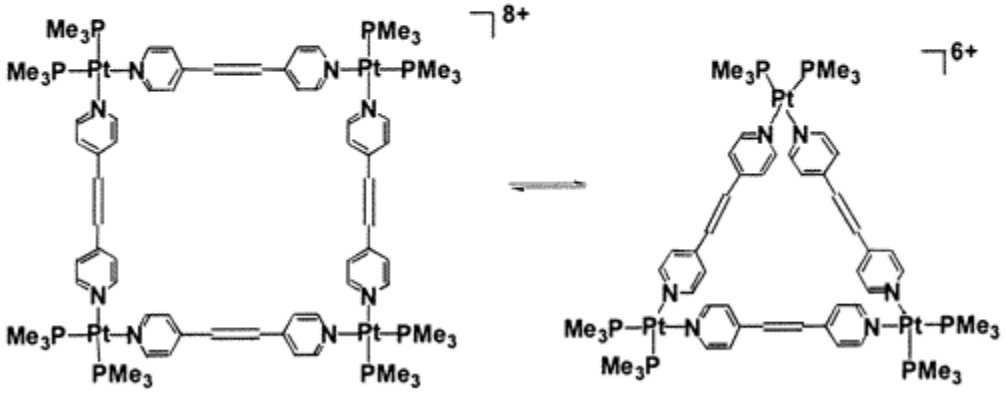


8 $CF_3SO_3^-$ 6 $CF_3SO_3^-$

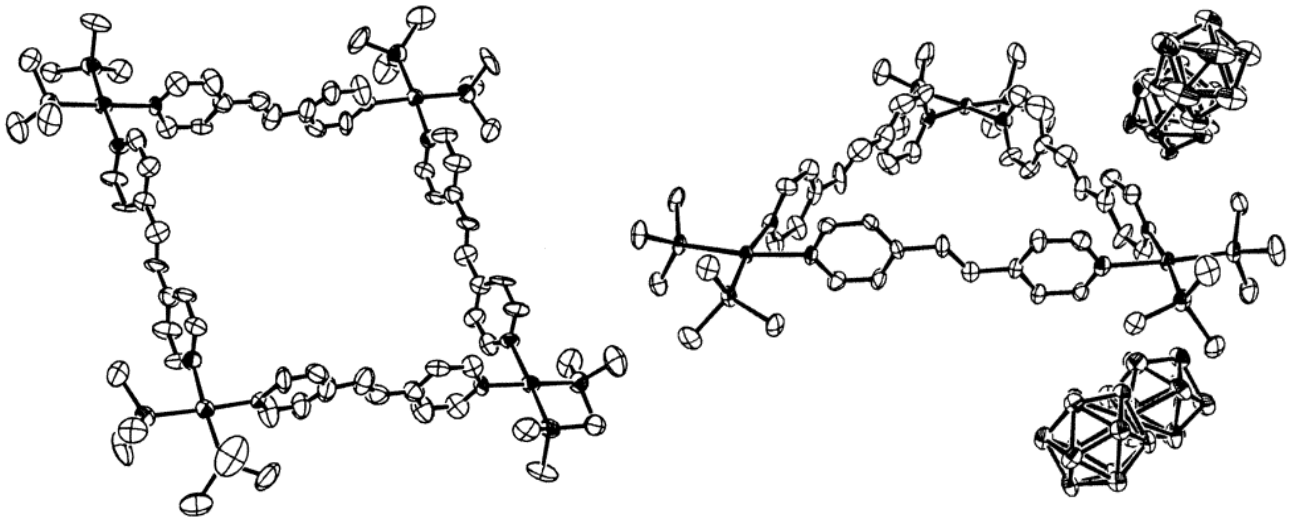

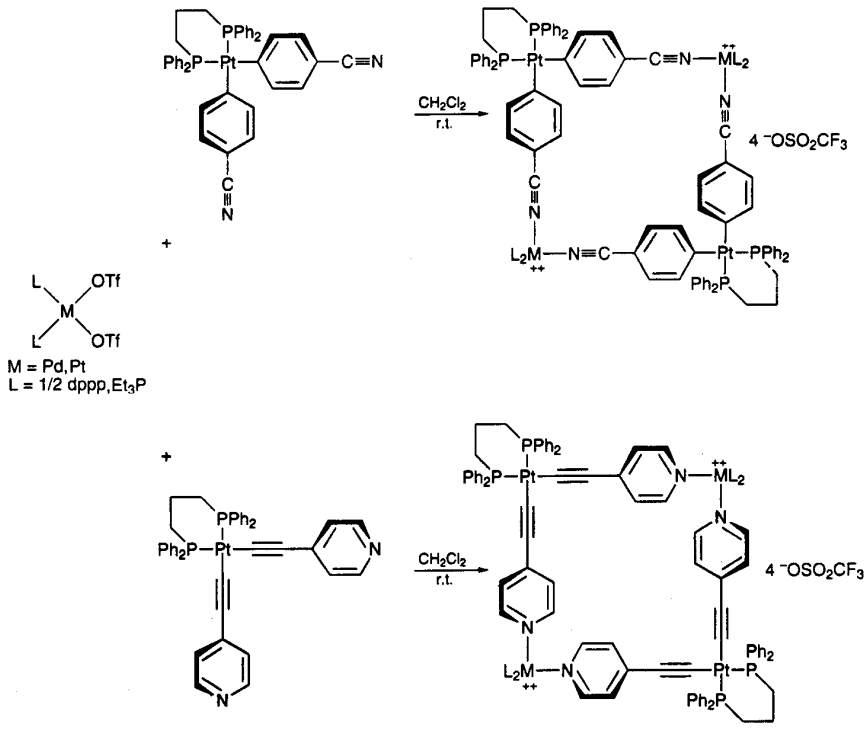


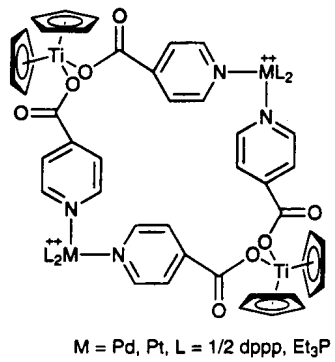


M = Pd, Pt, L = 1/2 dppp, $Et_3P$

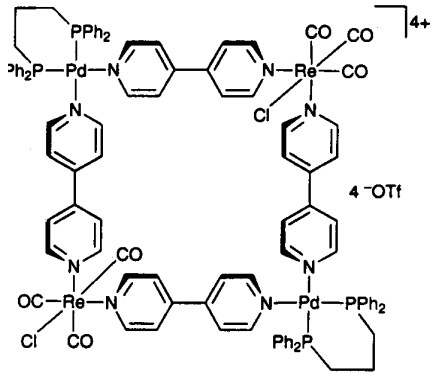

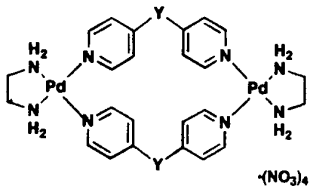

$\cdot(NO_3)_4$

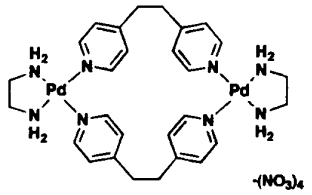

$\cdot(NO_3)_4$

Y = $CH_2$

Y = $C(OH)_2$

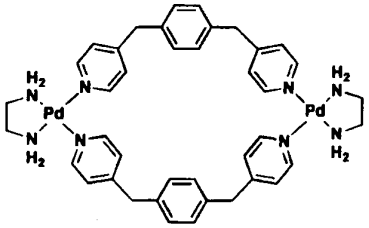

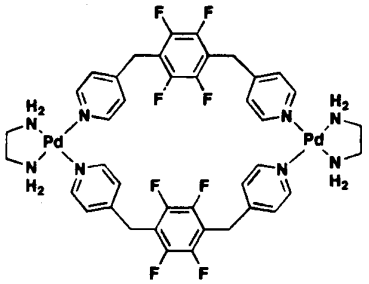

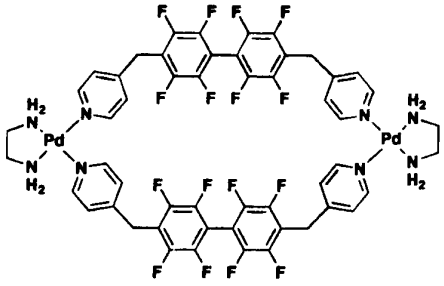

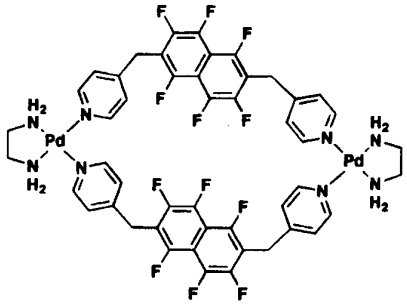

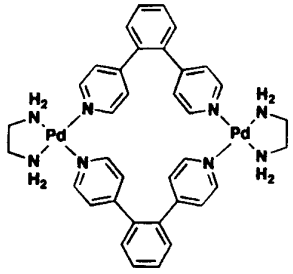

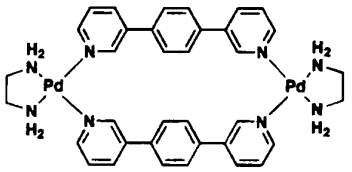

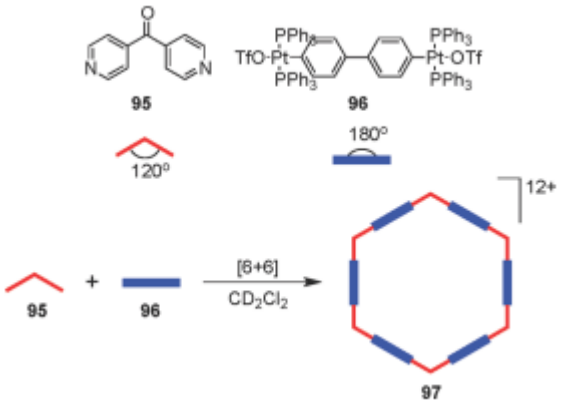
95
96
120°
180°
12+
[6+6]
CD2Cl2
97

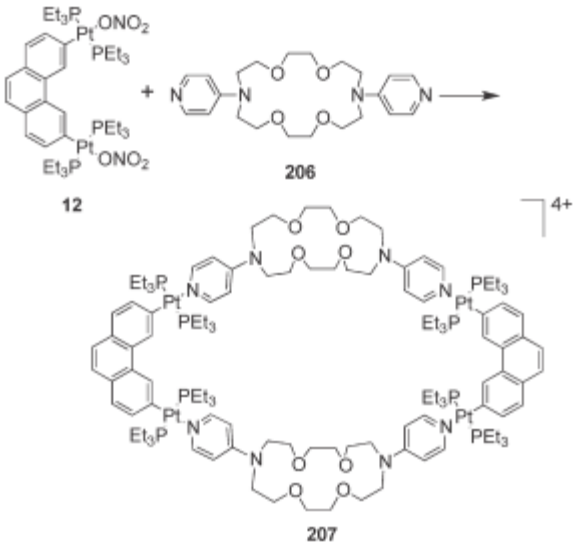
12
206
4+
207

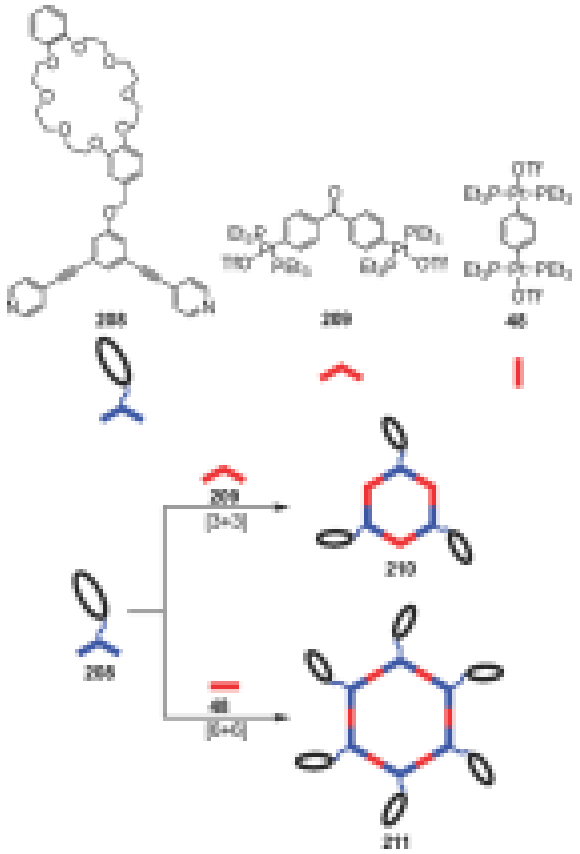
208
209
[3+3]
210
209
[6+6]
211

# Directonal Bonding Approach

**M** = bb acido, **L** = bb basico, definiti secondo il numero e geometria relativa dei siti acidi e basici

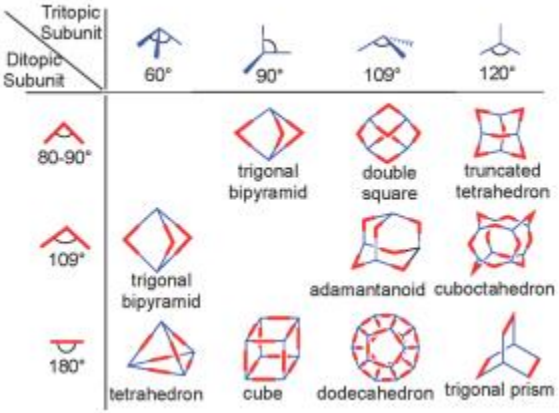

# Gabbie Molecolari

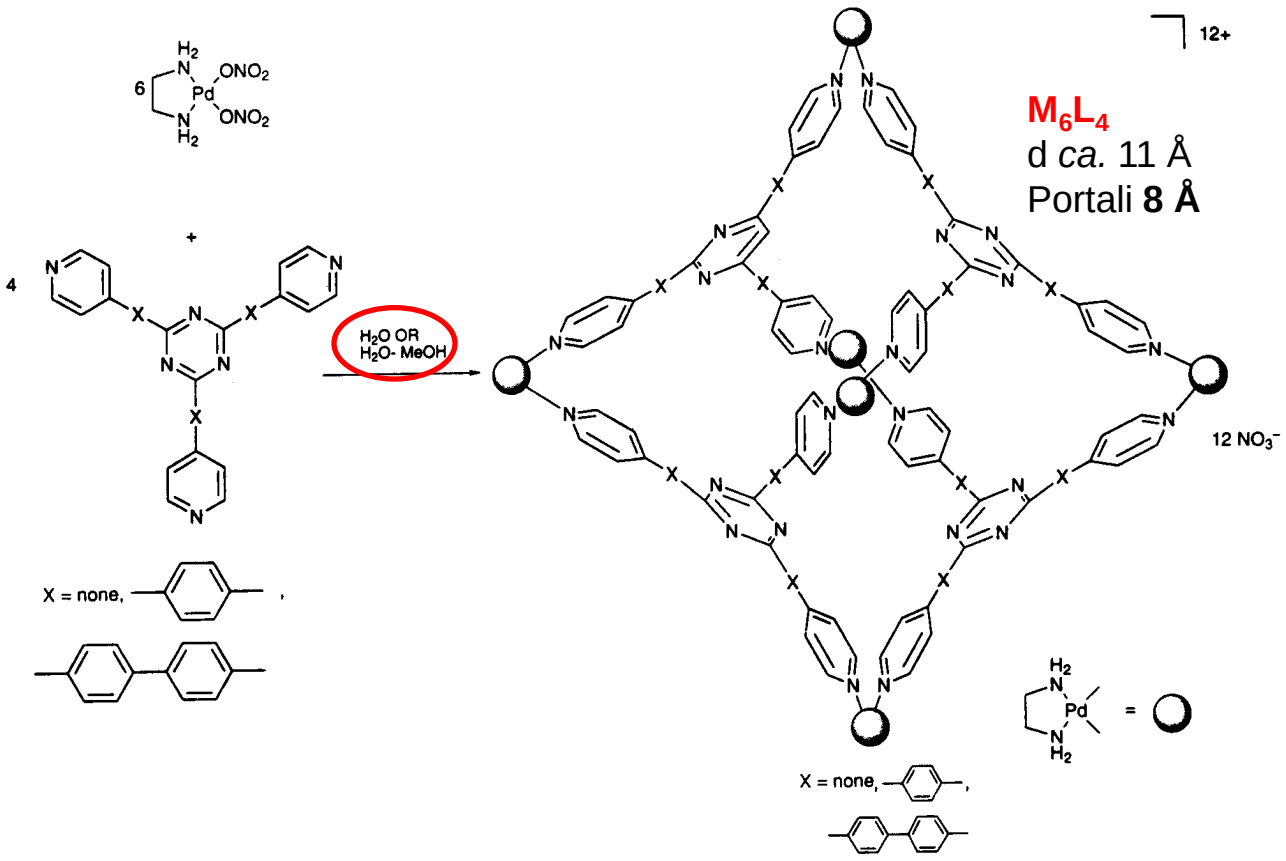

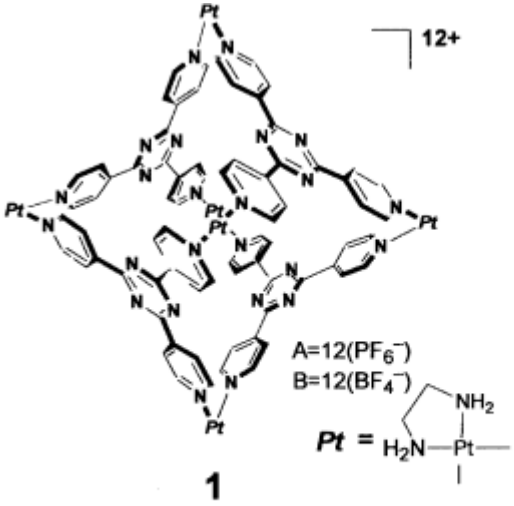


1

**a**: $(C_{84}H_{96}N_{36}Pt_6)^{12+}\cdot 12(PF_6^-)$
FW. 4519.98

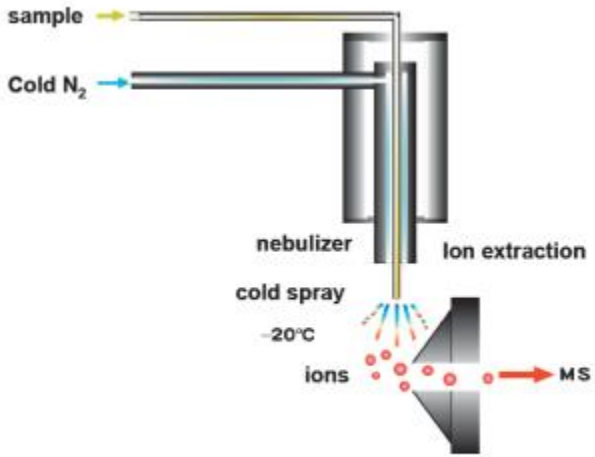


Fig. 1. Schematic illustration of the cold spray.

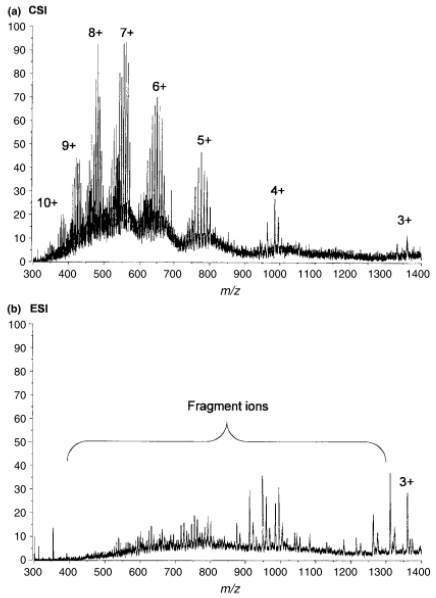


**Figure 3.** Comparison of (a) CSI and (b) ESI mass spectra of **1a**. Reprinted from Ref. 2 with permission from Elsevier.

a)

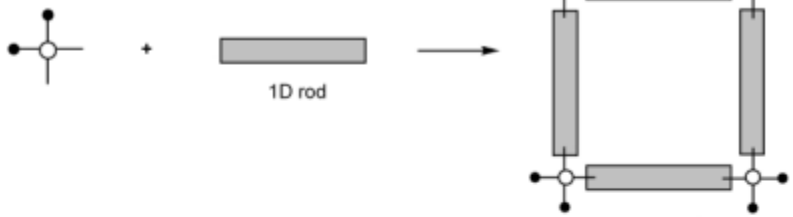


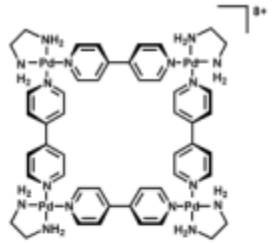


3

b)

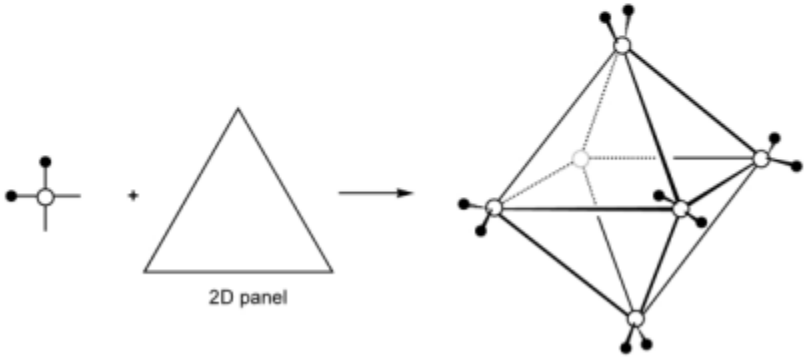


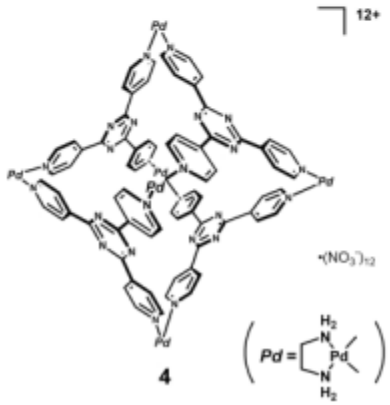


4

# *Molecular Paneling*

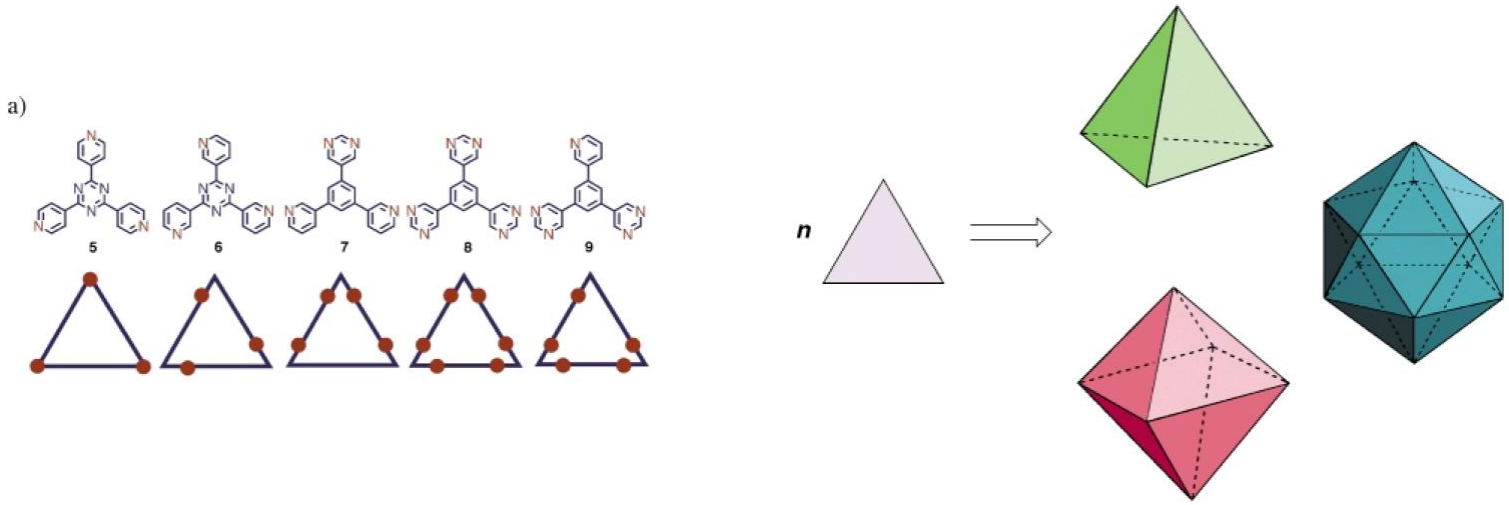


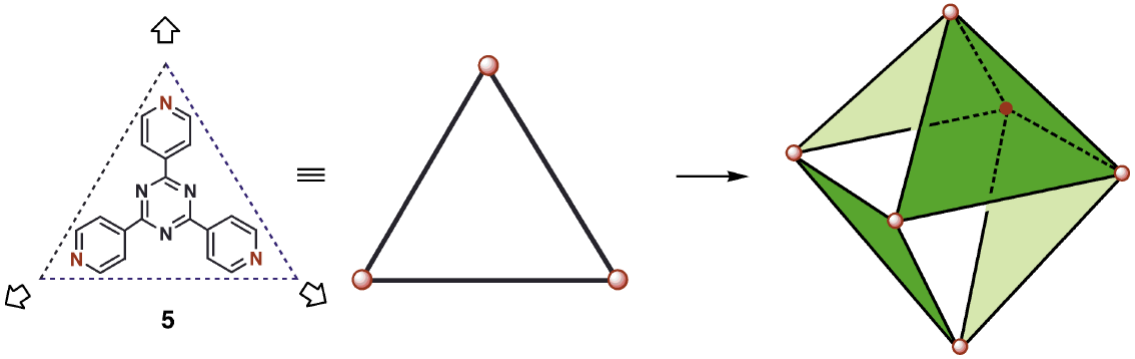

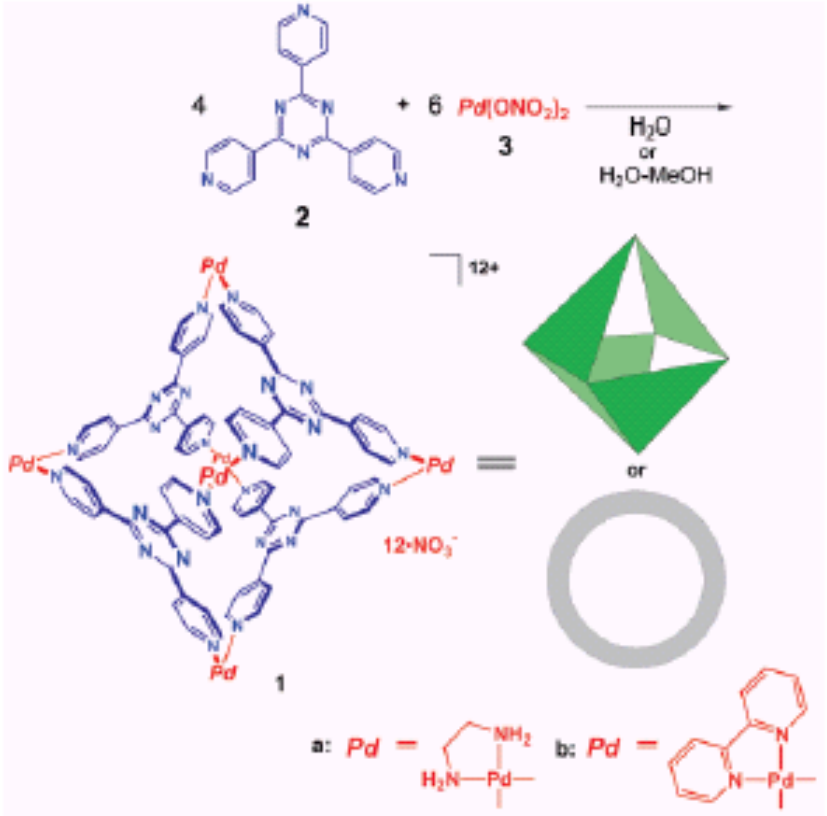
4
+ 6 Pd(ONO2)2
3
H2O
or
H2O-MeOH
2
12+
Pd
12·NO3−
or
1
a: Pd =
NH2
H2N—Pd—
b: Pd =
N
N—Pd—

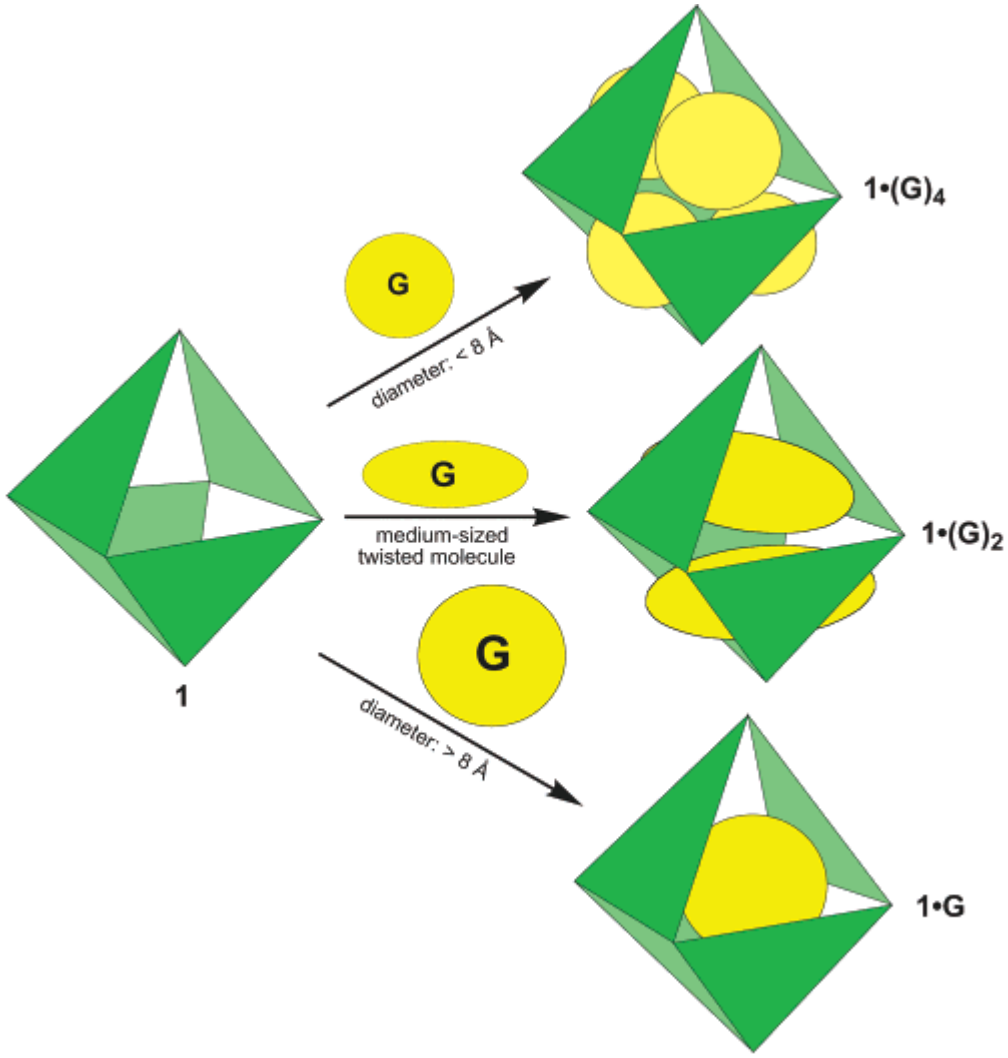
G
diameter: < 8 Å
1•(G)4
G
medium-sized
twisted molecule
1•(G)2
1
G
diameter: > 8 Å
1•G

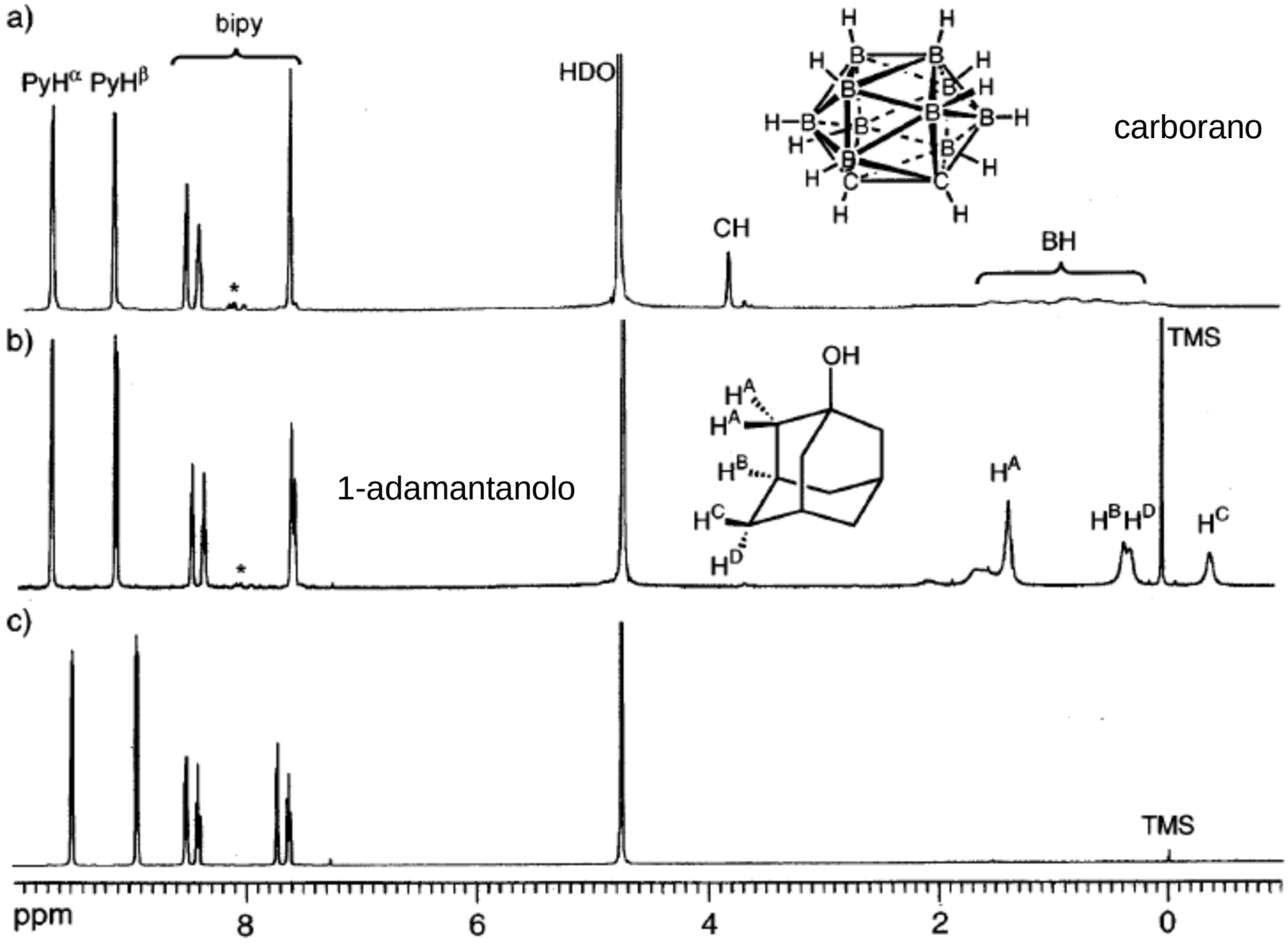


***Figure 1.*** $^{1}$H NMR observations of the enclathration of guest molecules in **1b**. (a) **1b**·(**4**)$_4$. (b) **1b**·(**5**)$_4$. (c) Empty **1b** (∗: impurities).

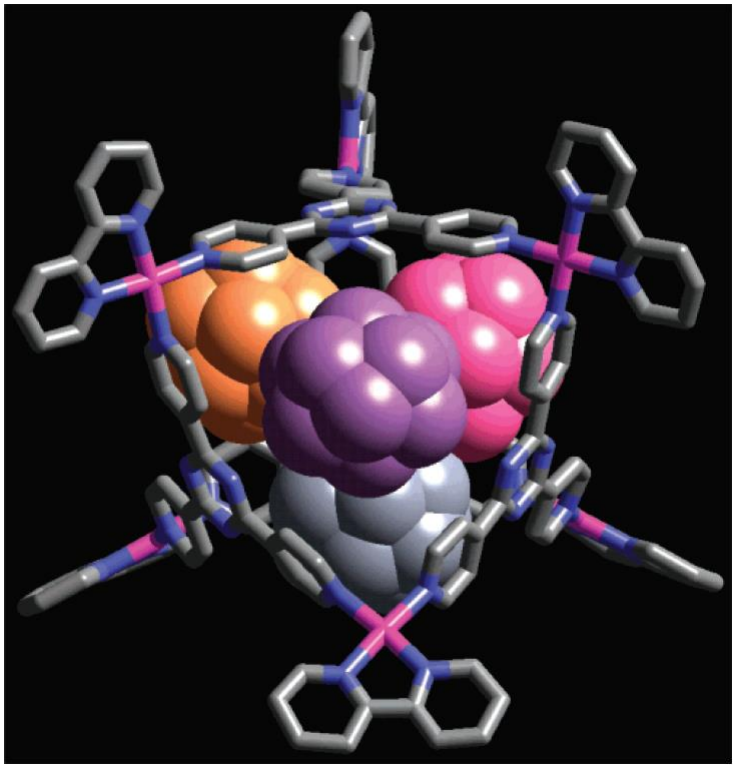

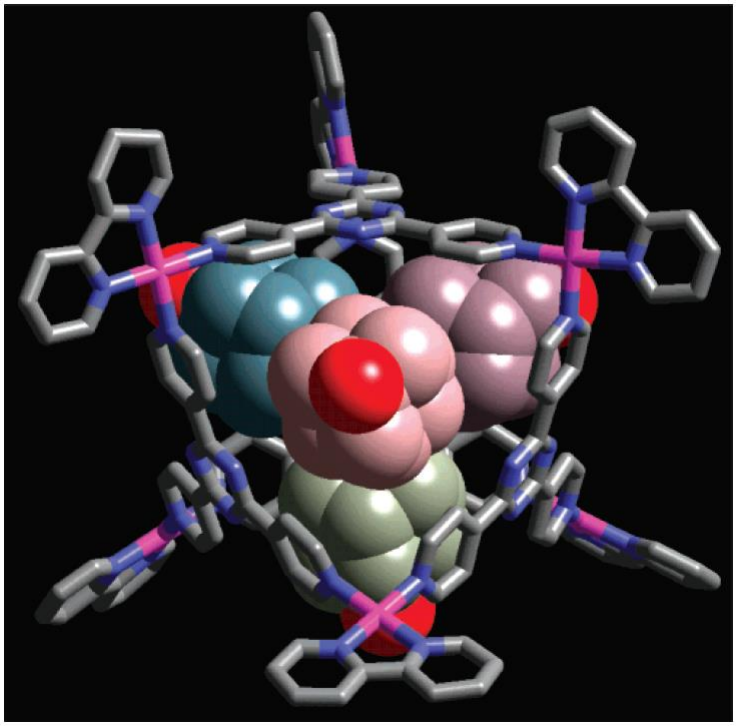

*Scheme 2*

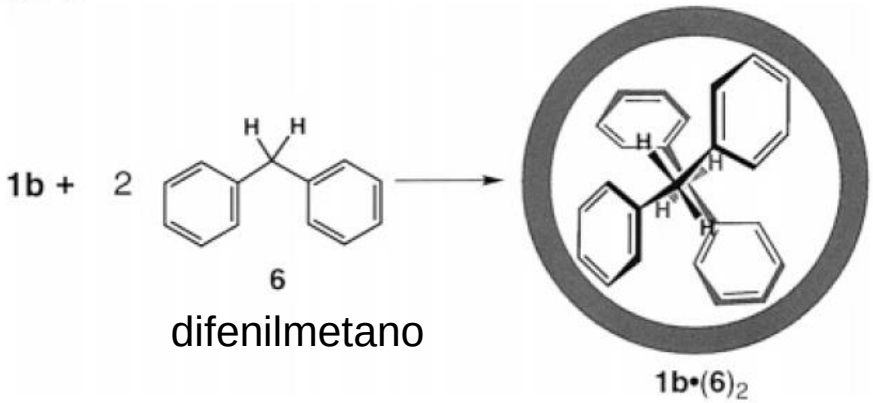


difenilmetano

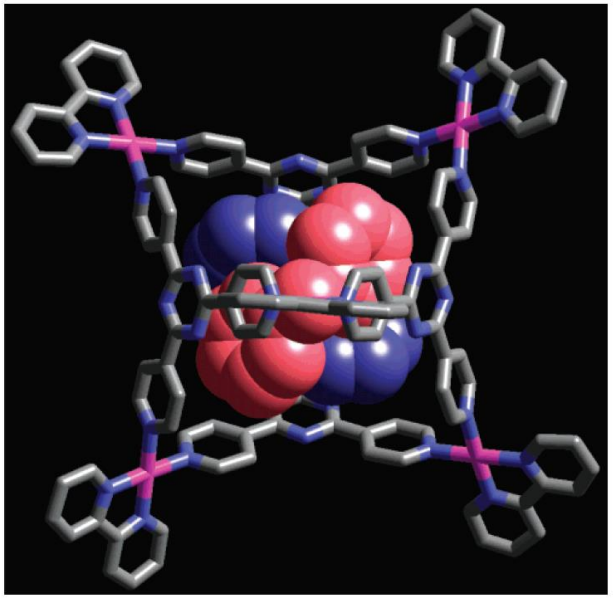

*cis*-azobenzene

*cis*-stilbene

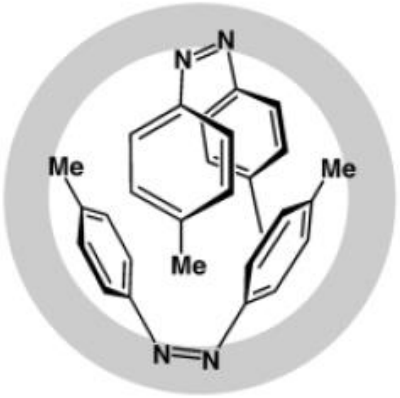


*Scheme 3*

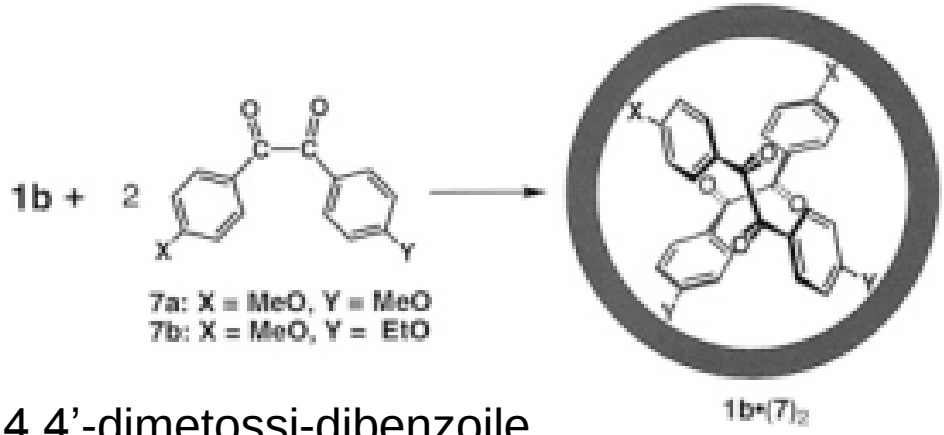


4,4’-dimetossi-dibenzoile

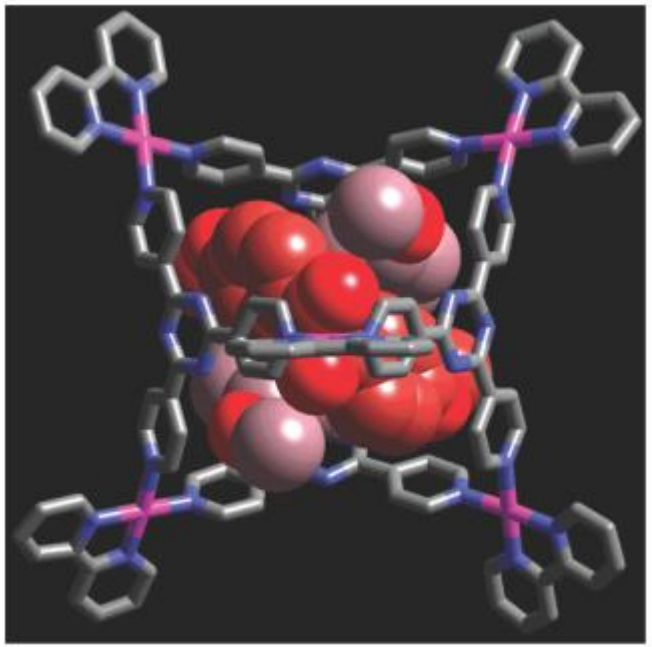

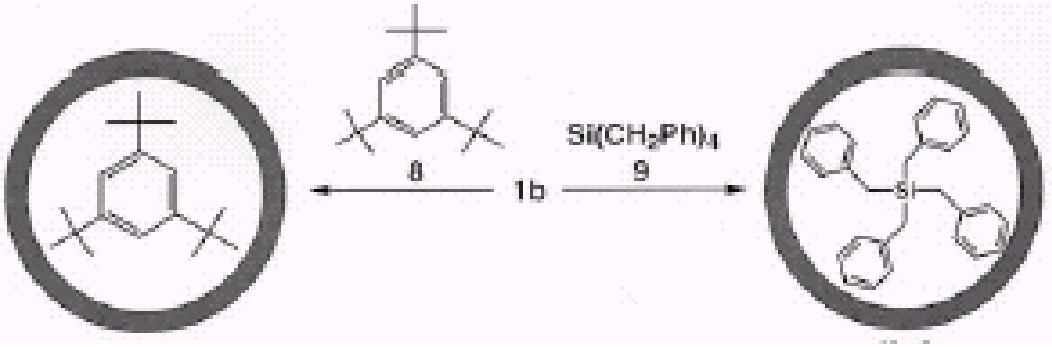


**tri-*tert*-butilbenzene** **tetrabenzilsilano**

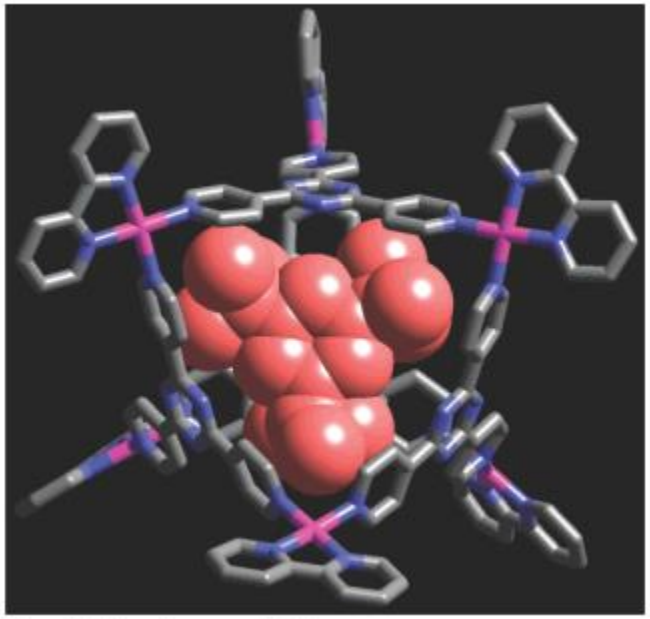

*Figure 8.* Crystal structure of **1b·8**.

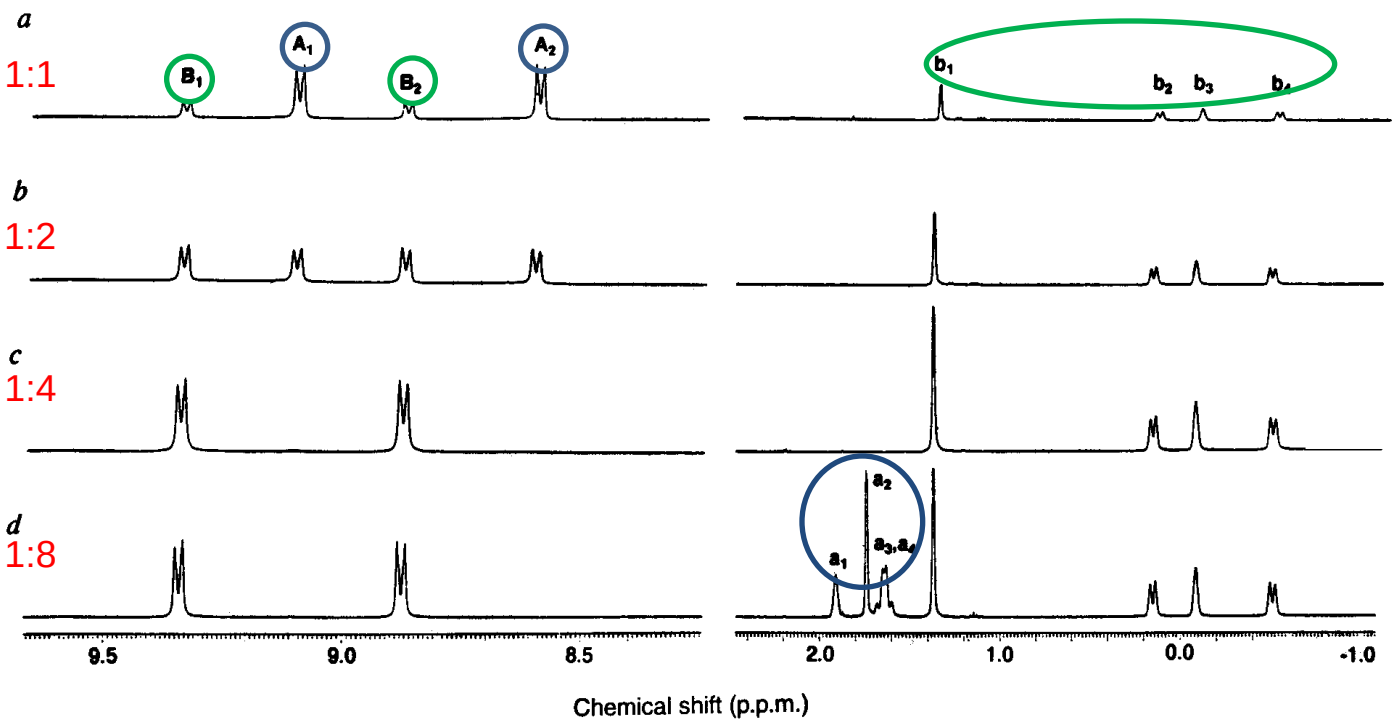


$M_6L_4$/adamantancarbossilato$_4$

**Effetto allosterico!**

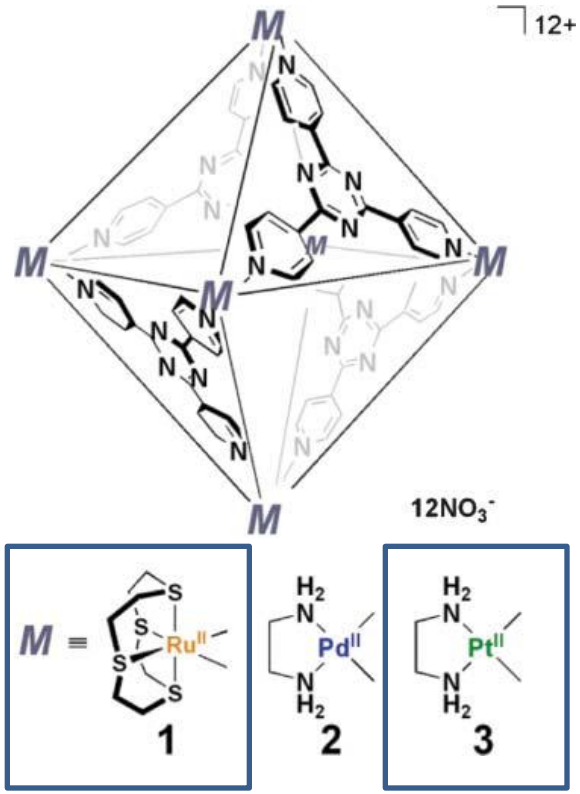
M
12+
12NO3-
M ≡
Ru^II
1
Pd^II
2
Pt^II
3

a)

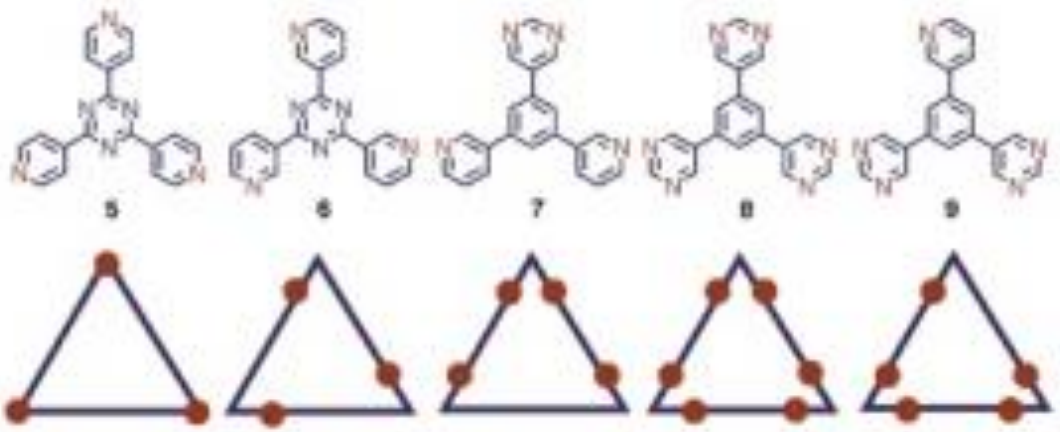


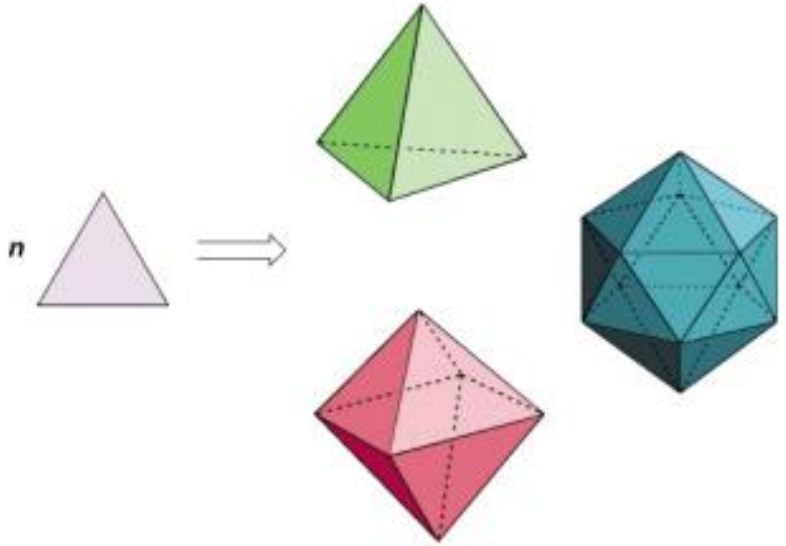

a)

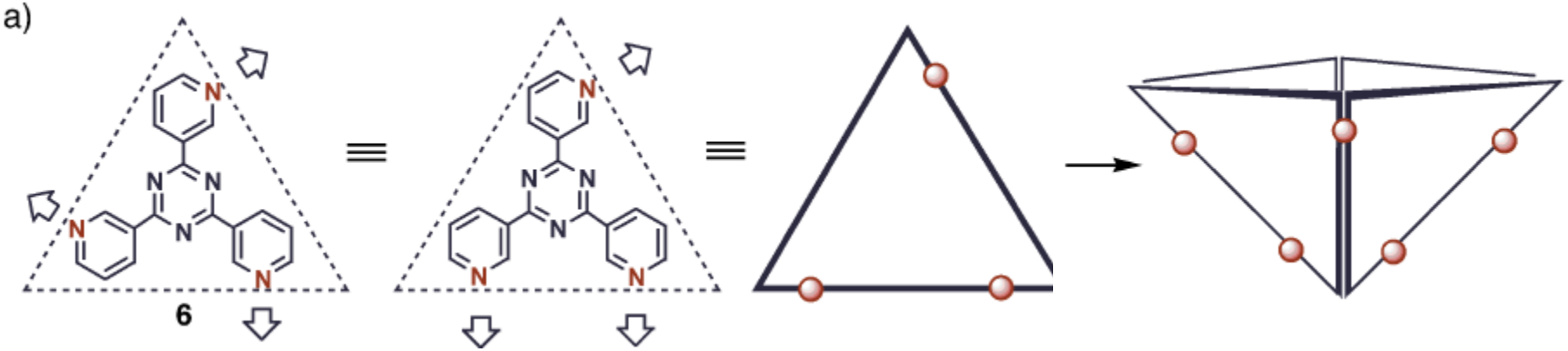

6

b)

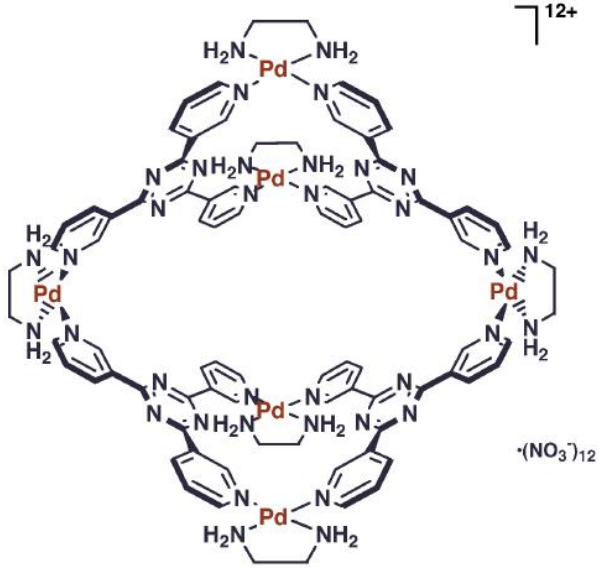

16

c)

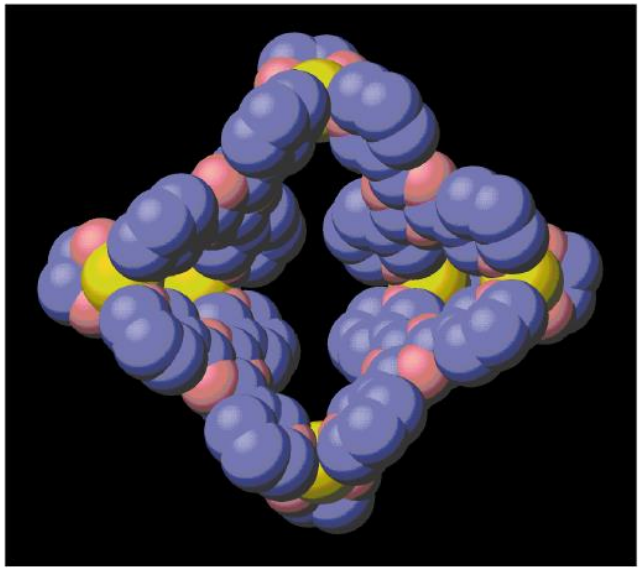

a)

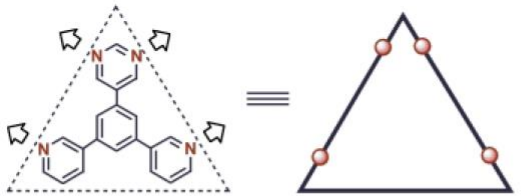

7

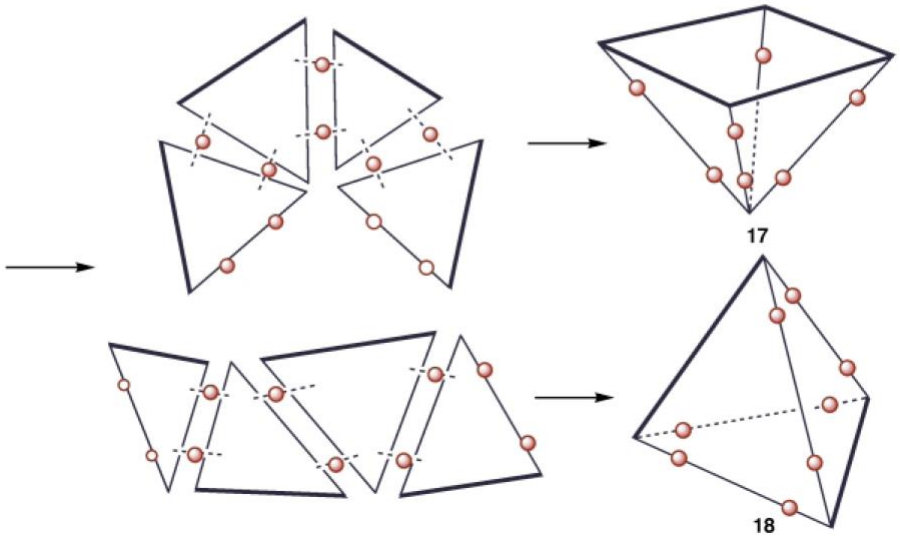

17

18

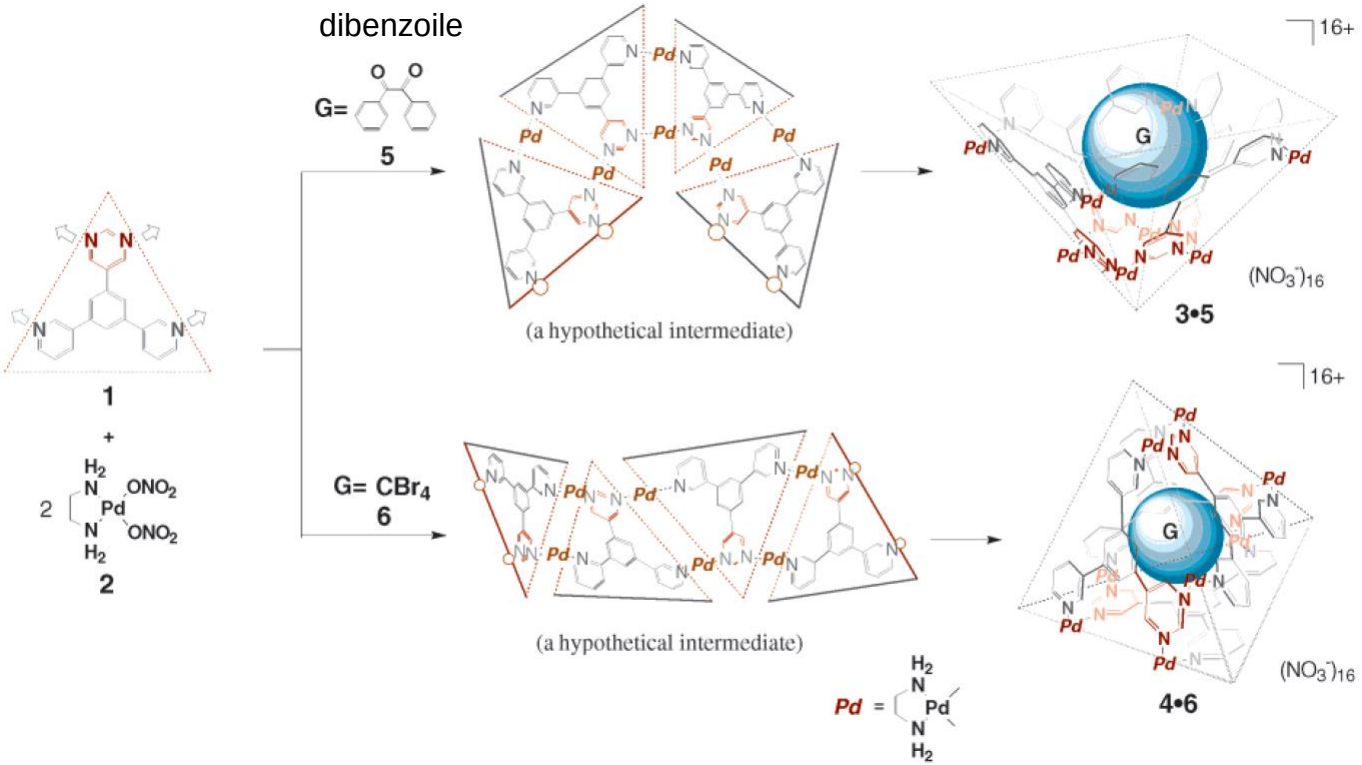
dibenzoile
G=
5
1
+
2
2
(a hypothetical intermediate)
3•5
16+
(NO3-)16
G= CBr4
6
(a hypothetical intermediate)
4•6
16+
(NO3-)16
Pd =

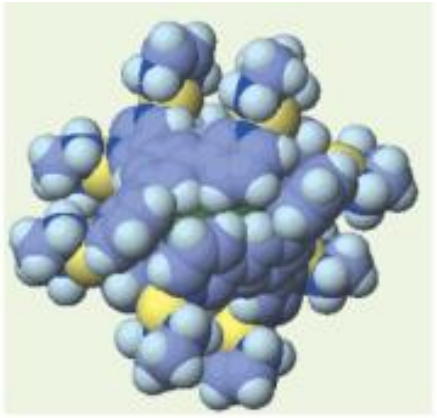

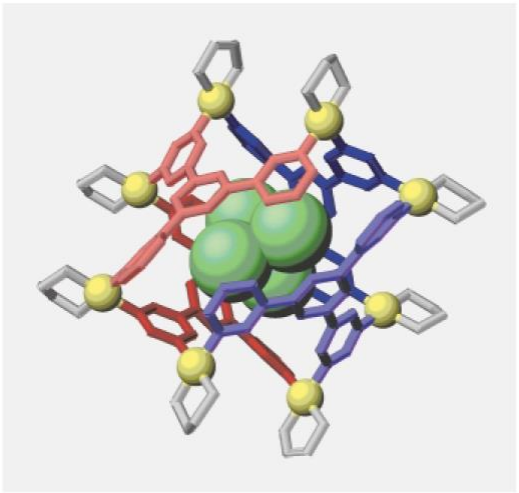

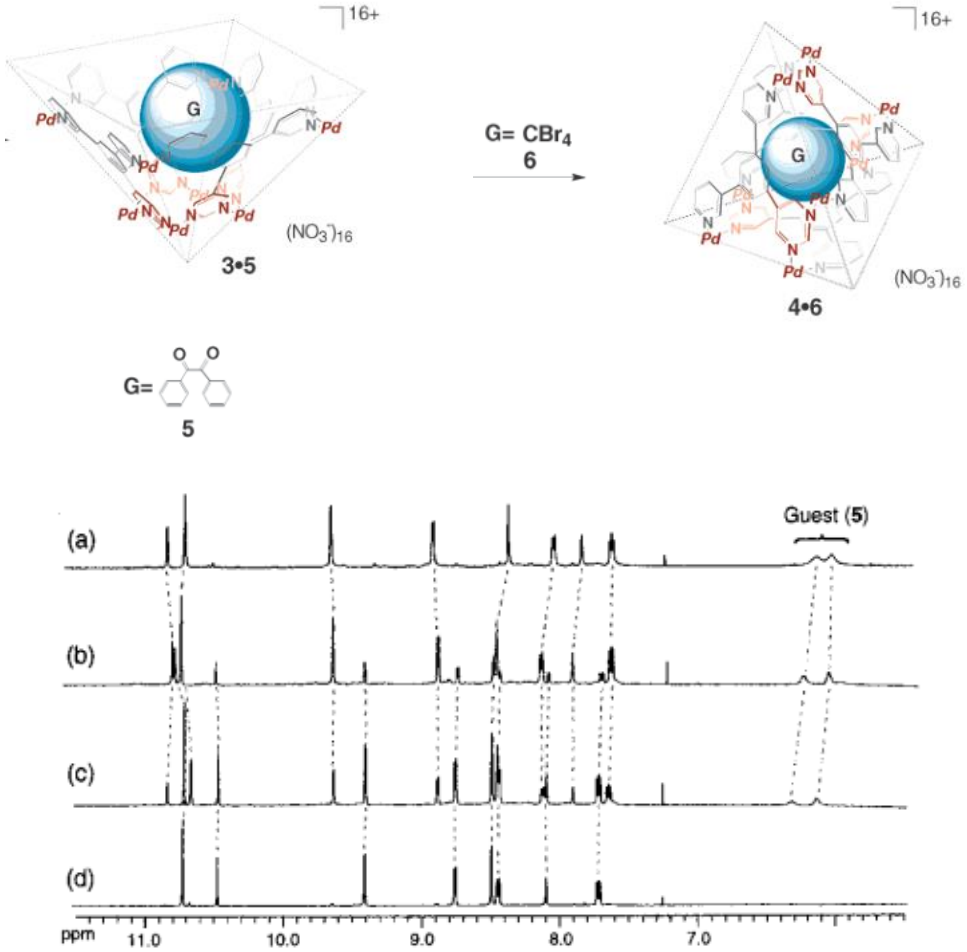


**Figure 2.** The $^1$H NMR monitoring of reorganization process from **3·5** to **4·6** via guest exchange. (a) **3·5** complex in $D_2O$; (b−d) After the addition of excess amount of **6** at 25 °C ((b) 3 h, (c) 8 h, (d) 24 h). Note that free **5** is immiscible in water and, after guest exchange, becomes invisible in the spectrum.

# A nanometre-sized hexahedral coordination capsule assembled from 24 components

NATURE | VOL 398 | 29 APRIL 1999 | www.nature.com

Nobuhiro Takeda*, Kazuhiko Umemoto†, Kentaro Yamaguchi‡ & Makoto Fujita*

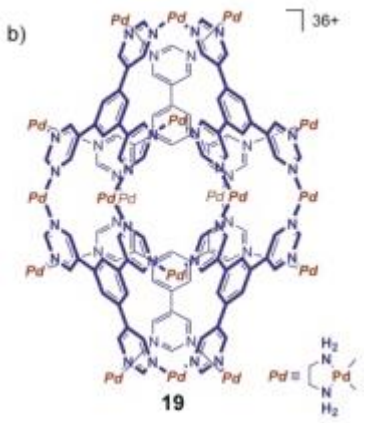


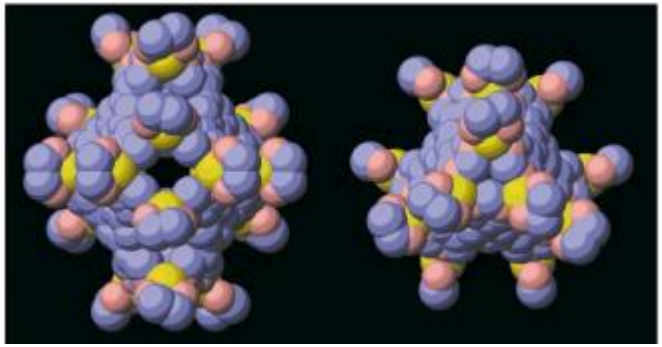

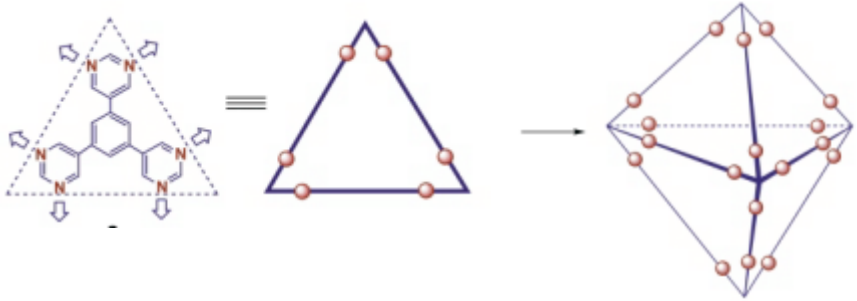

b)

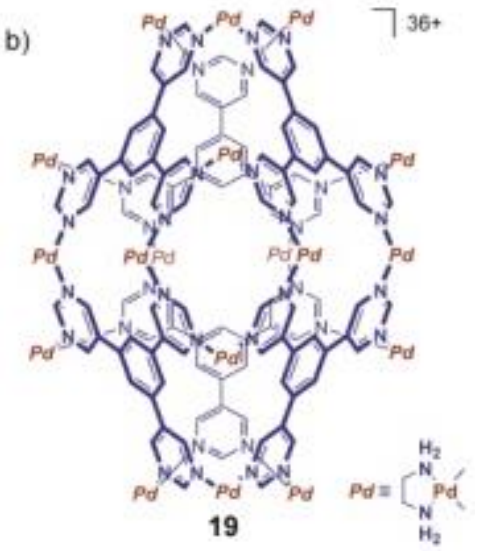


19

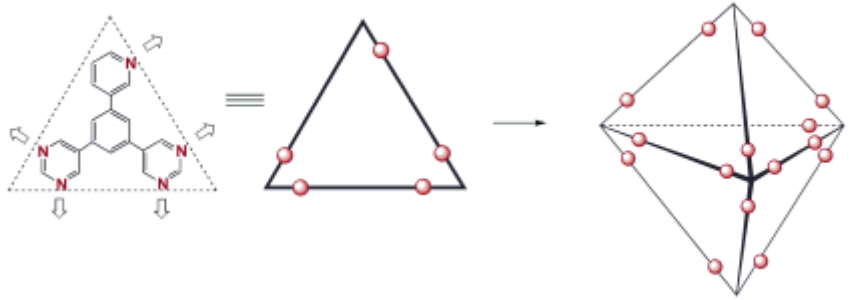

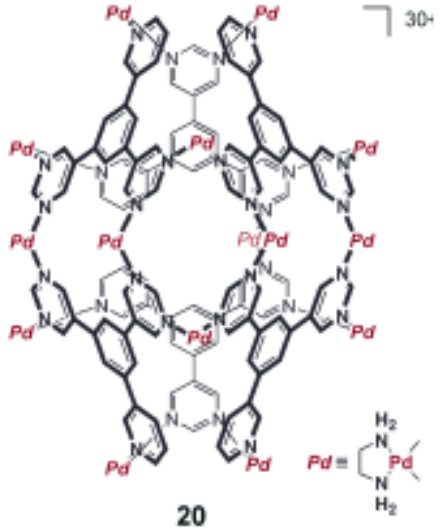


20

a)

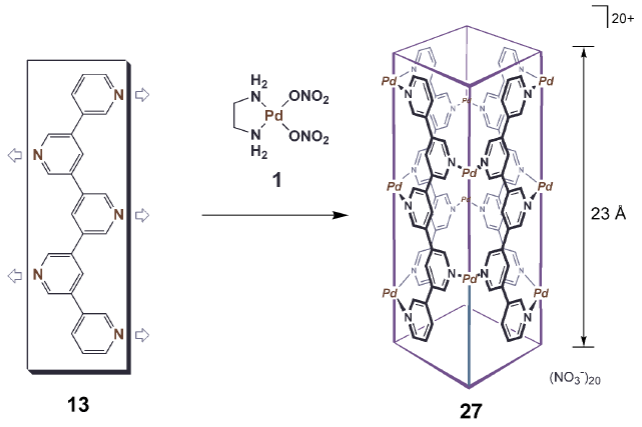
20+
23 Å
(NO3−)20
1
13
27

b)

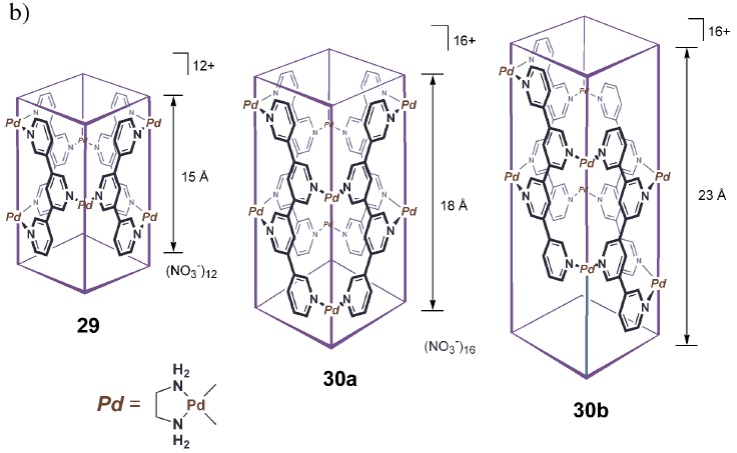
12+
15 Å
(NO3−)12
16+
18 Å
(NO3−)16
16+
23 Å
29
30a
30b
Pd =

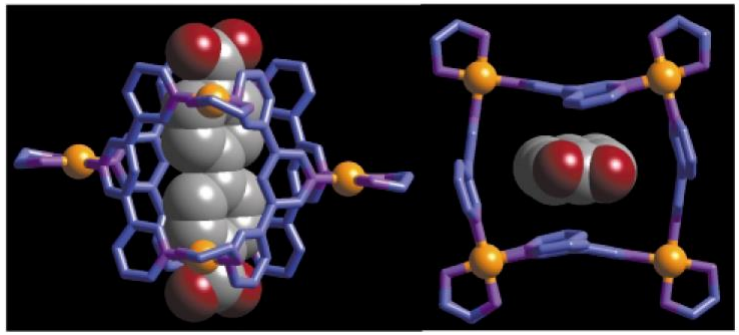

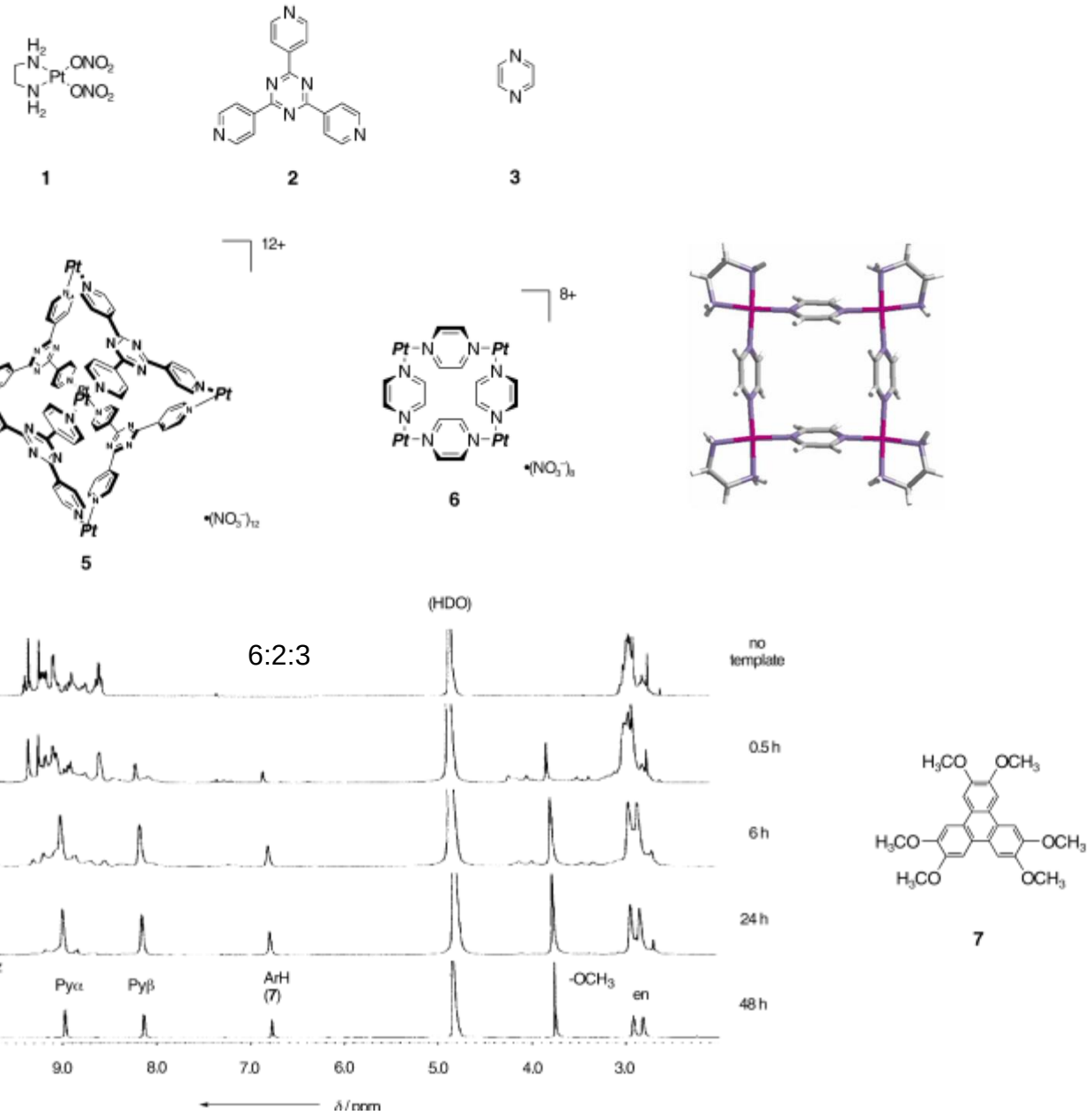


***Figure 1.*** $^1$H NMR spectra showing the guest-templated assembly of **7**⊂**4** complex (500 MHz, $D_2O$, 25 °C). a) A mixture of **1**, **2**, and **3**. Template **7** was added to this solution and the mixture was heated at 100 °C for b) 0.5 h, c) 6 h, d) 24 h, and e) 48 h. Pyz = pyrazine.

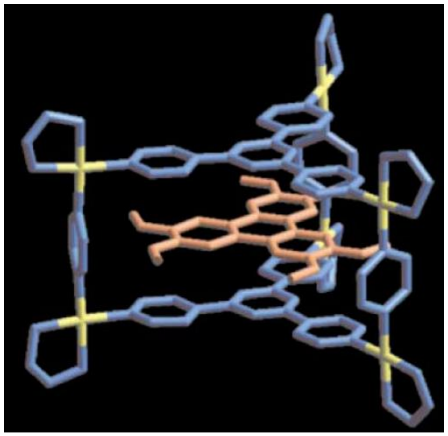

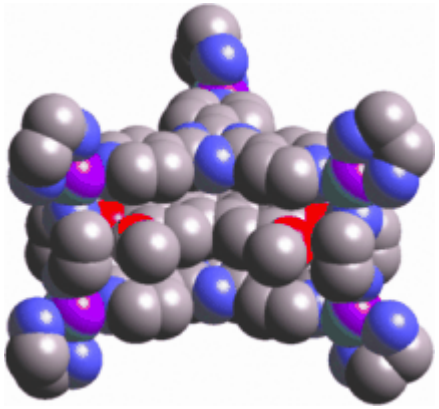

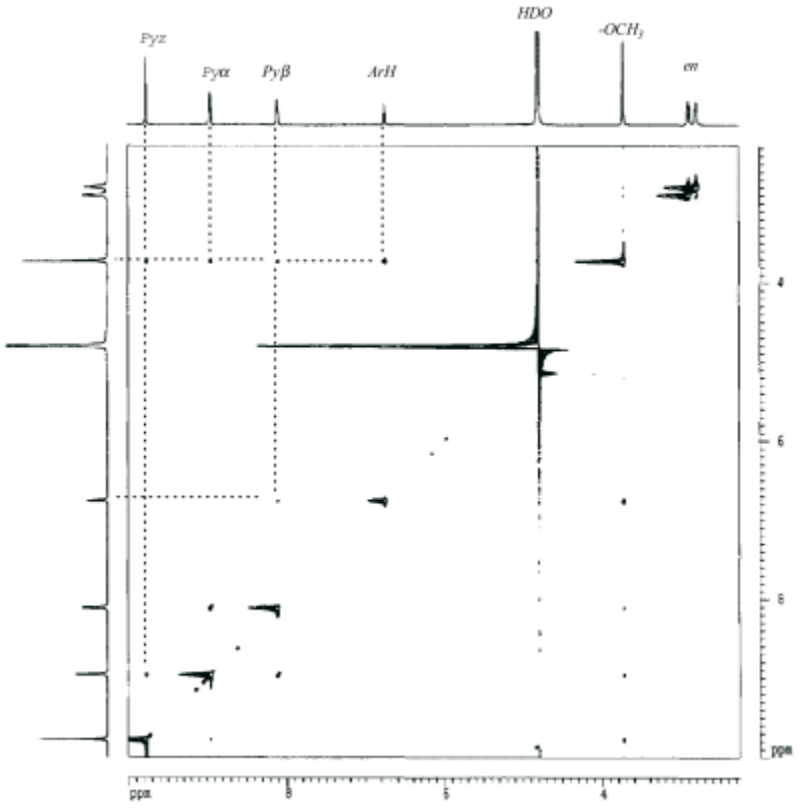


NOESY of 7⊂4

# DOSY

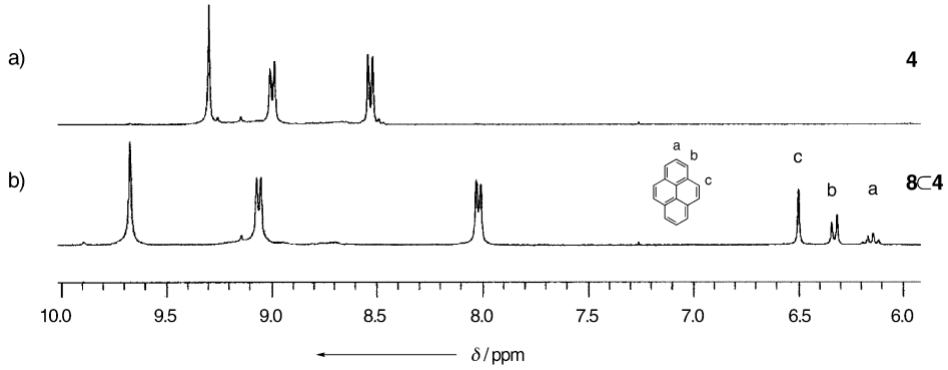


***Figure 4.*** $^{1}$H NMR spectra (300 MHz, $D_2O$, 25 °C) of aromatic regions of a) free **4** after extraction of template and b) **8**⊂**4** after the subsequent reinclusion of **8**.

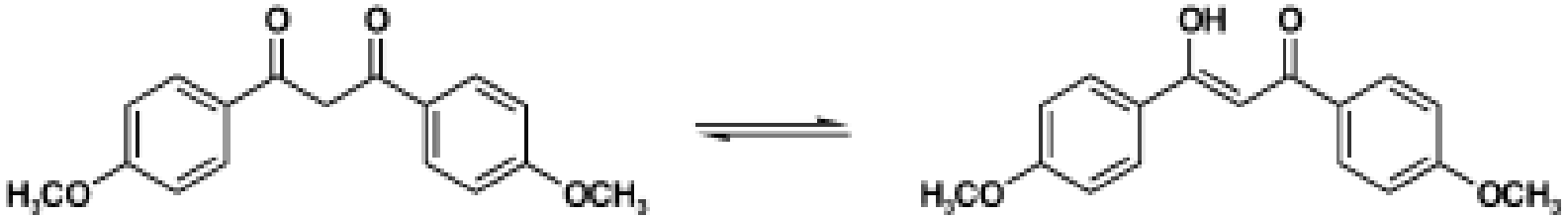
O
O
H3CO
OCH3
OH
O
H3CO
OCH3

keto **9** enol **9**

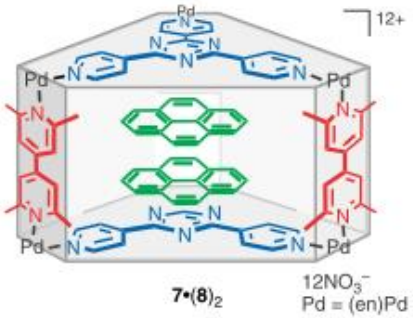
12+
Pd
N
7•(8)2
12NO3−
Pd = (en)Pd

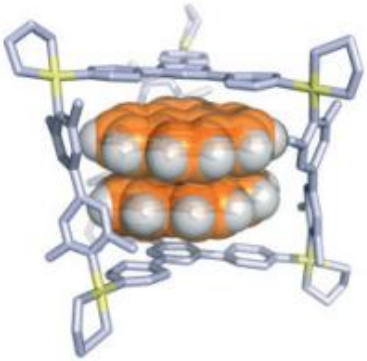

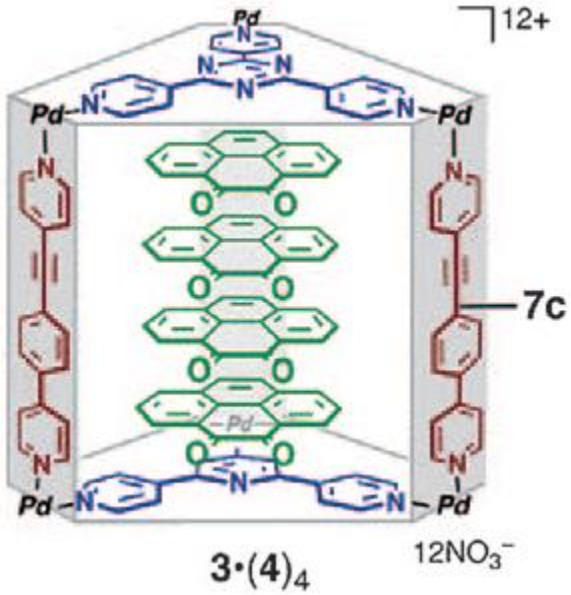
12+
Pd
N
O
7c
3•(4)4
12NO3−

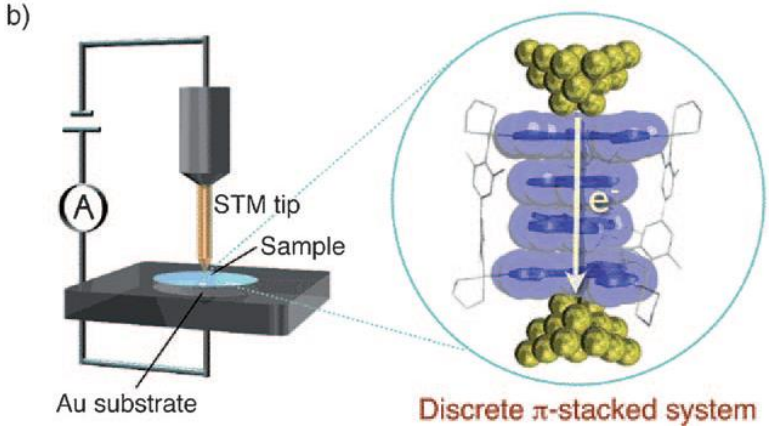
b)
A
STM tip
Sample
Au substrate
e−
Discrete π-stacked system

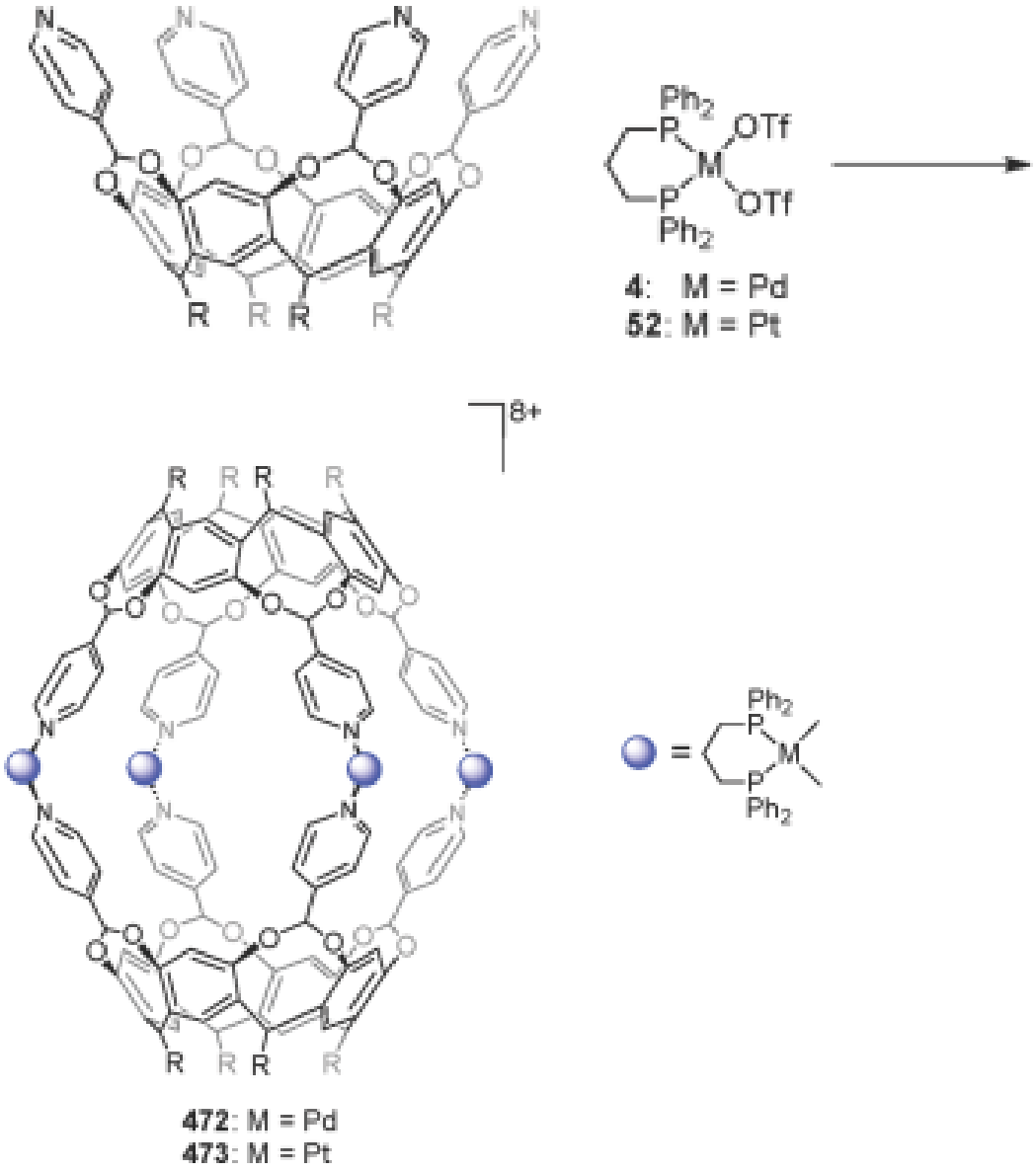
Ph2
P
M
OTf
OTf
P
Ph2
4: M = Pd
52: M = Pt
8+
R
472: M = Pd
473: M = Pt

# Stabilizzazione di intermedi reattivi: alcossi-silani ciclici
## *Ship in a Bottle*

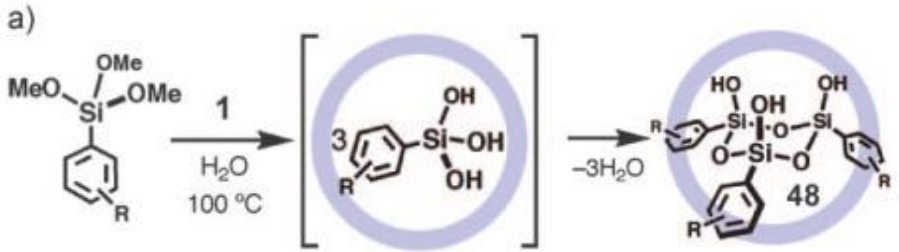


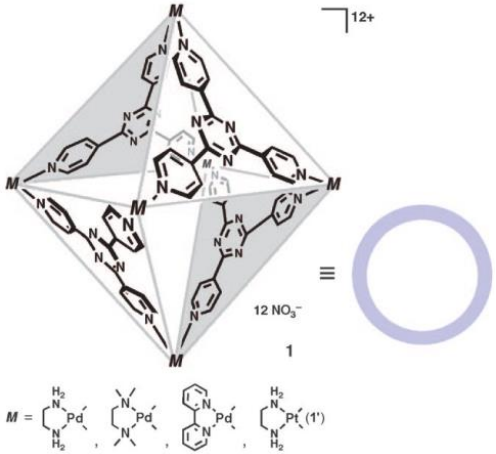


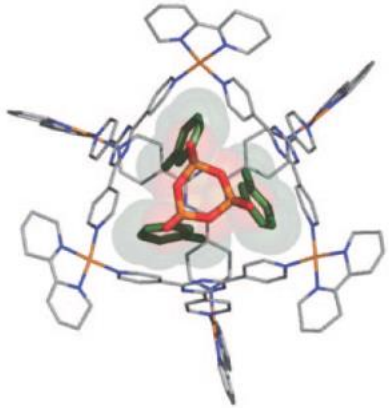

# Stabilizzazione di intermedi reattivi: Oligomerizzazione di tri alcossi-silani

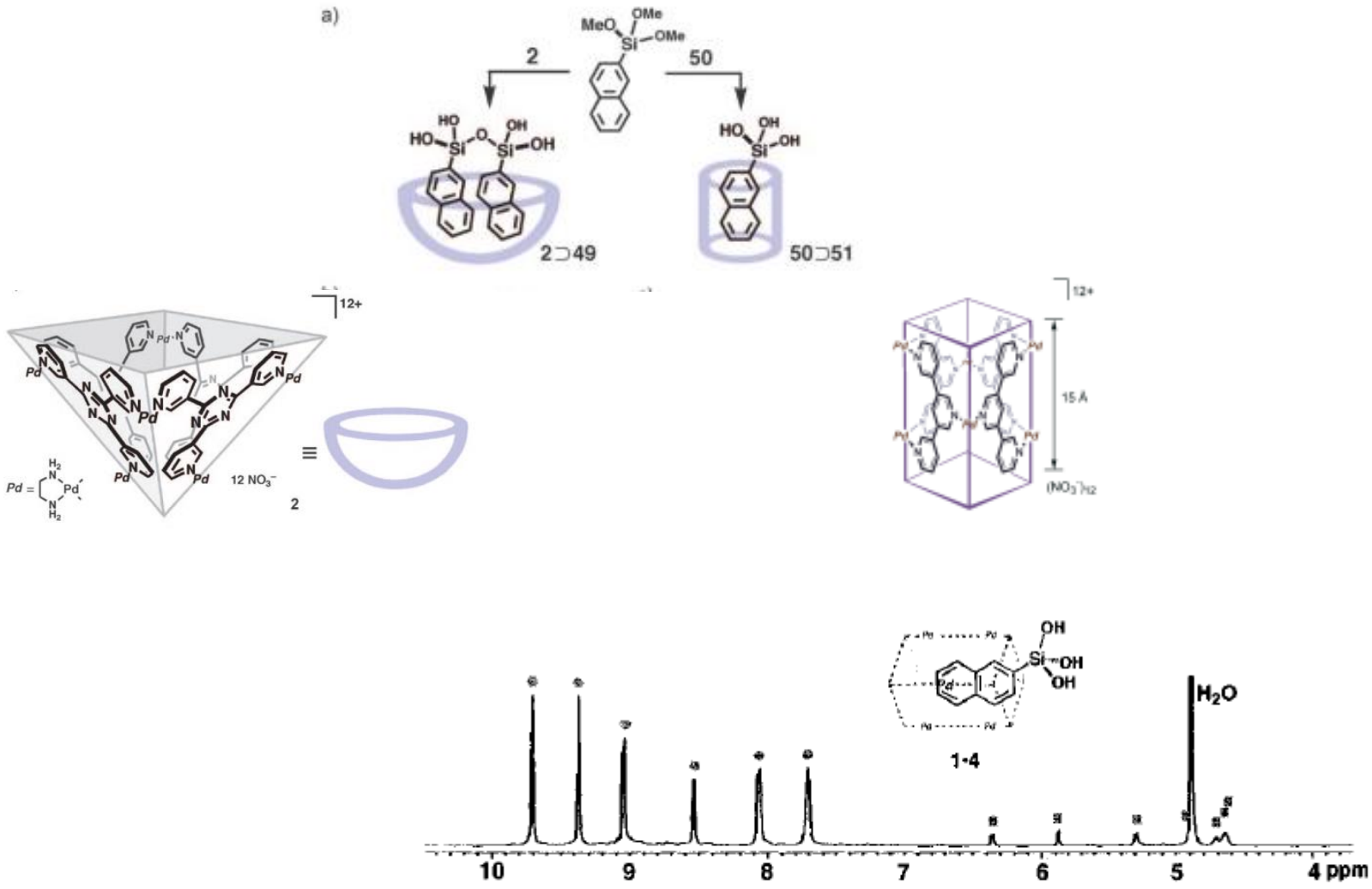


**Figure 1.** $^1$H NMR spectrum (500 MHz, $D_2O$, TMS as an external standard) of **1·4** at 27 °C. Circles and squares indicate host and guest signals, respectively.

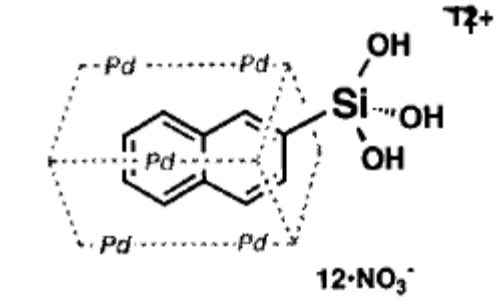


$12 \cdot NO_3^-$

**1•4**

## $^{29}Si$ NMR of 1•4

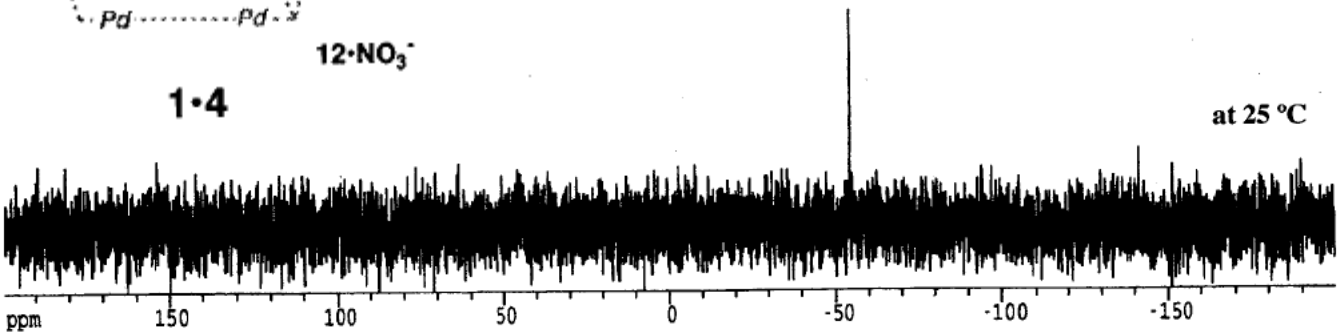

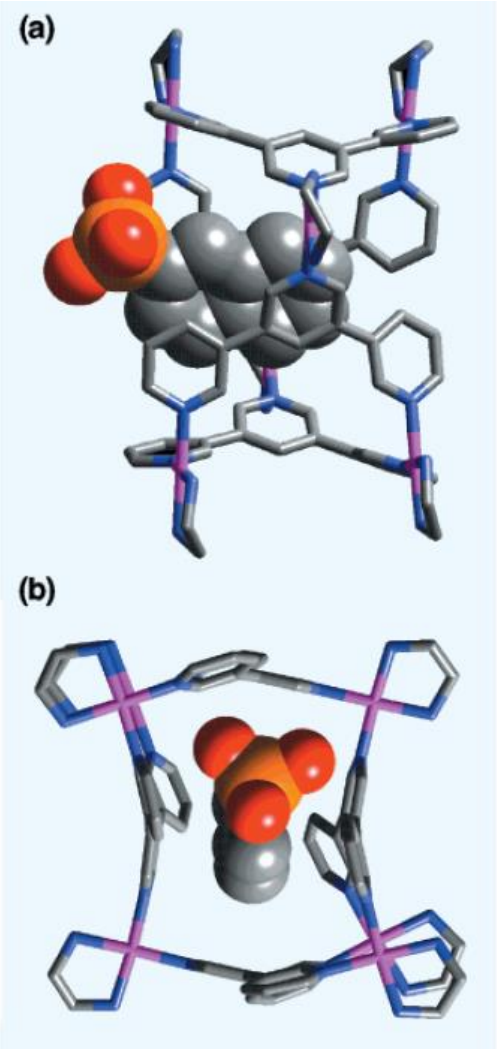


**Figure 2.** The crystal structure of **1·4**: (a) side view and (b) top view.

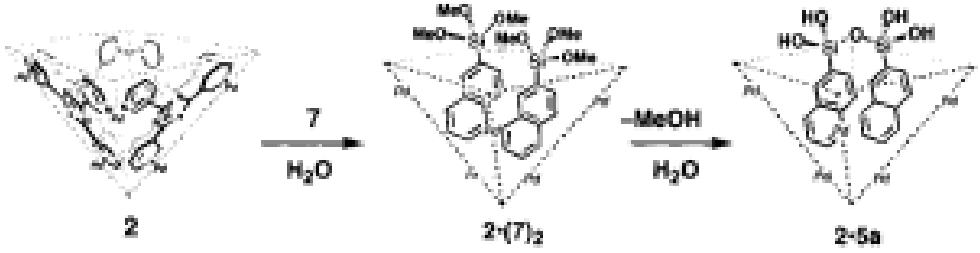


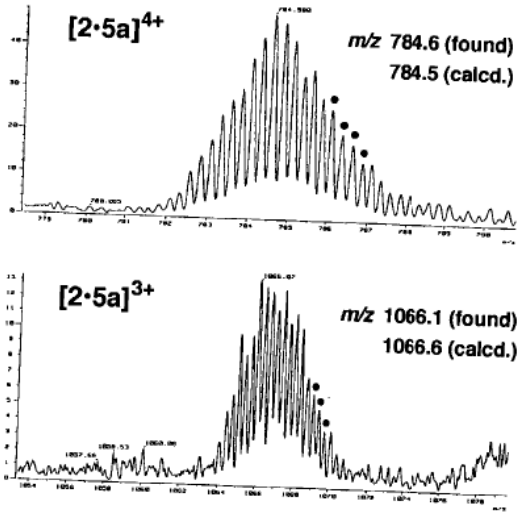


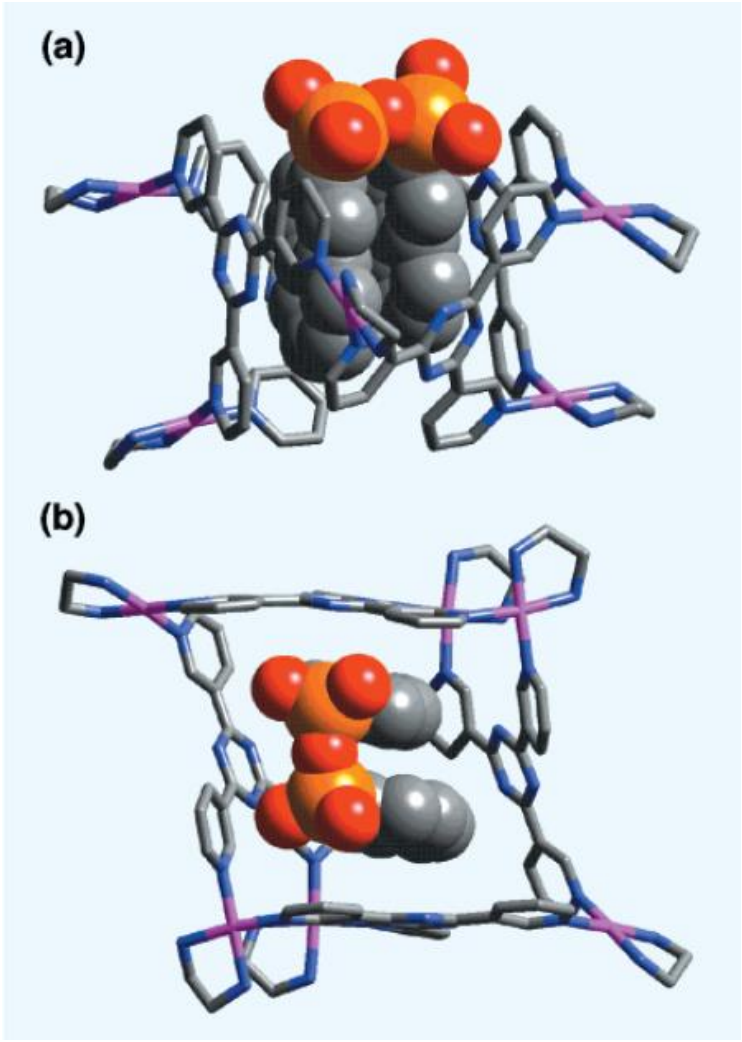


**Figure 4.** The crystal structureof **2·5a**: (a) side view and (b) top view.

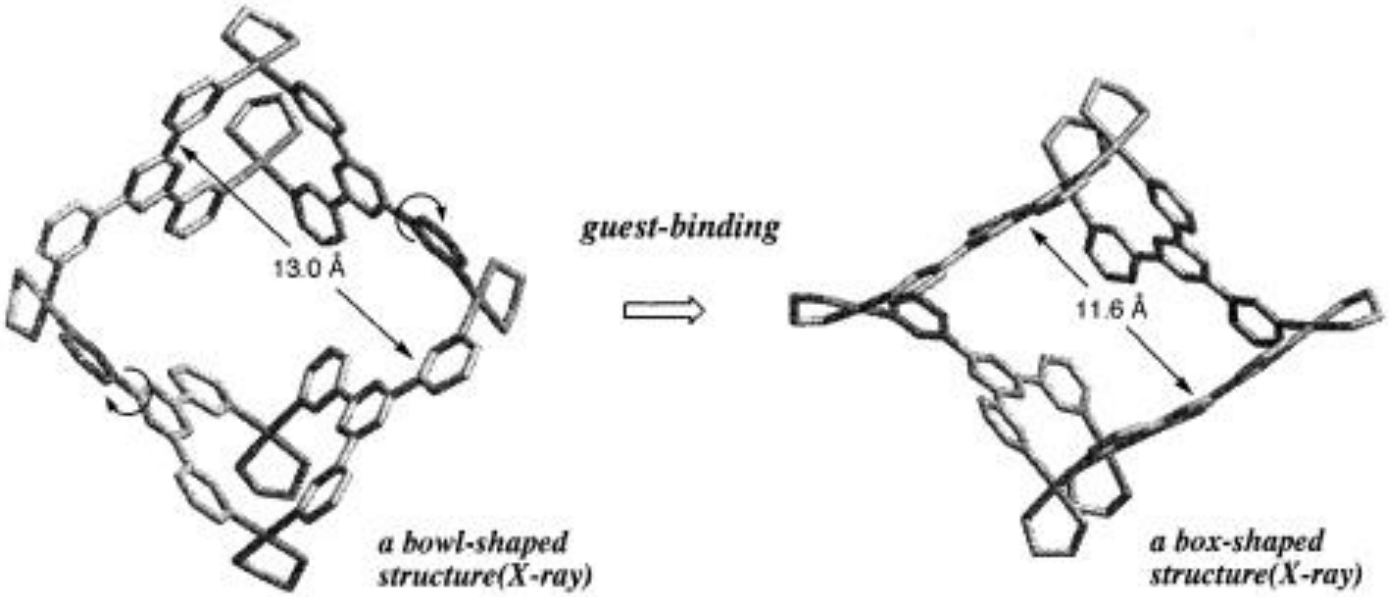


**Figure 5.** Bowl-to-box conformational change of **2·5a** is triggered by the guest binding. For clarity, guest molecules are omitted.

# Fotodimerizzazioni 2+2

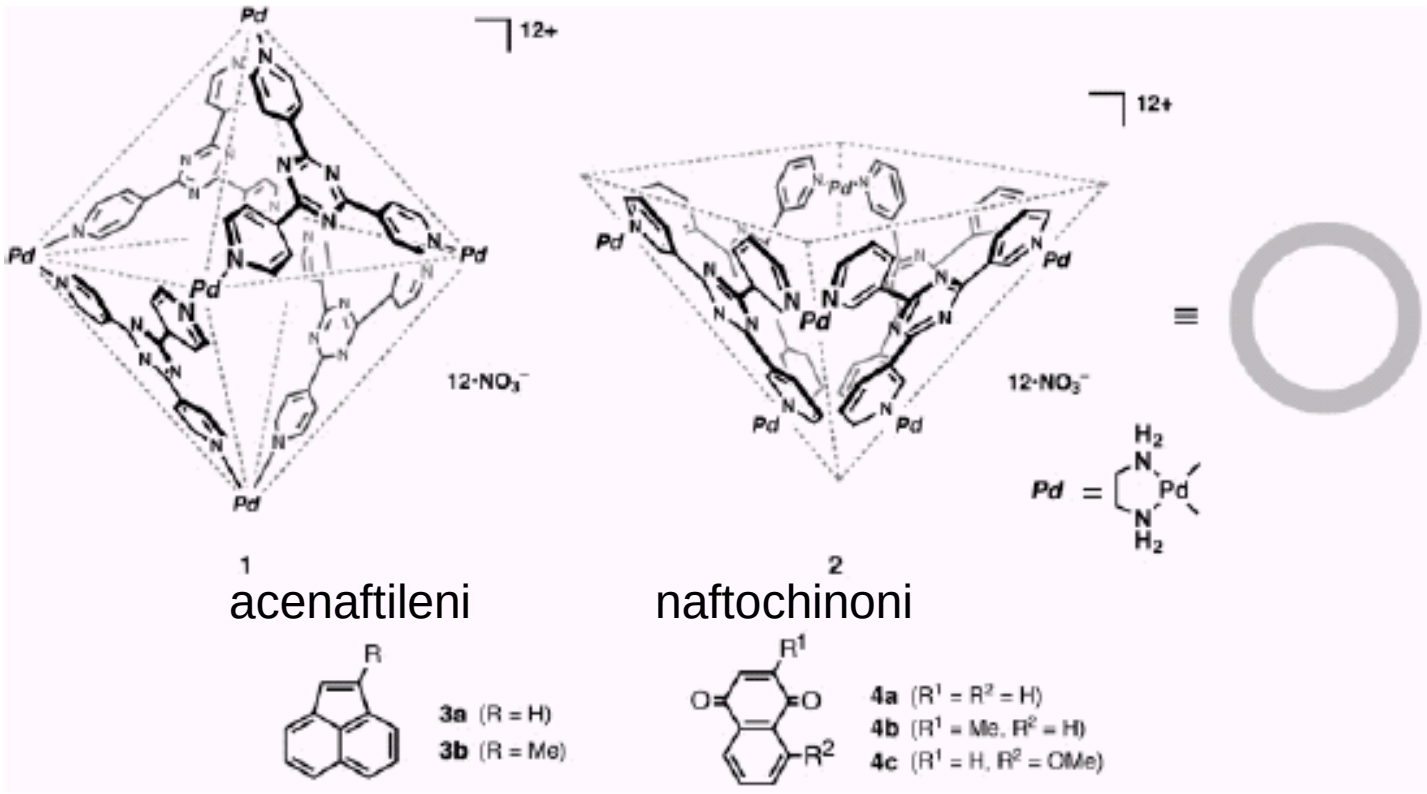


1 acenaftileni

2 naftochinoni




**3a** (R = H)
**3b** (R = Me)




**4a** ($R^1 = R^2 = H$)
**4b** ($R^1$ = Me, $R^2$ = H)
**4c** ($R^1$ = H, $R^2$ = OMe)

acenaftilene

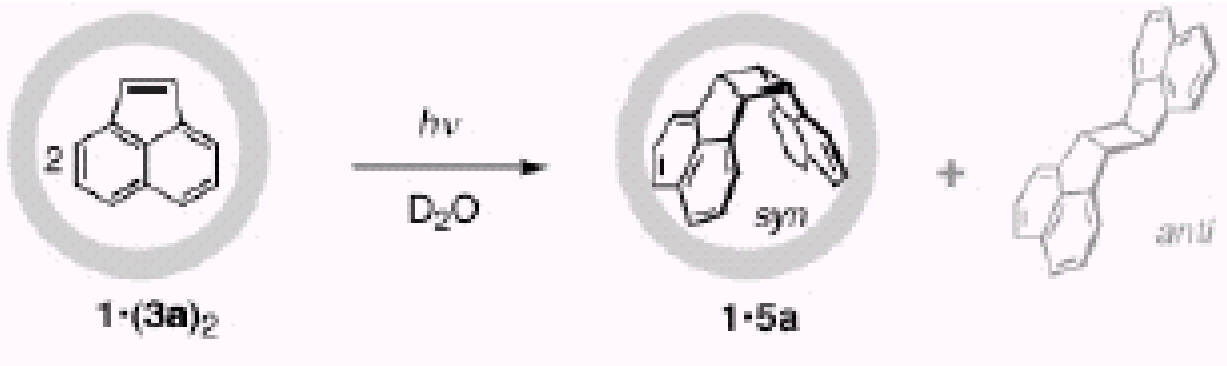


controllo stereochimica, [ ] 2mM resa > 98%

benzene: [ ] 150mM, 3h, resa 40%, no stereoselettività

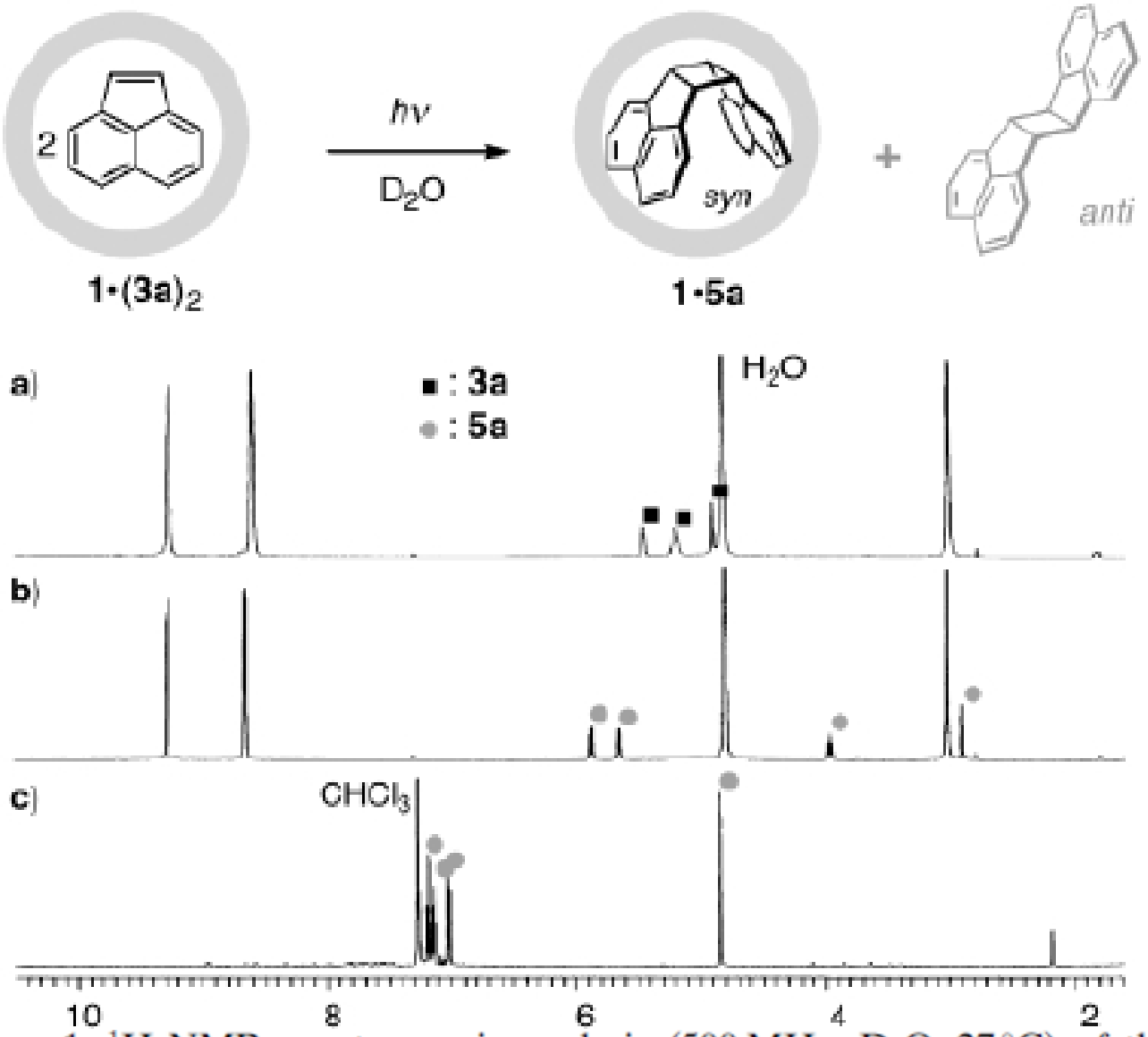


Figure 1. $^1$H NMR spectroscopic analysis (500 MHz, $D_2O$, 27 °C) of the photodimerization of **3a** within cage **1:** a) before irradiation ($\mathbf{1}\cdot(\mathbf{3a})_2$) in $D_2O$; b) after irradiation (400 W) for 0.5 h; c) after extraction with $CDCl_3$.

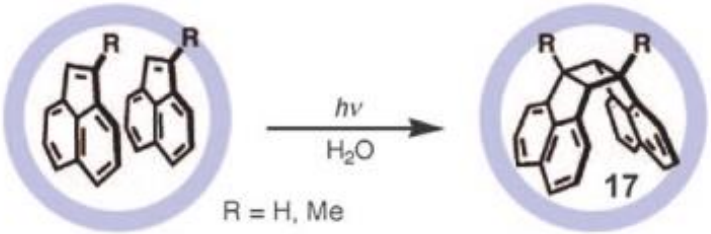
R
R
hν
H2O
R = H, Me
R
R
17

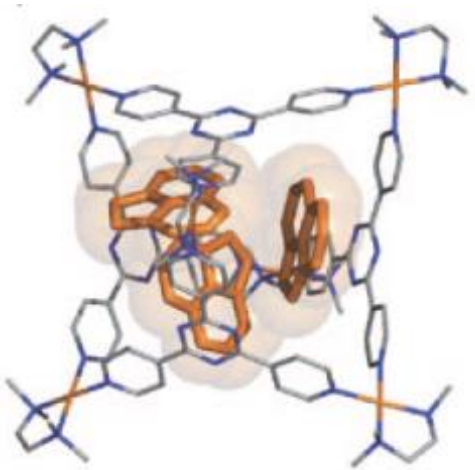

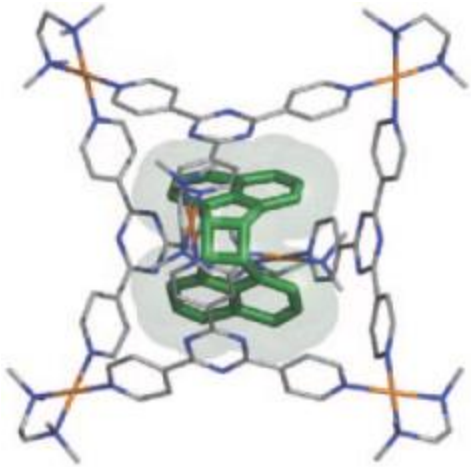

1-metil-acenaftilene

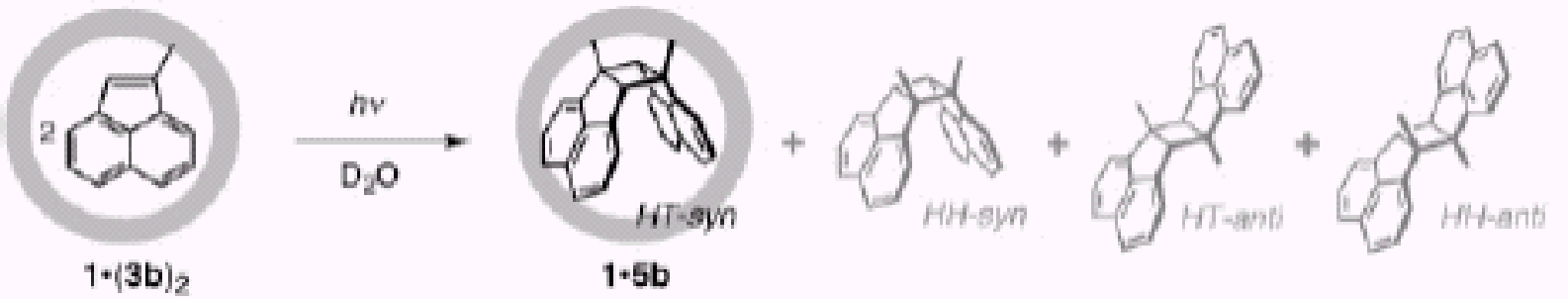


Controllo regiochimica, [ ] 2mM resa > 98%

naftochinone

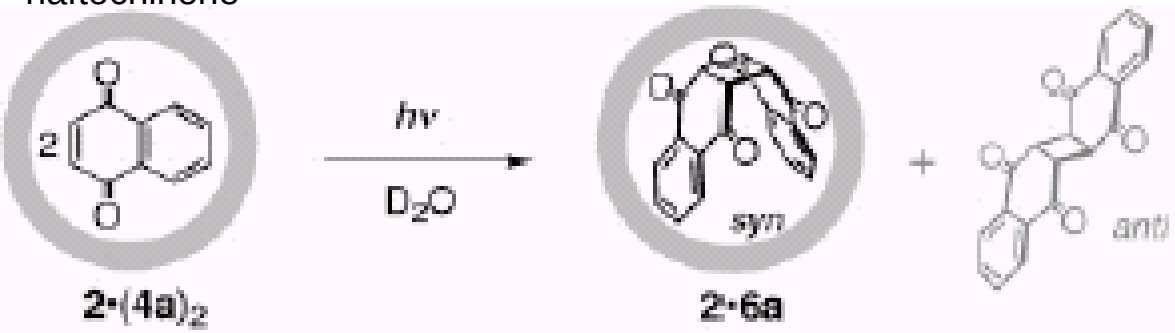


controllo stereochimica, [ ] 2mM resa > 98%

benzene: [ ] > >, t > >, resa 25%, 21% *anti*

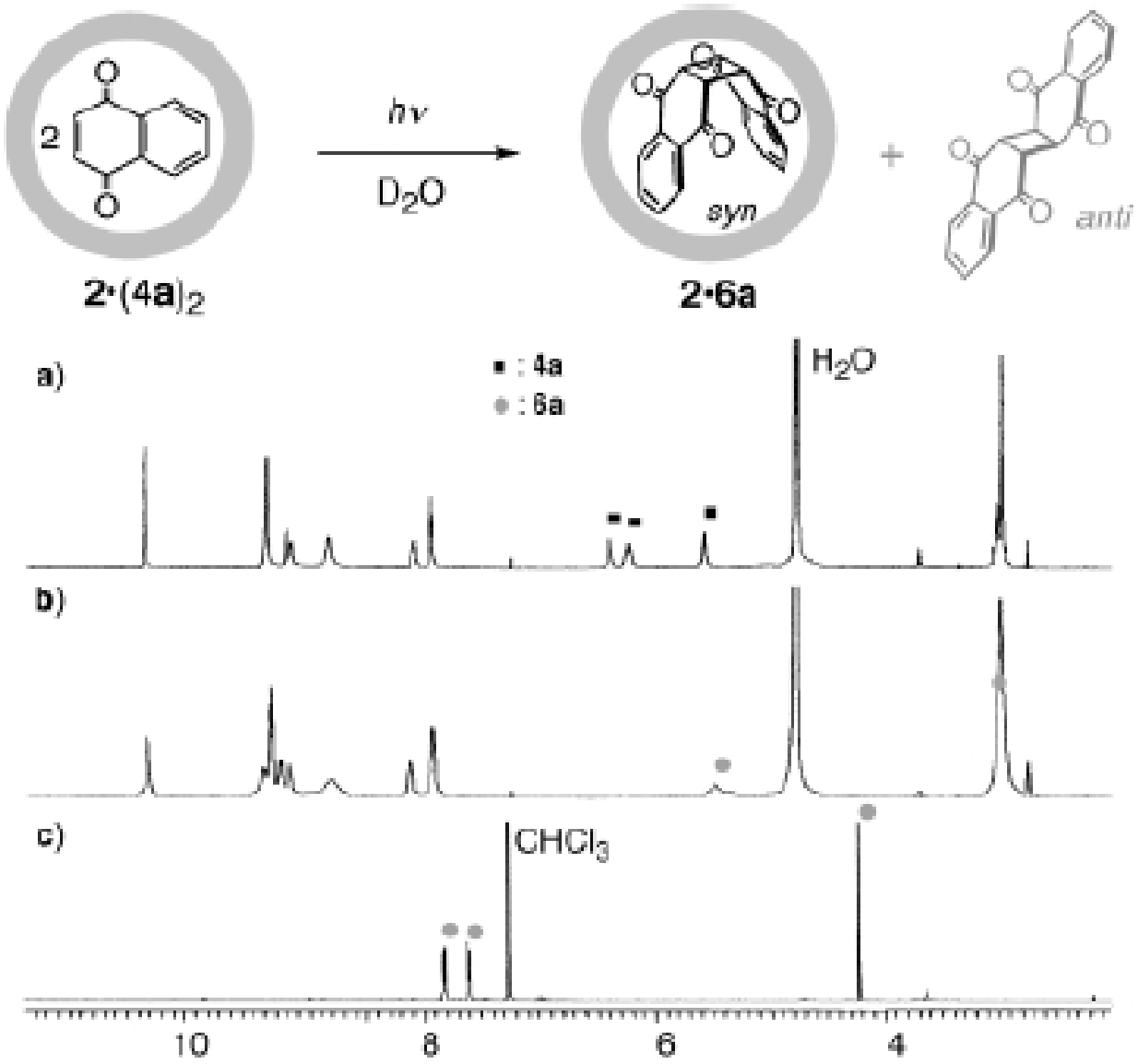


Figure 2. $^1$H NMR spectroscopic analysis (500 MHz, $D_2O$, 27 °C) of the photodimerization of **4a** within bowl **2**: a) before reaction (**2**·(**4a**)$_2$) in $D_2O$; b) after irradiation (400 W) for 3 h; c) after extraction with $CDCl_3$.

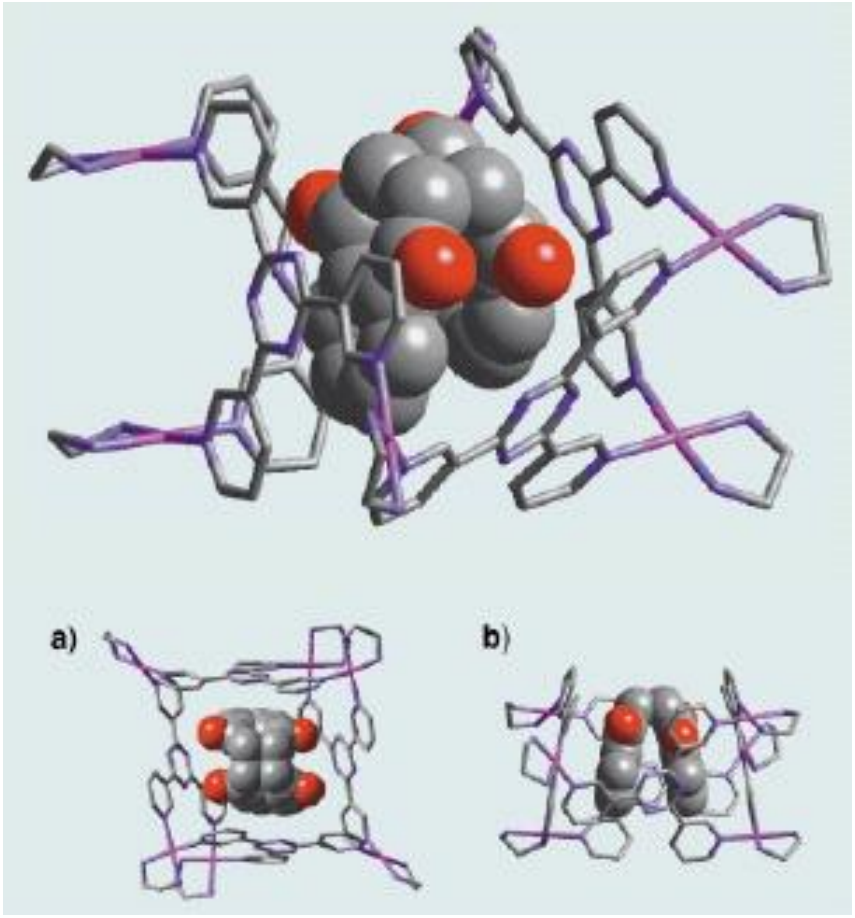
a)
b)

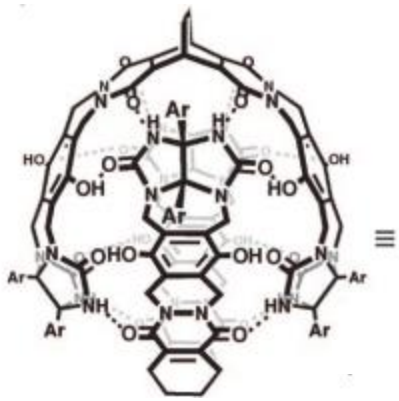

≡



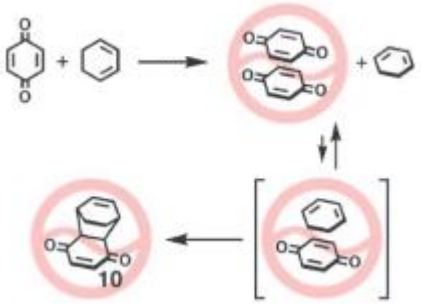
10

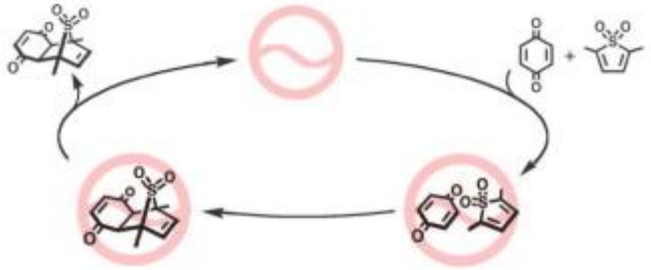

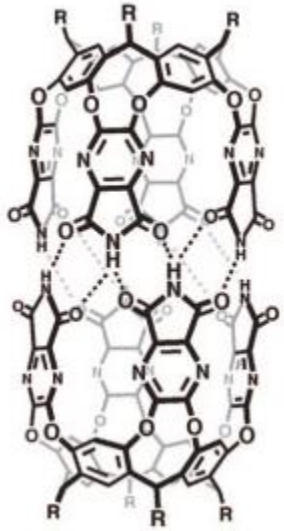

≡



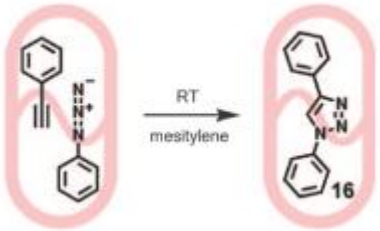
RT
mesitylene
16

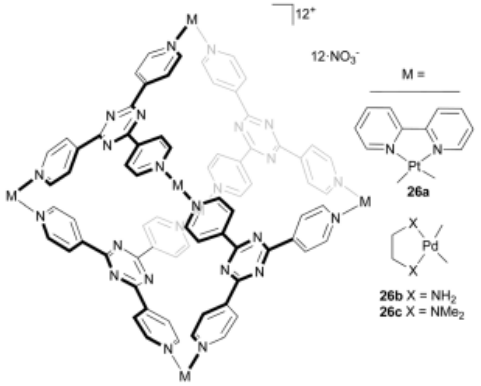


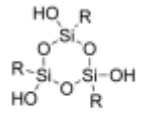

**28a** R = Ph
**28b** R = *m*-xylyl
**28c** R = Napth

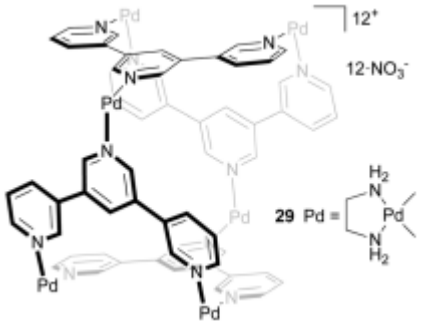


**27a** R = Ph
**27b** R = *m*-xylyl
**27c** R = Napth

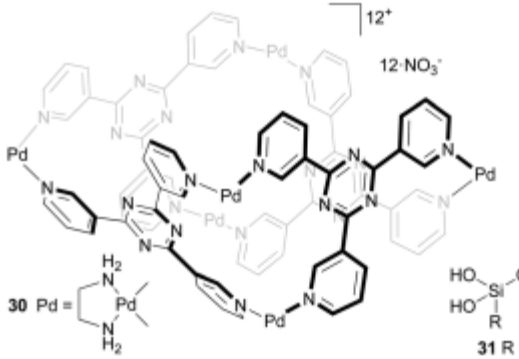


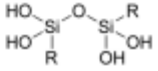

**31** R = Napth

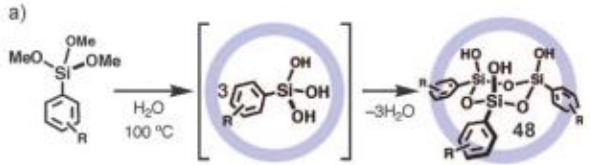


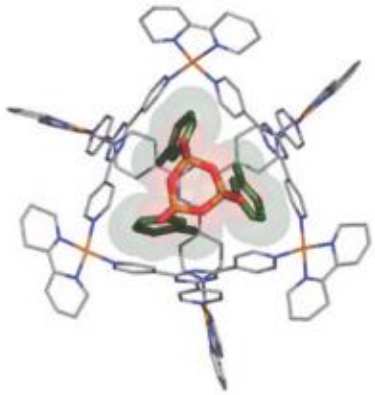


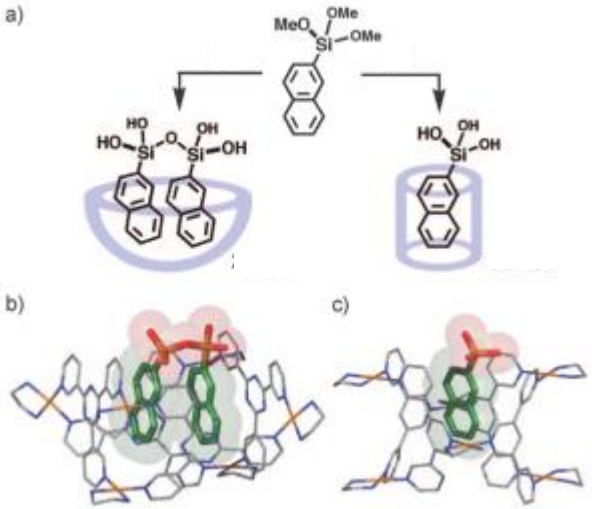

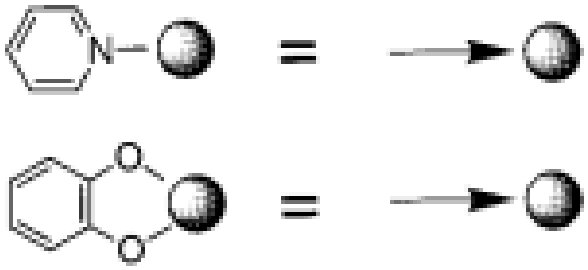
N
O
O

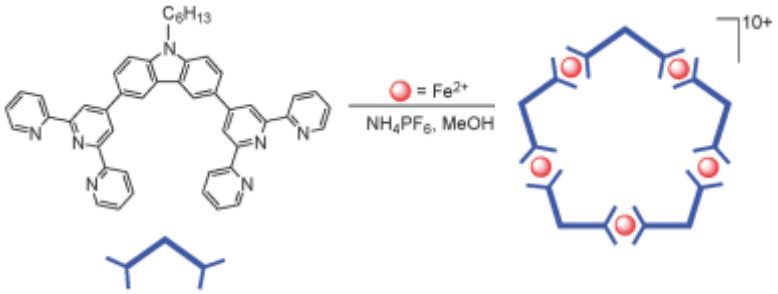
C6H13
N
N
N
N
N
N
= Fe2+
NH4PF6, MeOH
10+

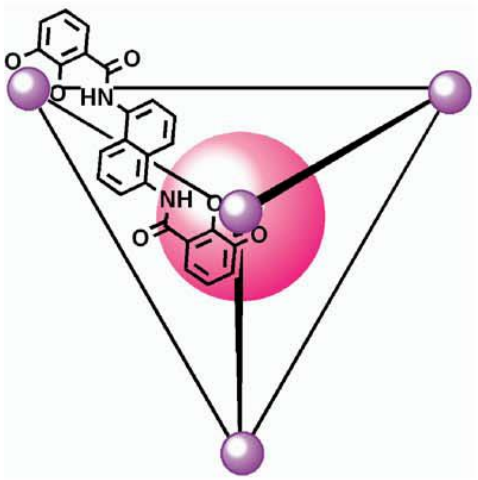

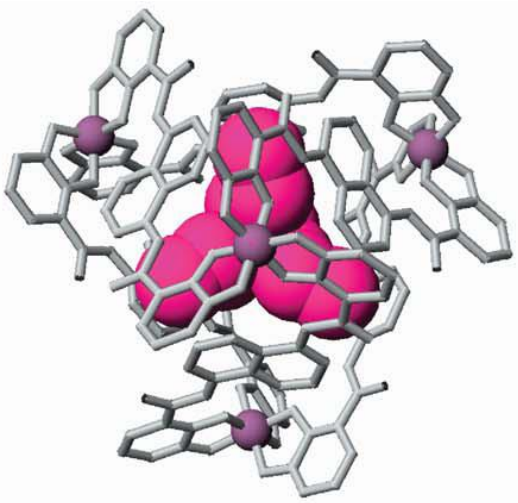

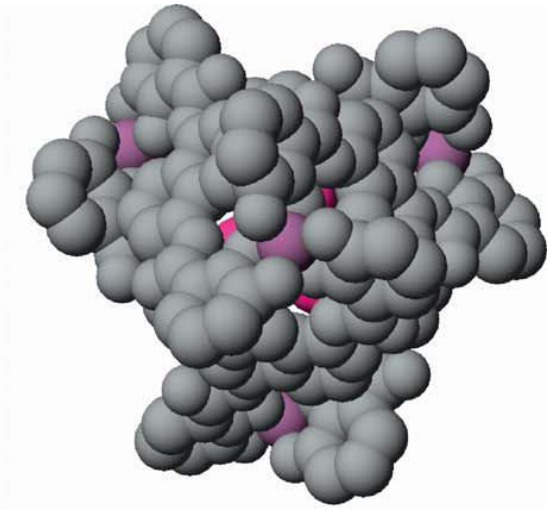

$M_4L_6$, ($Ga^{3+}$, $Fe^{3+}$; biscatecol-amidi) $12^-$, $\Delta\Delta\Delta\Delta$, $\Lambda\Lambda\Lambda\Lambda$, 300-350 Å
Stabilizzazione di cationi organici

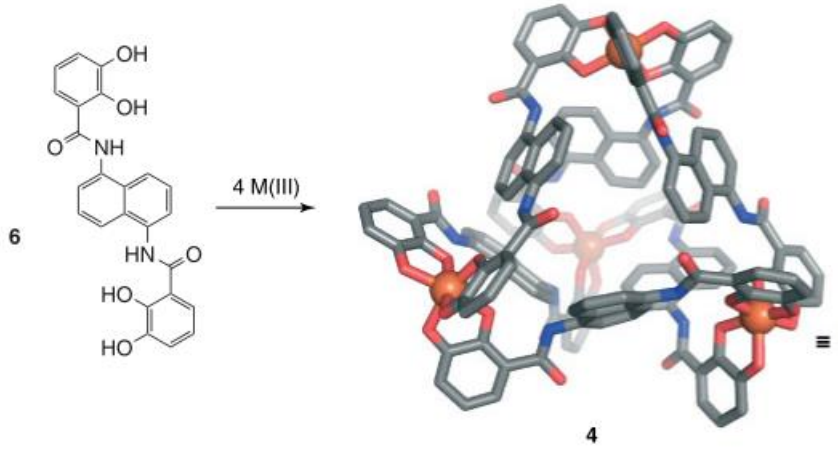


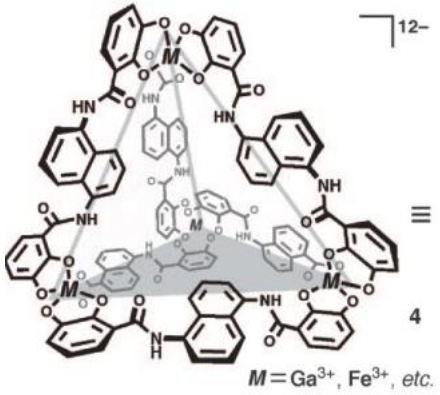

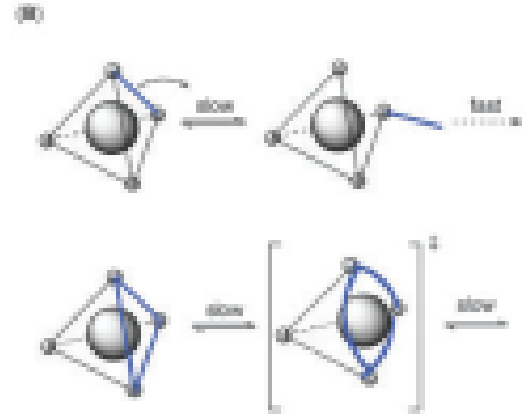
(B)
slow
fast
slow
slow

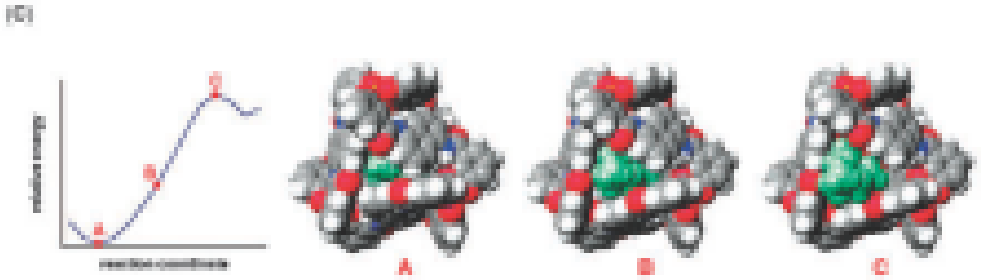
(C)
relative energy
reaction coordinate
A
B
C

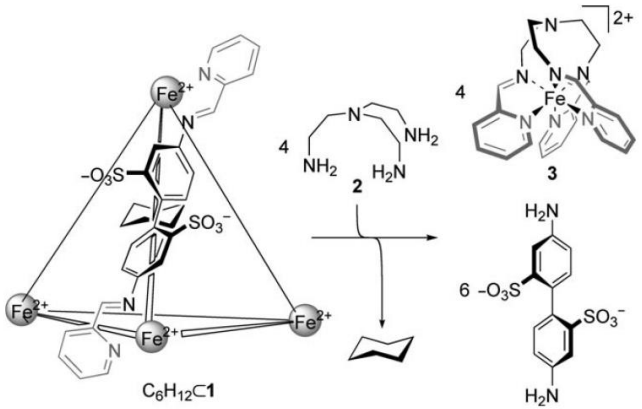


***Scheme 3.*** Liberation of the cyclohexane guest within **1** by the addition of chelating amine **2**.

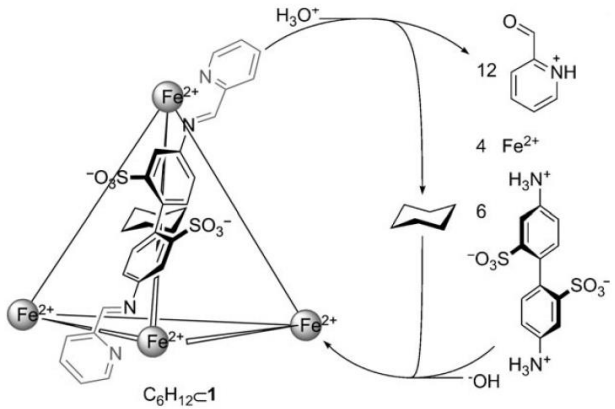


***Scheme 4.*** "Unlocking" of cage **1** through the addition of acid and subsequent base-driven "relocking" of cyclohexane within **1**.

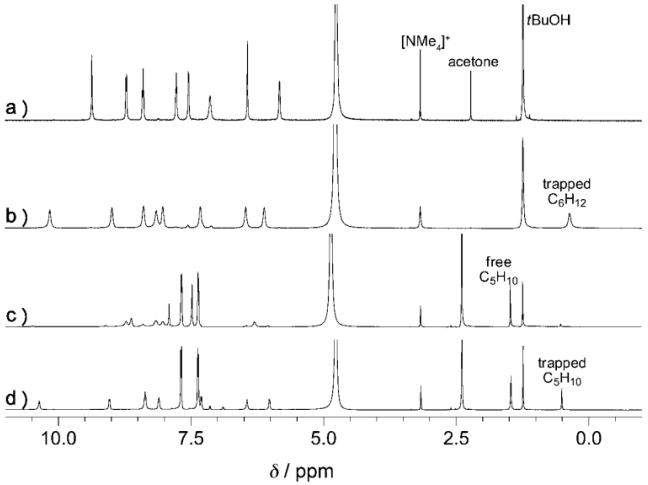


***Figure 2.*** $^1$H NMR spectra of a) cage **1**, b) $C_6H_{12}\subset$**1**, c) $C_6H_{12}\subset$**1** after reaction with tosylic acid (10 equiv) and in presence of excess cyclopentane, d) generation of complex $C_5H_{10}\subset$**1** after the addition of sodium bicarbonate (15 equiv).

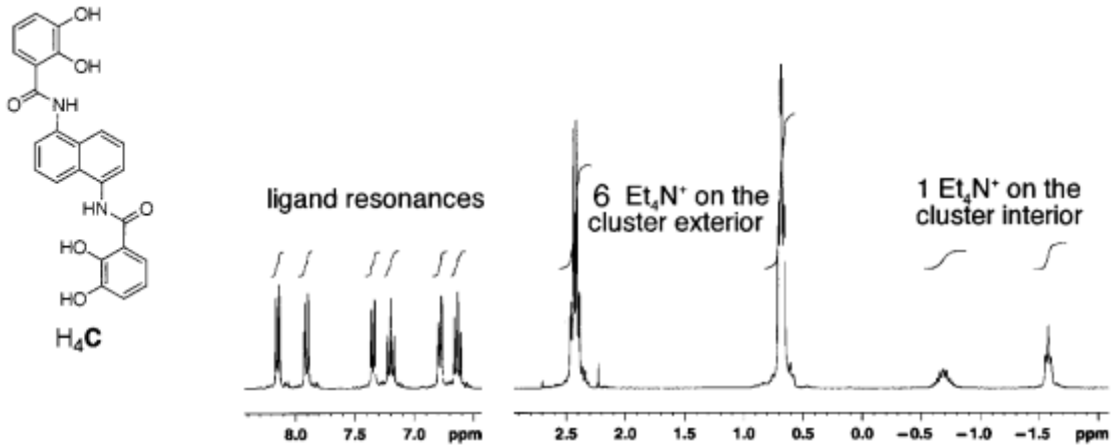


**Figure 14.** $^1$H NMR ($D_2O$) of $K_5(Et_4N)_7[Ga_4C_6]$ depicting the two sets of $Et_4N^+$ resonances characteristic of the exterior and encapsulated cations.

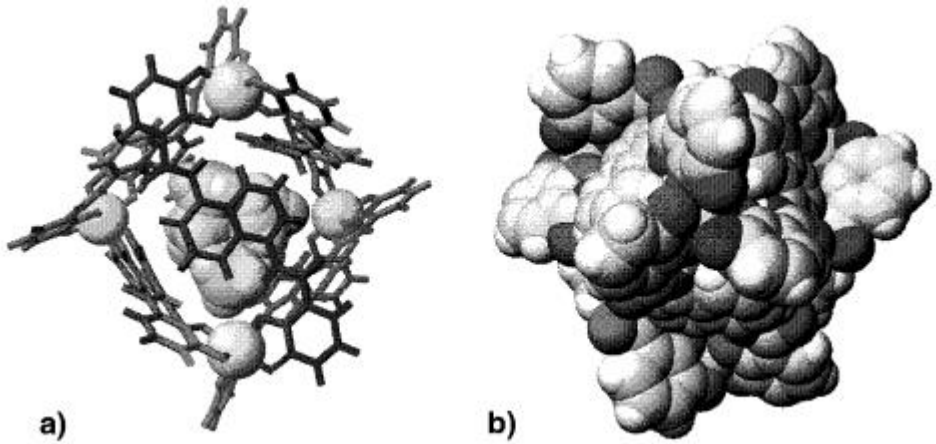


**Figure 15.** Based on the X-ray structure coordinates, $Et_4N^+\subset[Fe_4C_6]^{12-}$ in both (a) wire-frame and (b) space-filling representations.

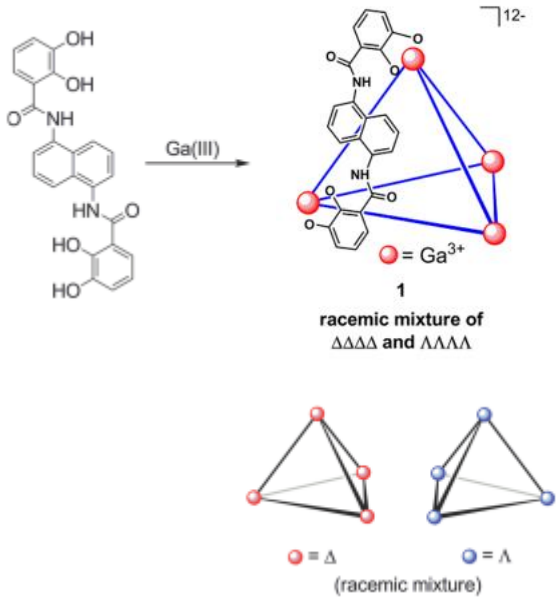
Ga(III)
12-
= Ga3+
1
racemic mixture of
ΔΔΔΔ and ΛΛΛΛ
= Δ
= Λ
(racemic mixture)

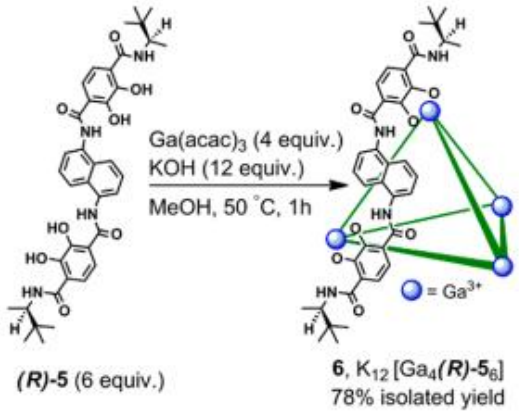
Ga(acac)3 (4 equiv.)
KOH (12 equiv.)
MeOH, 50 °C, 1h
= Ga3+
(R)-5 (6 equiv.)
6, K12 [Ga4(R)-56]
78% isolated yield

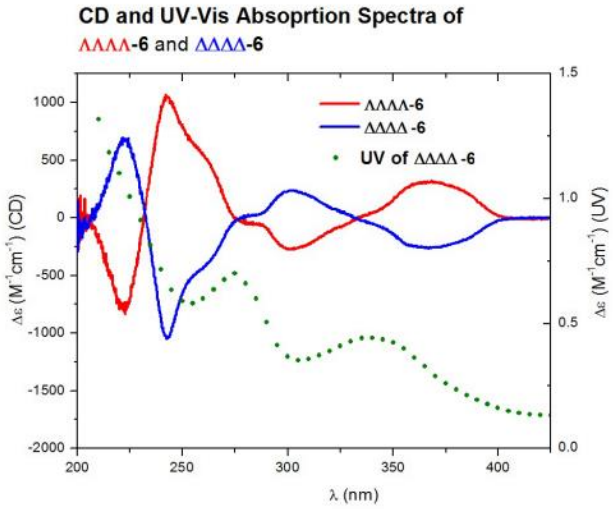
CD and UV-Vis Absoprtion Spectra of
ΛΛΛΛ-6 and ΔΔΔΔ-6
ΛΛΛΛ-6
ΔΔΔΔ -6
UV of ΔΔΔΔ -6
Δε (M-1cm-1) (CD)
Δε (M-1cm-1) (UV)
λ (nm)

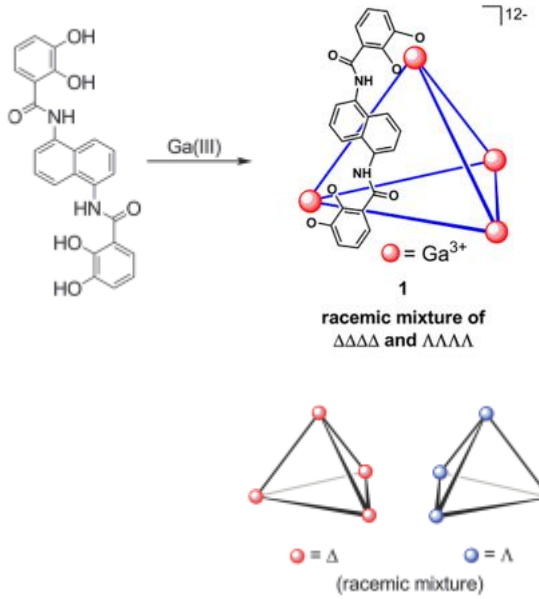
OH
OH
NH
HN
O
HO
HO
Ga(III)
12-
NH
O
= Ga3+
1
racemic mixture of
ΔΔΔΔ and ΛΛΛΛ
= Δ
= Λ
(racemic mixture)

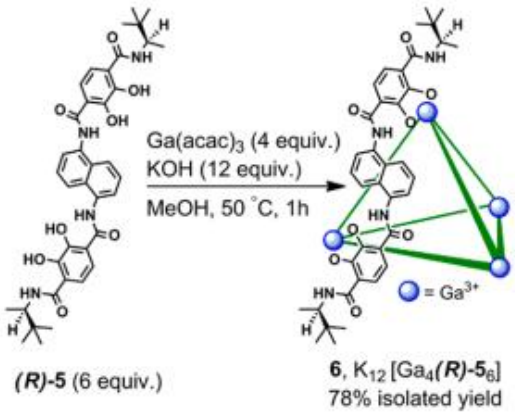
Ga(acac)3 (4 equiv.)
KOH (12 equiv.)
MeOH, 50 °C, 1h
= Ga3+
(R)-5 (6 equiv.)
6, K12 [Ga4(R)-56]
78% isolated yield

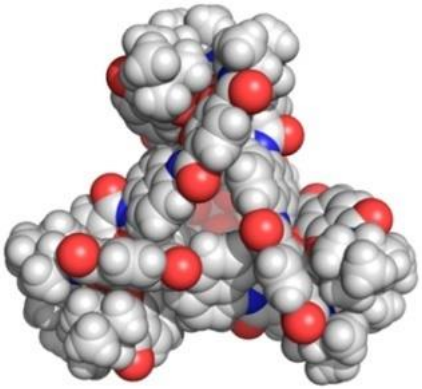

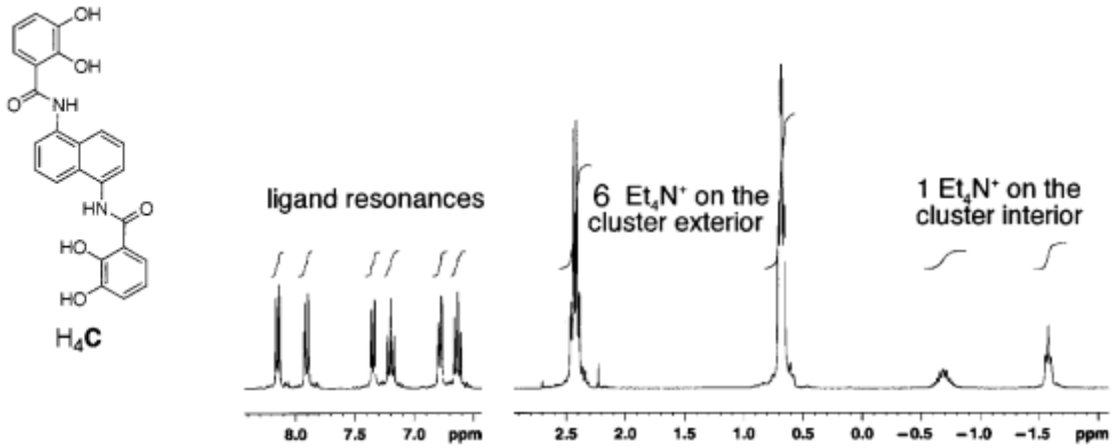


**Figure 14.** $^1$H NMR ($D_2O$) of $K_5(Et_4N)_7[Ga_4C_6]$ depicting the two sets of $Et_4N^+$ resonances characteristic of the exterior and encapsulated cations.

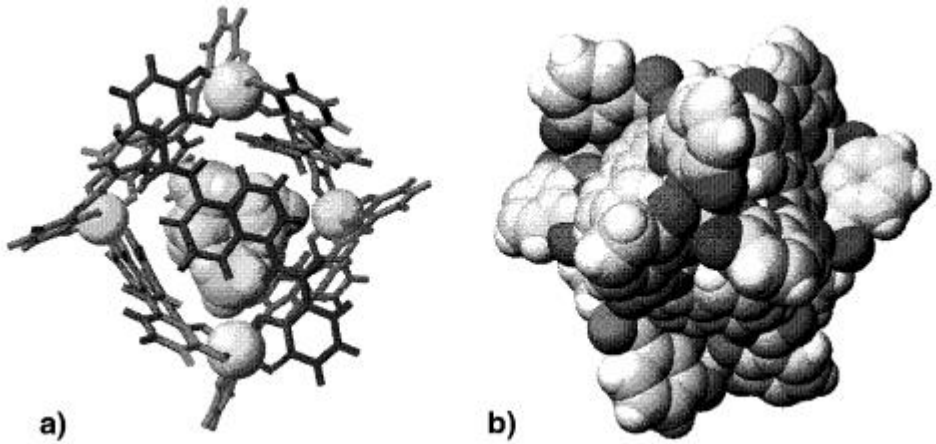


**Figure 15.** Based on the X-ray structure coordinates, $Et_4N^+\subset[Fe_4C_6]^{12-}$ in both (a) wire-frame and (b) space-filling representations.

Host–Guest Systems

DOI: 10.1002/anie.200803066

*Angew. Chem. Int. Ed.* **2008**, *47*, 8297–8301

# An Unlockable–Relockable Iron Cage by Subcomponent Self-Assembly**

*Prasenjit Mal, David Schultz, Kodiah Beyeh, Kari Rissanen,* and Jonathan R. Nitschke**

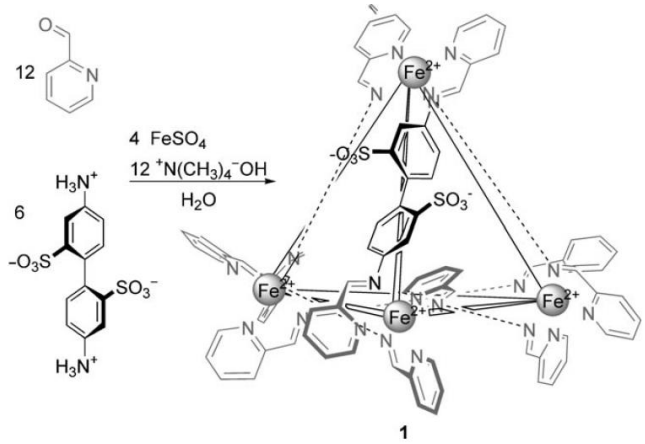


***Scheme 1.*** Preparation of tetrahedral cage **1** salt by aqueous subcomponent self-assembly;[14] the structure of only one edge is fully shown for clarity.

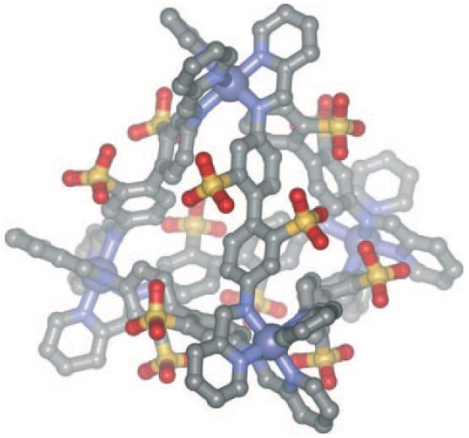

***Figure 1.*** View of the crystal structure of **1**; cations, hydrogen atoms, and solvent of crystallization are not shown for clarity. Fe violet-gray, N blue, S yellow, O red, C gray.

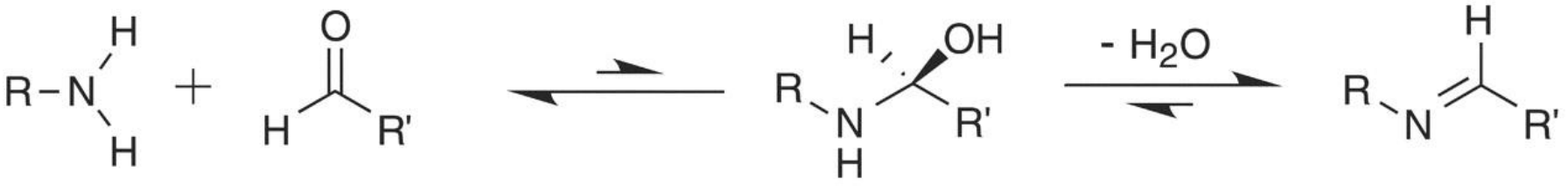
- $H_2O$
Hemiaminal
Imine


6
12
12 $Me_4NOH$
4 $FeSO_4.7H_2O$
$H_2O$
1

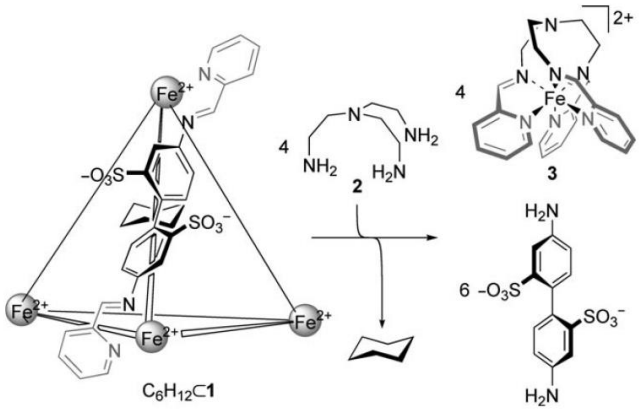


***Scheme 3.*** Liberation of the cyclohexane guest within **1** by the addition of chelating amine **2**.

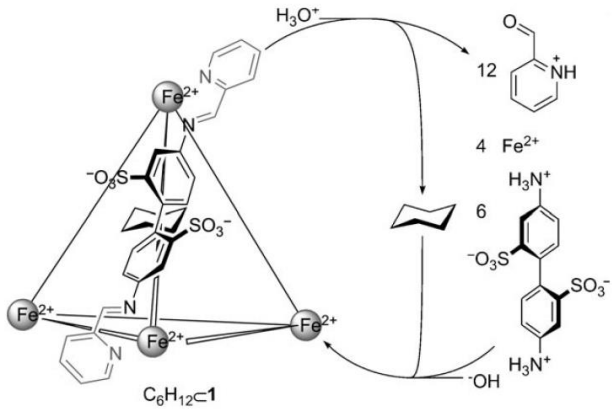


***Scheme 4.*** "Unlocking" of cage **1** through the addition of acid and subsequent base-driven "relocking" of cyclohexane within **1**.

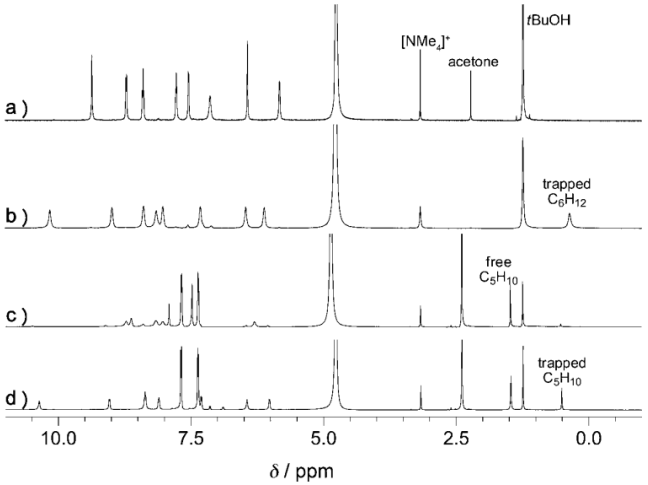


***Figure 2.*** $^1$H NMR spectra of a) cage **1**, b) $C_6H_{12}\subset$**1**, c) $C_6H_{12}\subset$**1** after reaction with tosylic acid (10 equiv) and in presence of excess cyclopentane, d) generation of complex $C_5H_{10}\subset$**1** after the addition of sodium bicarbonate (15 equiv).

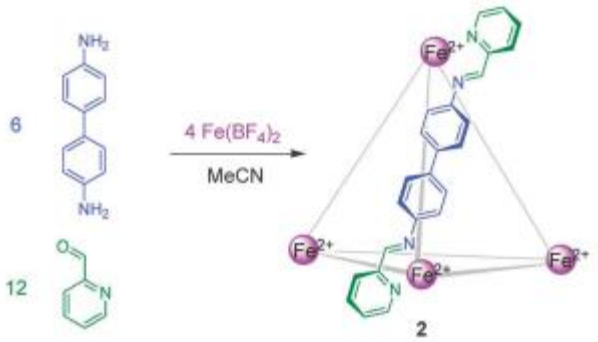
6
12
4 Fe(BF4)2
MeCN
2

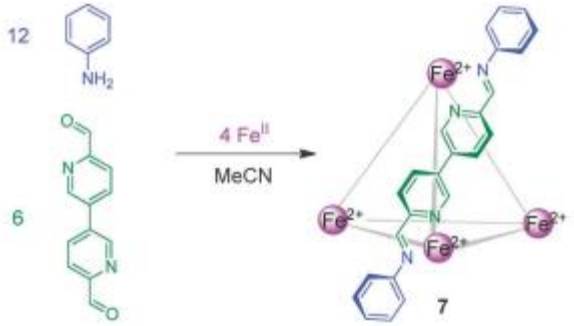
12
6
4 FeII
MeCN
7

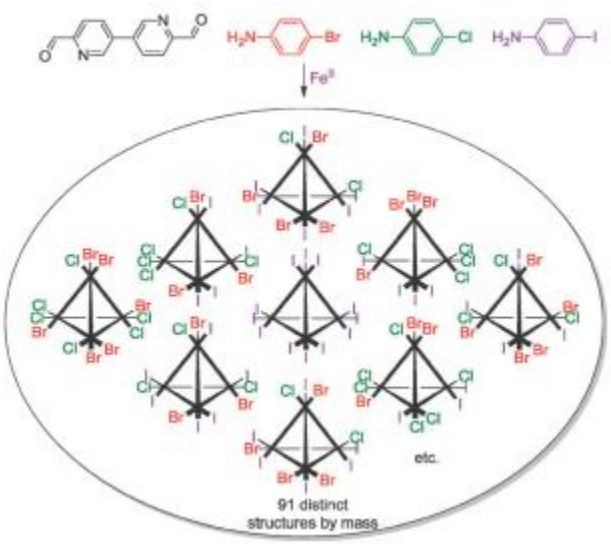
Fe3
etc.
91 distinct
structures by mass

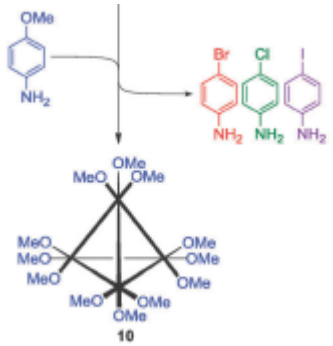
10

# Catalisi Supramolecolare

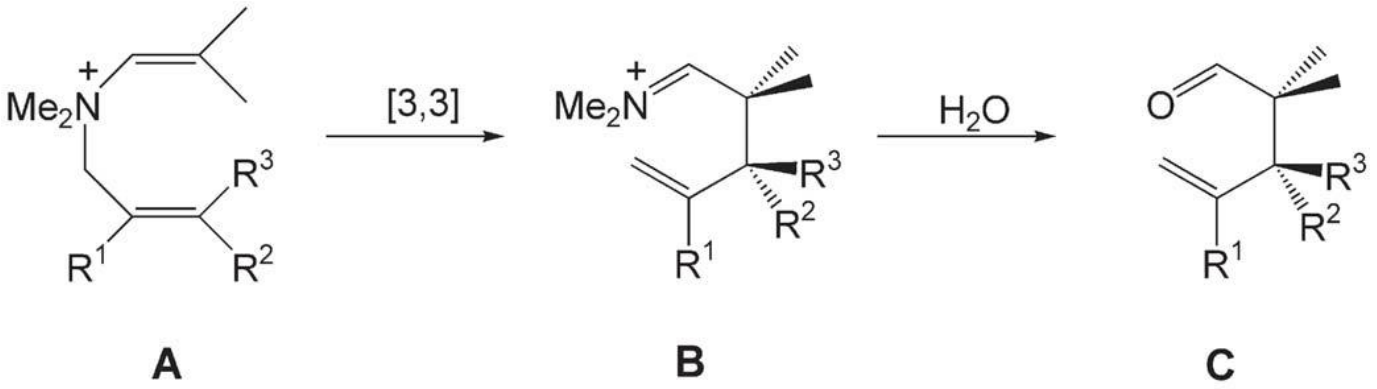


Riarrangiamento 3-aza-Cope ione enammonio

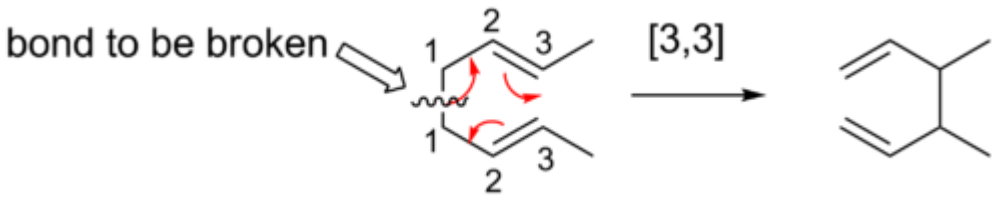

| Substrate | $R^1$ | $R^2$ | $R^3$ | Acceleration |
|---|---|---|---|---|
| **1** | H | H | H | 5 |
| **2** | Me | H | H | 26 |
| **3** | H | Et | H | 141 |
| **4** | H | H | Et | 90 |
| **5** | H | *n*Pr | H | 150 |
| **6** | H | H | *n*Pr | 44 |
| **7** | H | *i*Pr | H | 854 |

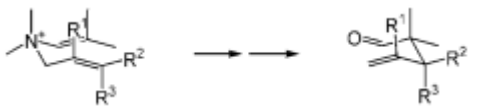

| Substrate | $R^1$ | $R^2$ | $R^3$ |
|---|---|---|---|
| **1** | H | H | H |
| **2** | Me | H | H |
| **3** | H | Et | H |
| **4** | H | H | Et |
| **5** | H | *n*Pr | H |
| **6** | H | H | *n*Pr |
| **7** | H | *i*Pr | H |

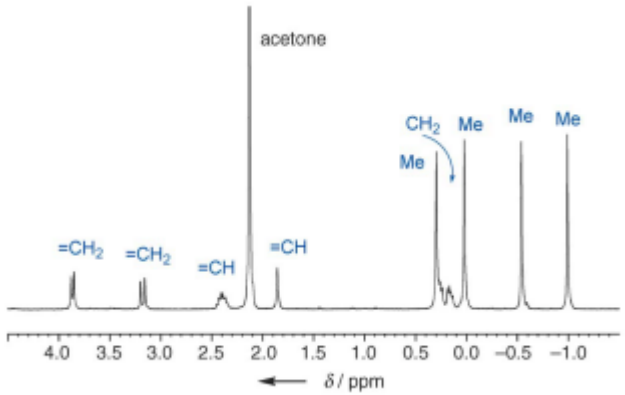


: $^1$H NMR spectrum of $[\mathbf{1}\subset Ga_4L_6]^{11-}$ (**1**: $R^1$, $R^2$, $R^3$ = H). The observed upfield shift of guest resonance signals illustrates the close contact between host and guest.

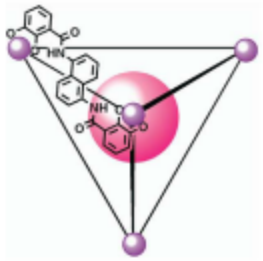

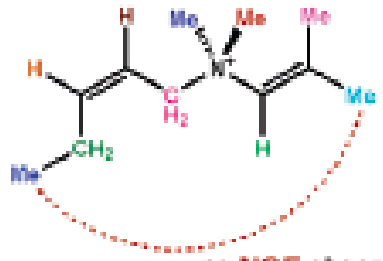


no **NOE** observed

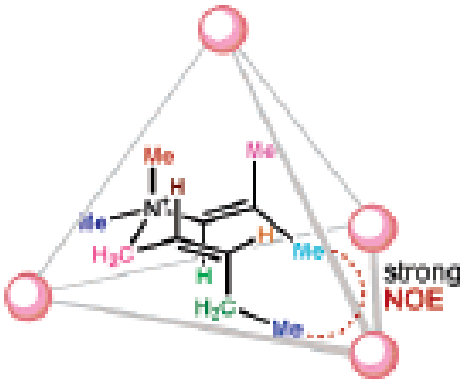


strong **NOE**

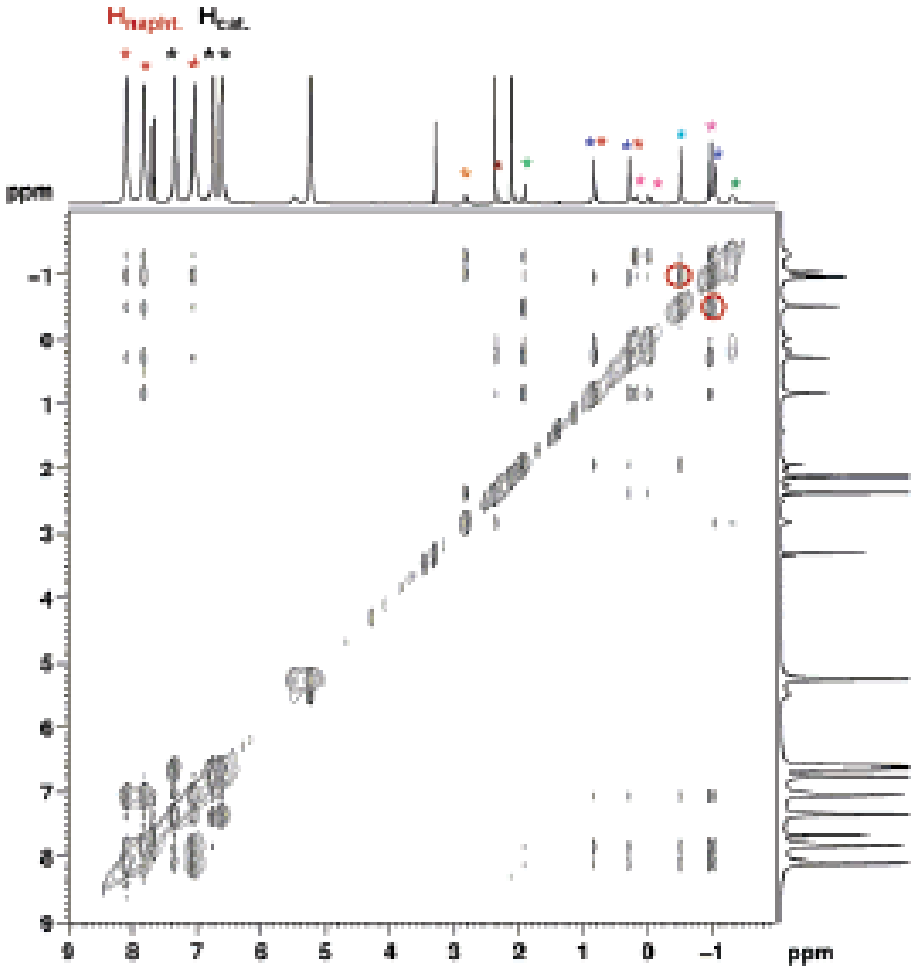

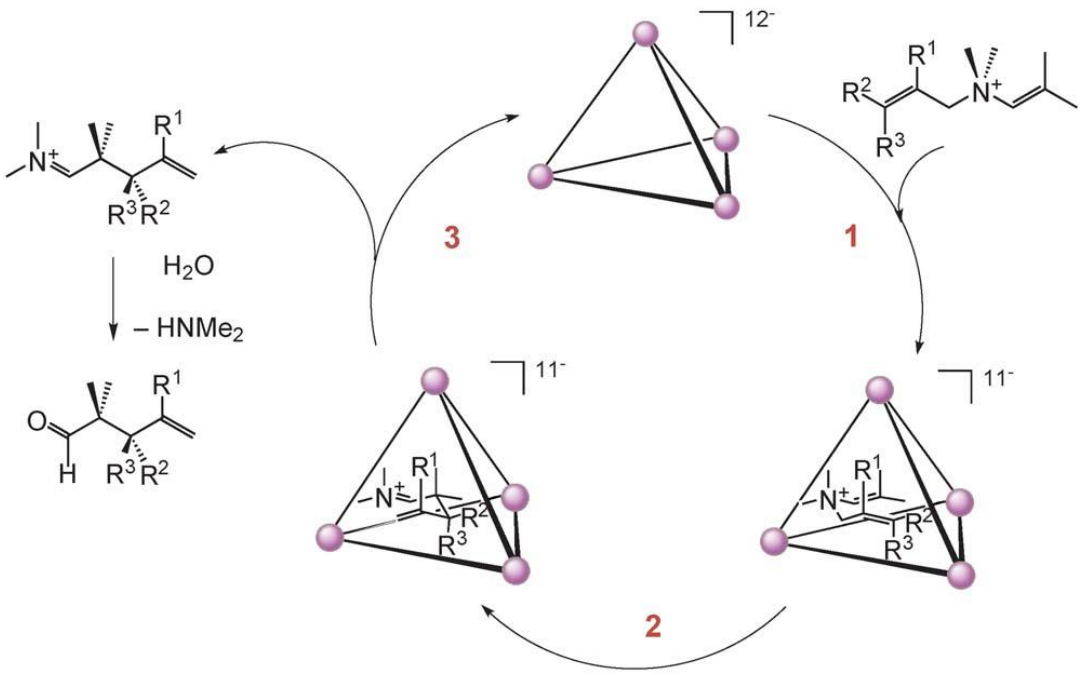
12-
11-
11-
1
2
3
H2O
– HNMe2

# Diels-Alder in Aqueous Molecular Hosts: Unusual Regioselectivity and Efficient Catalysis

Michito Yoshizawa, Masazumi Tamura, Makoto Fujita*

SCIENCE VOL 312 14 APRIL 2006



## ERRATUM

*Post date 9 June 2006*

**Reports:** "Diels-Alder in aqueous molecular hosts: unusual regioselectivity and efficient catalysis" by M. Yoshizawa *et al.* (14 Apr. 2006, p. 251). Due to a nomenclature error, all references to "phthalimides" in the text and Supporting Online Material should instead refer to "maleimides." The chemical structures in the schemes and figures are all correct as drawn.

**Fig. 1.** Self-assembled coordination cages (**1** and **2**), which are prepared by simple mixing of an exo-tridentate organic ligand and an end-capped Pd(II) ion in a 4:6 ratio in water.

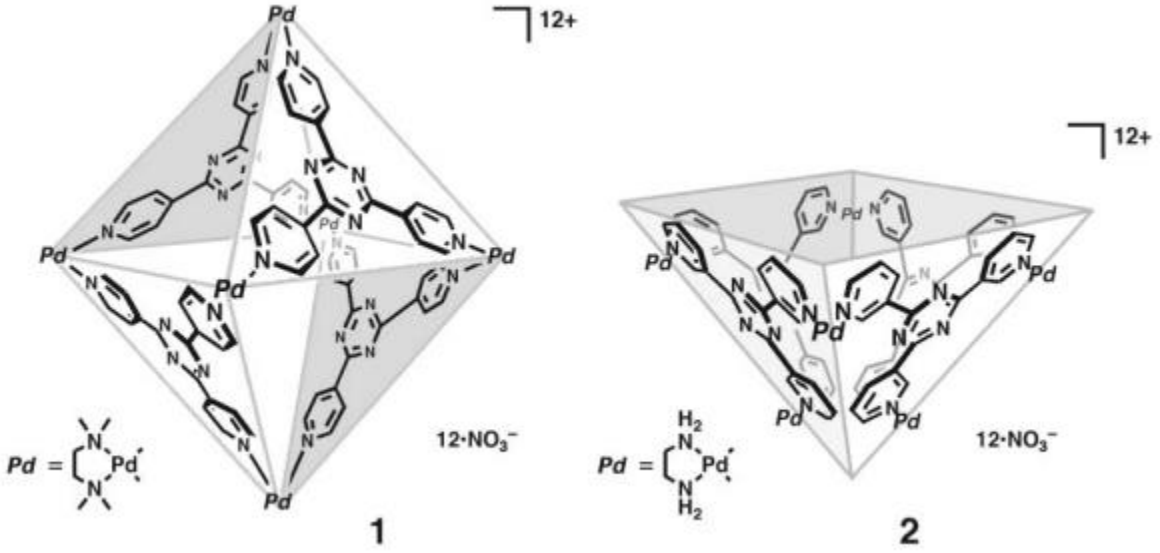

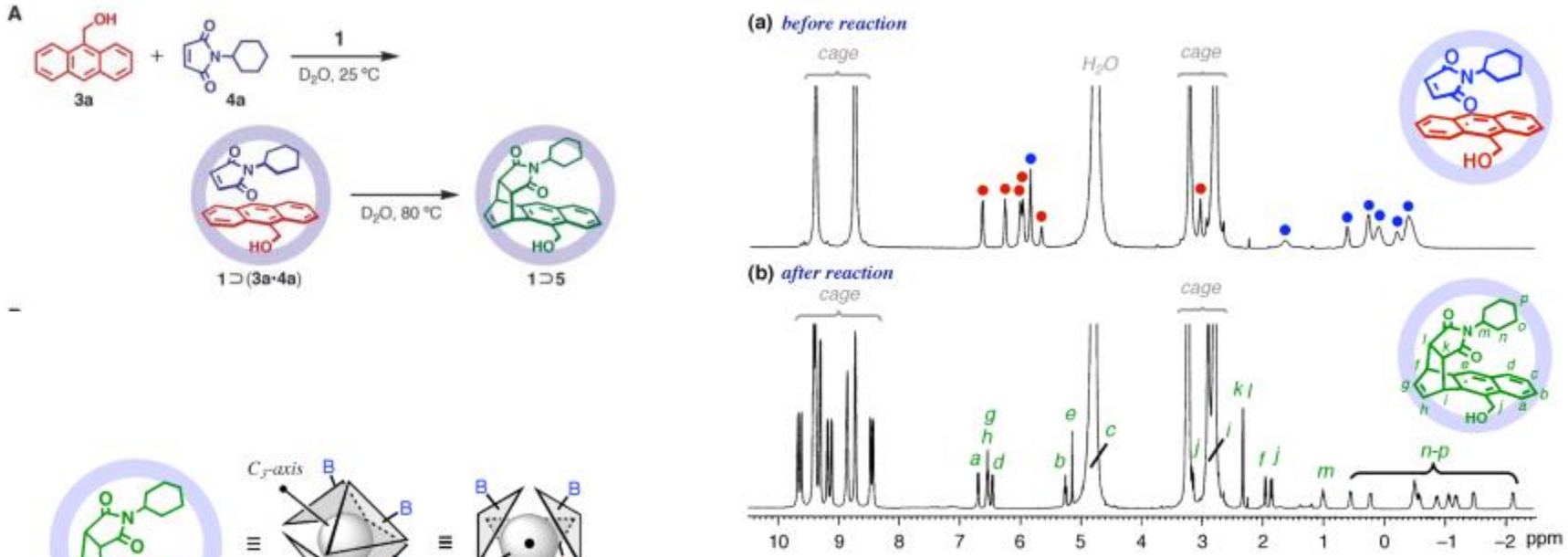


**Fig. S1.** $^1$H-NMR spectra (500 MHz, $D_2O$, r.t.) of (**a**) **1**⊃(**3a•4a**) and (**b**) **1**⊃**5**.

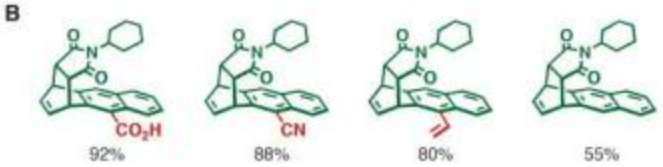

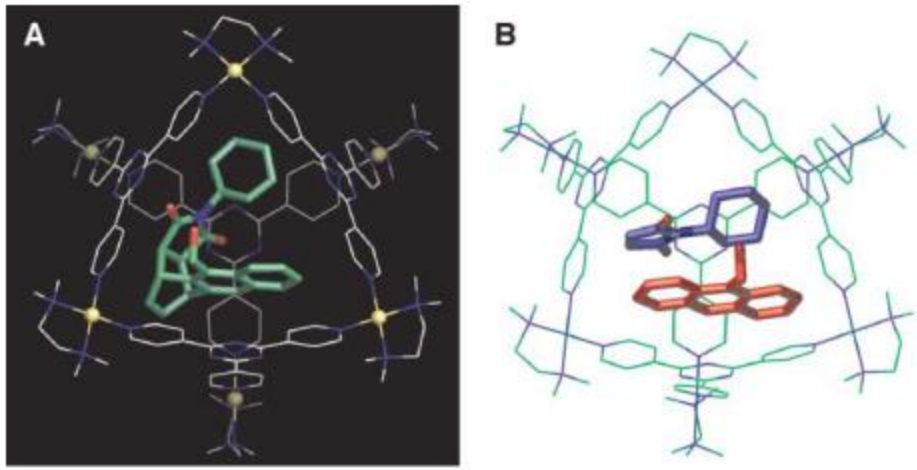


**Fig. 3.** (**A**) Crystal structure of **1** ⊃ **5** and (**B**) optimized structure of **1** ⊃ (**3a**•**4a**) by a force-field calculation.

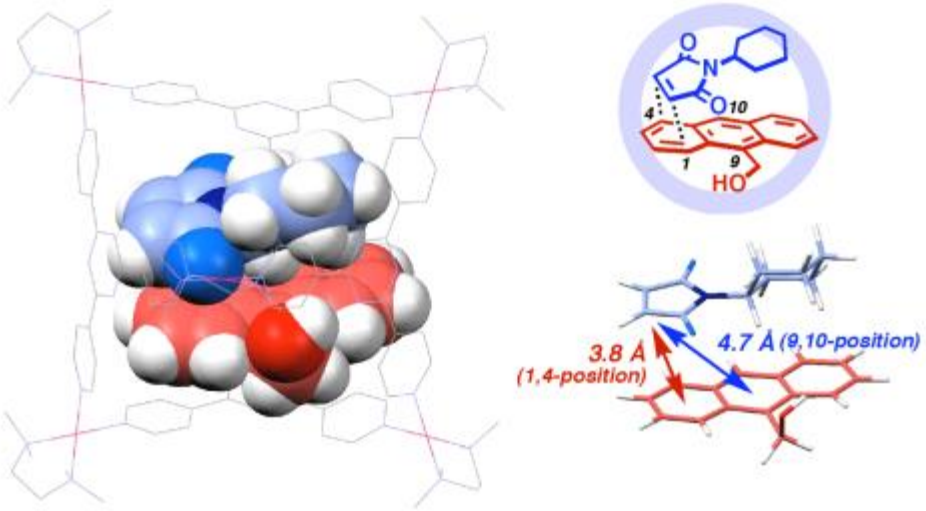


**Fig. S17.** Optimized structure of **1**⊃(**3a**•**4a**) by a force-field calculation and the distance between the C=C bond of **4a** and the 1,4-position or 9,10-position of **3a**.

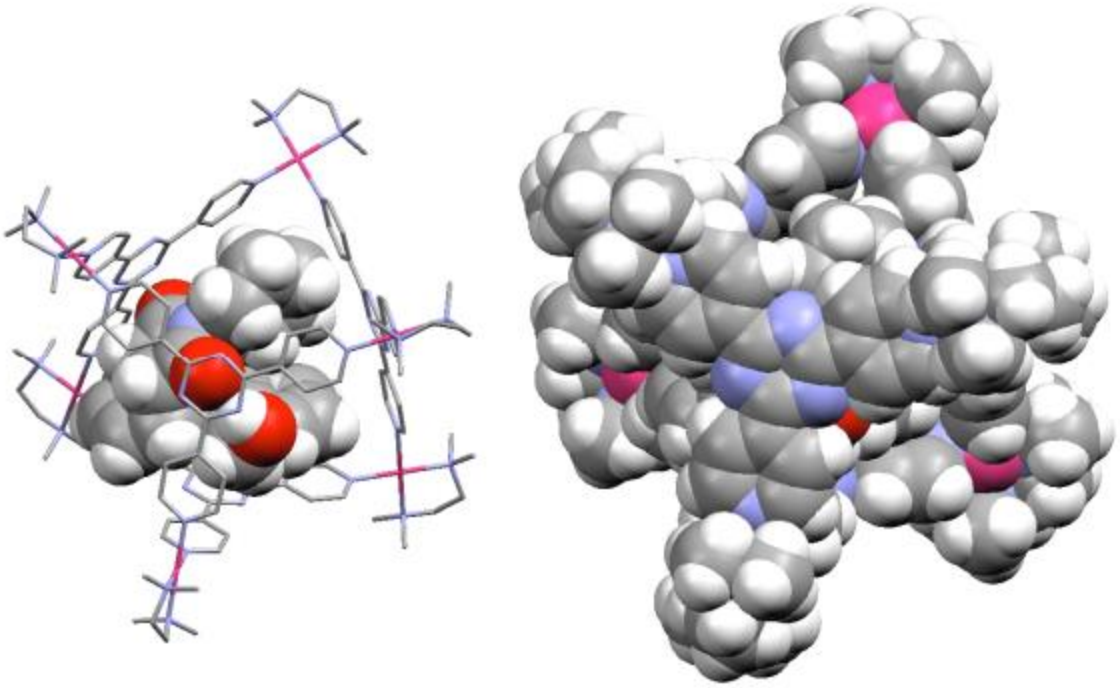

**Fig. S16.** Cylinder and/or Space-filling drawing of **1**⊃**5**.

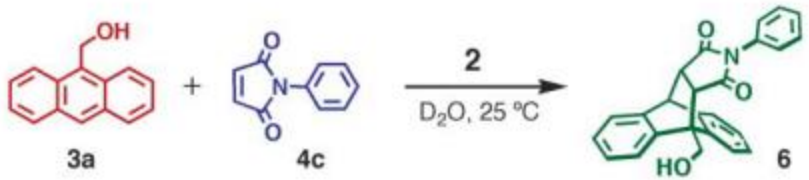


**Fig. 4.** Catalytic Diels-Alder reaction of 9-hydroxymethylanthracene (**3a**) and *N*-phenylphthalimide (**4c**) in the aqueous solution of bowl **2**, leading to 9,10-adduct **6**.

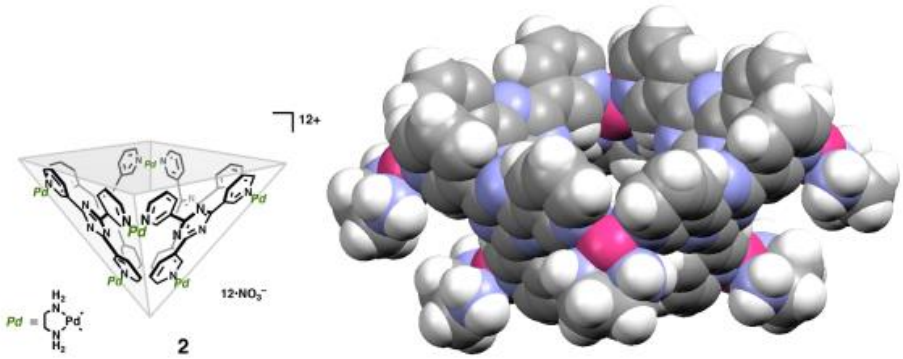


**Fig. S18.** Chemical structure of **2** and the Space-filling drawing.

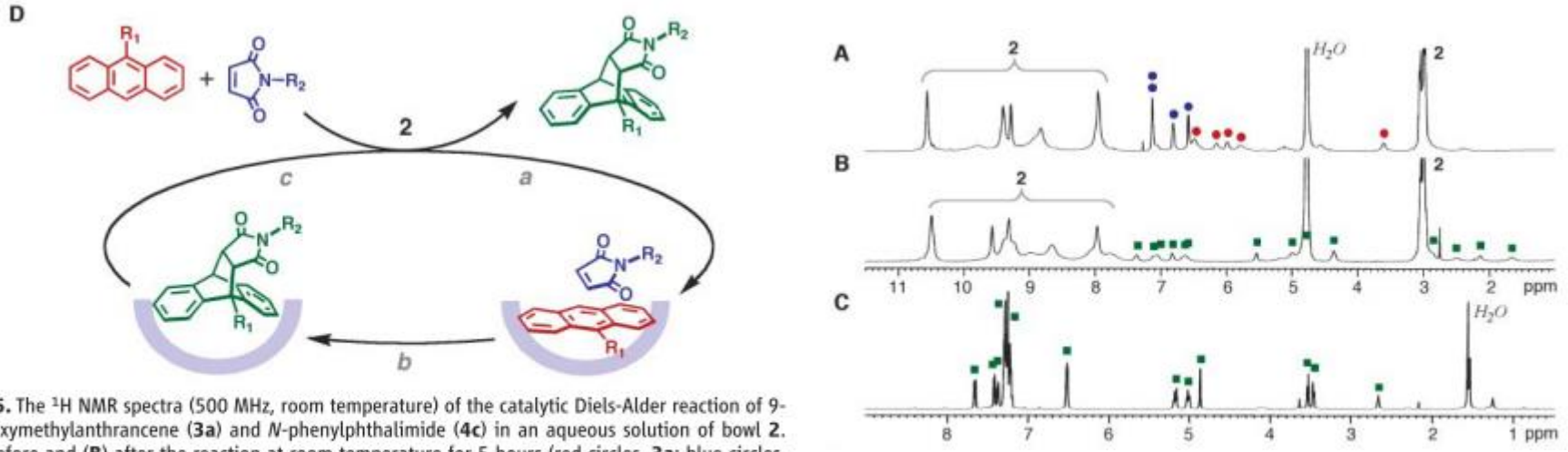


**Fig. 5.** The $^1$H NMR spectra (500 MHz, room temperature) of the catalytic Diels-Alder reaction of 9-hydroxymethylanthrancene (**3a**) and *N*-phenylphthalimide (**4c**) in an aqueous solution of bowl **2**. (**A**) Before and (**B**) after the reaction at room temperature for 5 hours (red circles, **3a**; blue circles, **4c**; and green squares, **6**). (**C**) Diels-Alder product **6** after extraction with $CDCl_3$. (**D**) Schematic representation of the catalytic Diels-Alder reaction of anthracenes and phthalimide in the presence of bowl **2**. Autoinclusion of substrates into **2** (step a) and autoexclusion of the product from **2** (step c) underlie the efficient catalytic Diels-Alder reaction.

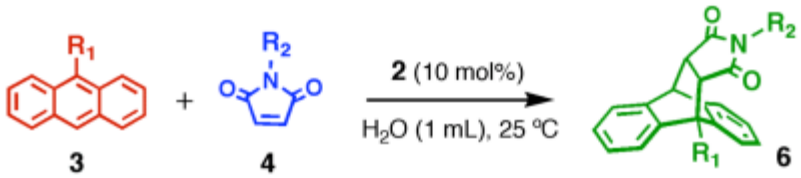


3 + 4 → 6

| Entry | Substrate | | Time | Yield(%) of **6** | | |
|---|---|---|---|---|---|---|
| | **3** ($R_1$) | **4** ($R_2$) | | with **2** | without **2** | in $CHCl_3$[†] |
| 1 | -$CH_2OH$ | propyl | 5 h | >99 | 8 | 0 |
| 2 | -$CH_2OH$ | cyclohexyl | 15 h | 98 | 0 | 6 |
| 3 | -$CH_2OH$ | phenyl | 5 h | >99[*,†] | 3 | 9 |
| 4 | -$CH_2OH$ | phenyl | 15 h | 6 | 7 | 21 |
| 5 | -$CH_2OH$ | benzyl | 5 h | >99 | trace | 0 |
| 6 | -$CH_2OH$ | xylyl | 15 h | 94 | 0 | 17 |
| 7 | -$CH_3$ | cyclohexyl | 7 h | >99 | 0 | 5 |
| 8 | -$CH_3$ | phenyl | 3 h | >99 | 5 | 17 |
| 9 | -$CH{=}CH_2$ | phenyl | 1 d | 88 | 0 | trace |
| 10 | -$CH{=}CH_2$ | benzyl | 1 d | 97 | 5 | 4 |
| 11 | -$CO_2H$ | benzyl | 1 d | 12 | 0 | 0 |
| 12 | -$CH_2OH$ | phenyl | 1 d | >99[‡] | — | — |

[*] (en)$Pd(NO_3)_2$: 10 mol% [†] without **2** [‡] **2** : 1 mol%, hexane (1 mL)

# White Phosphorus Is Air-Stable Within a Self-Assembled Tetrahedral Capsule

Prasenjit Mal,[1] Boris Breiner,[1] Kari Rissanen,[2] Jonathan R. Nitschke[1]*

SCIENCE VOL 324 26 JUNE 2009



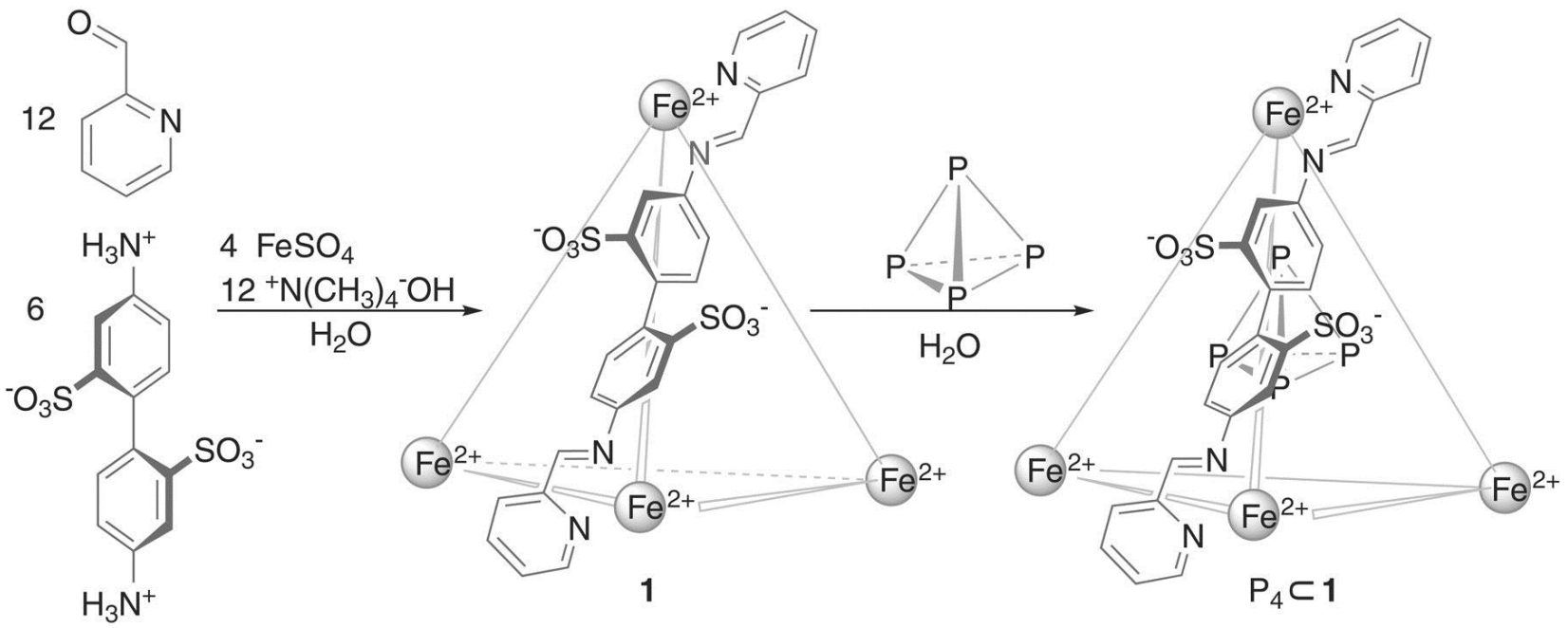


**Fig. 1 Synthesis of tetrahedral cage 1 and subsequent incorporation of P4.**

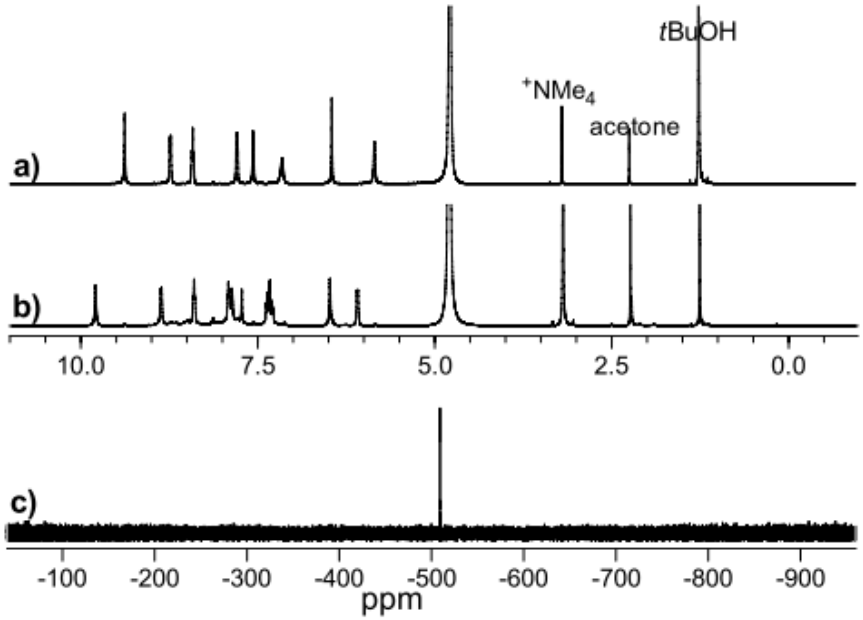


**Figure S1.** $^{1}$H NMR spectra in $D_2O$ of cage **1** (top), of $P_4\subset$**1** (middle), and $^{31}$P NMR spectrum of $P_4\subset$**1** (bottom).

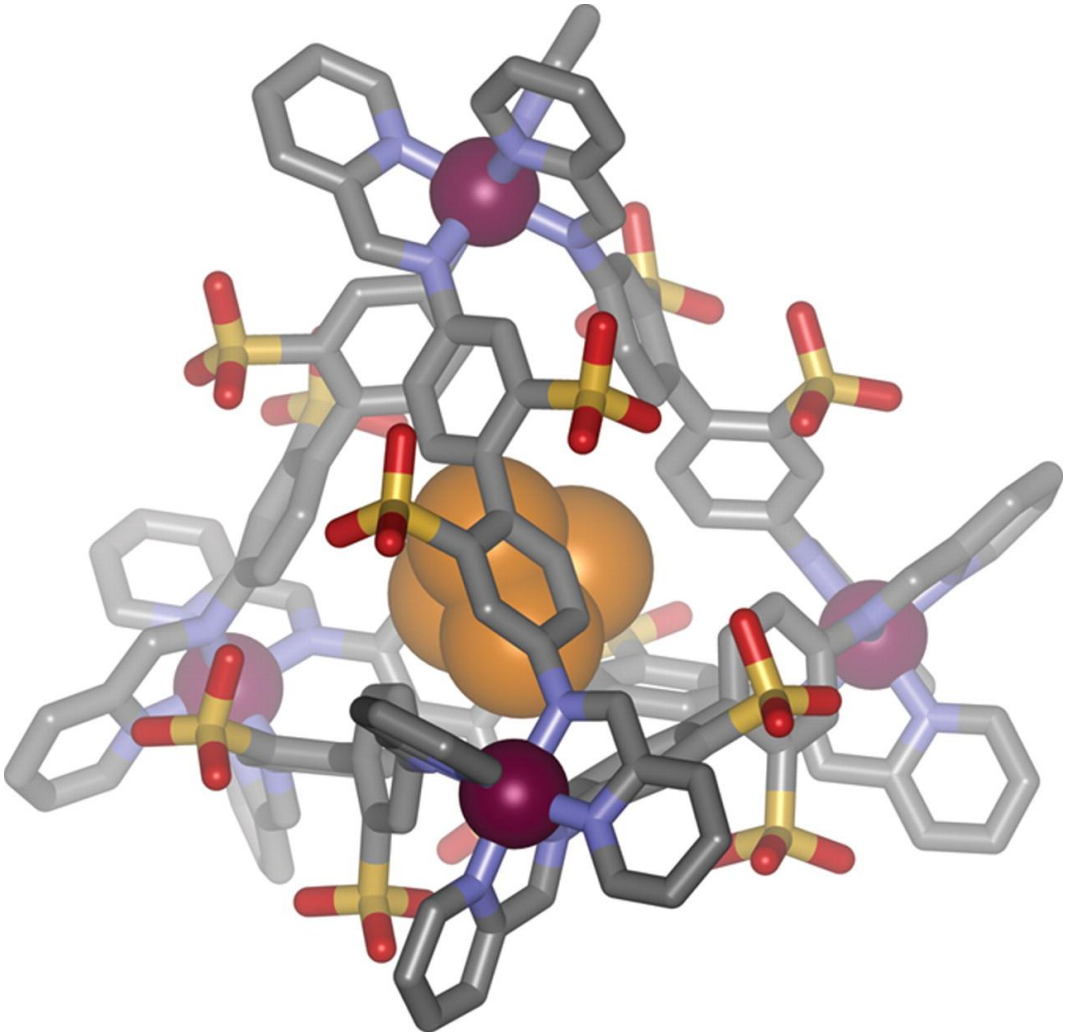

**Fig. 2 Crystal structure of P4⊂1.**

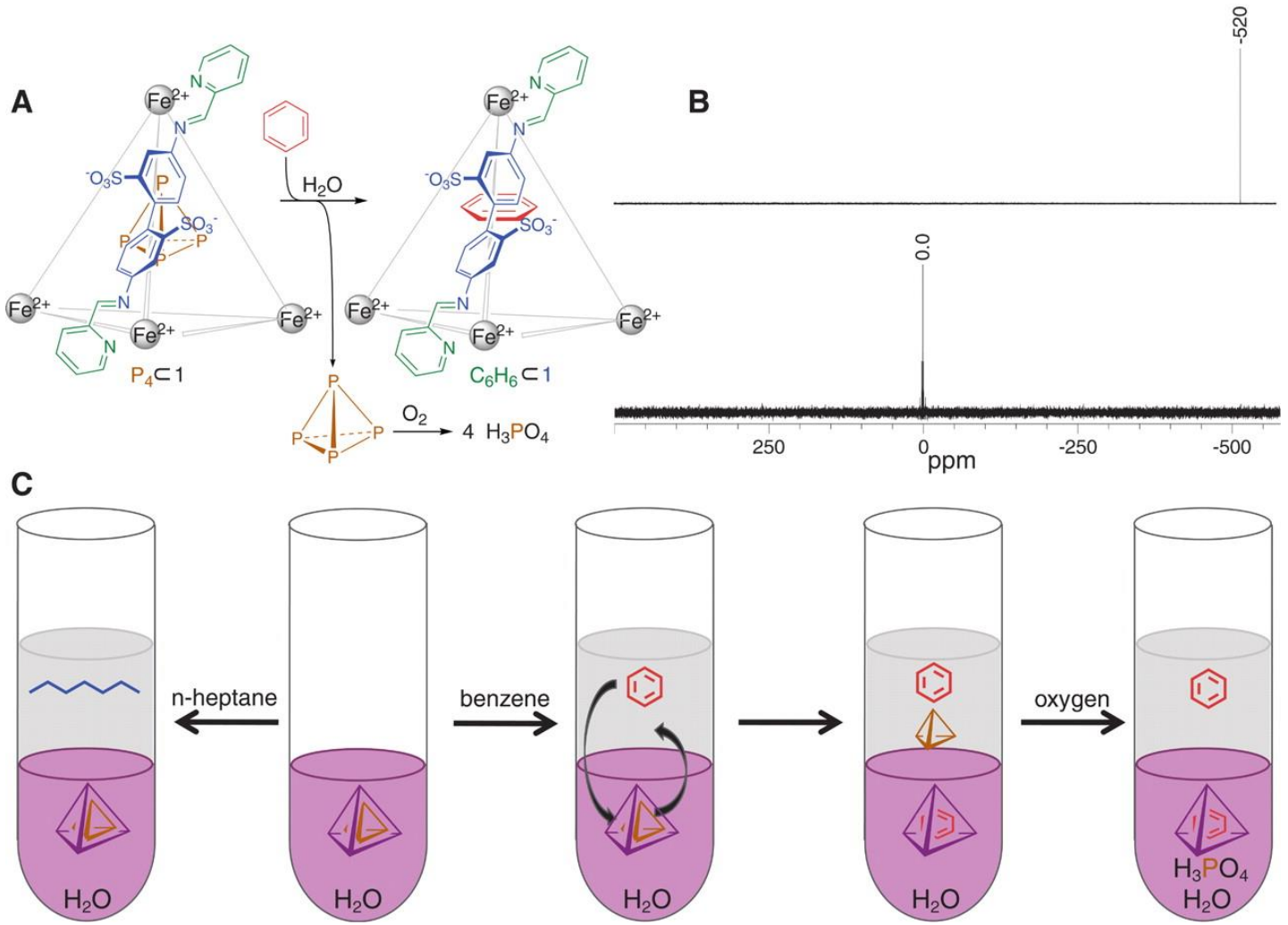


**Fig. 3 Extraction of P4 from 1 by n-heptane is not possible, whereas replacing P4 with another suitable guest (benzene or cyclohexane) results in the facile removal of P4 into the organic solvent.**

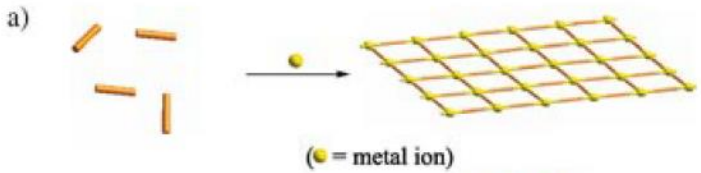


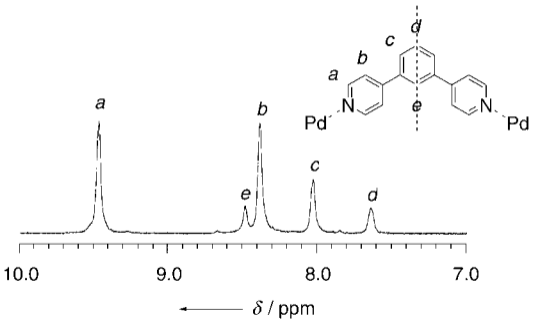


When ligand **1a** (0.02 mmol) was treated with $Pd(NO_3)_2$ (0.01 mmol) in $[D_6]$DMSO (1.0 mL) at 70 °C for 4 h, the quantitative self-assembly of a single product was detected by $^1$H NMR spectroscopy.[6] Only five signals are observed indicating that all the ligands are located equivalently in the product and have same inherent symmetry (Figure 2). The

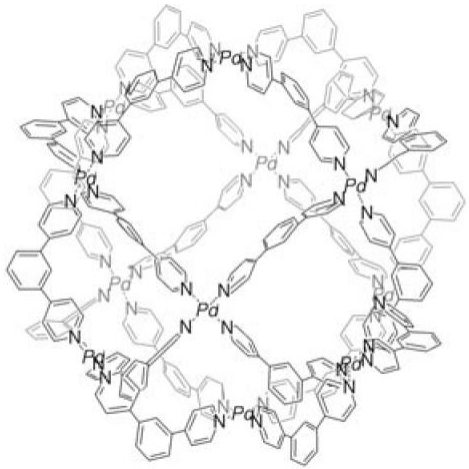

$[M_{12}L_{24}]^{12+}$

complexation. Diffusion-ordered NMR spectroscopy (DOSY) showed a single band at the diffusion coefficiency of $1.1 \times 10^{-10}$ m$^2$s$^{-1}$, from which the diameter of the product was roughly estimated to be 3.6 nm.[7] After anion exchange from $[NO_3]^-$ to $[PF_6]^-$ ions, cold-spray ionization mass spectrometry (CSI-MS)[8] clearly indicated an $M_{12}L_{24}$ composition with the molecular weight of 10330 Da by a series of $[M-(PF_6^-)_n]^{n+}$ ($n$ = 6–13) peaks (Figure 3).[9] Fragmentation in the MS measurement was hardly observed except the dissociation of counteranions, which demonstrates the remarkable stability of the product in solution. Elemental analysis was also consistent with the $M_{12}L_{24}$ composition.

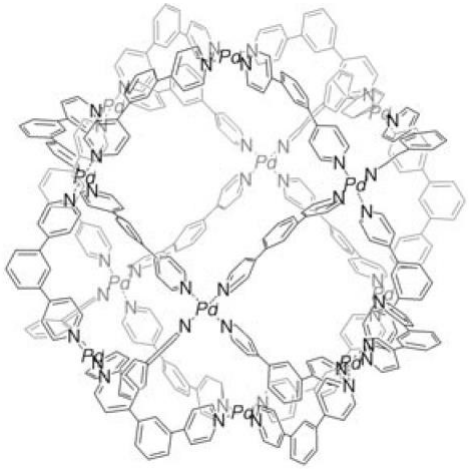

$[M_{12}L_{24}]^{12+}$

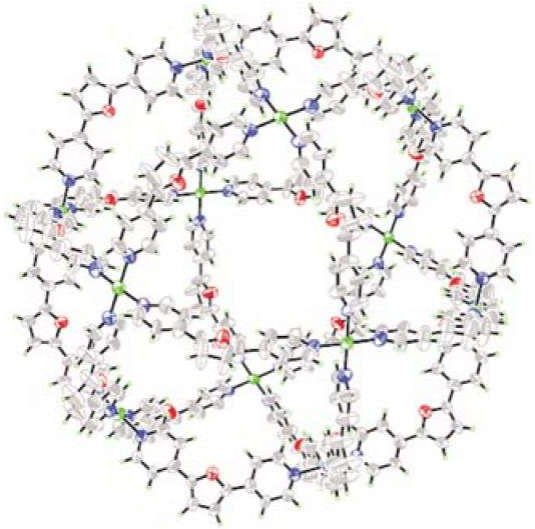

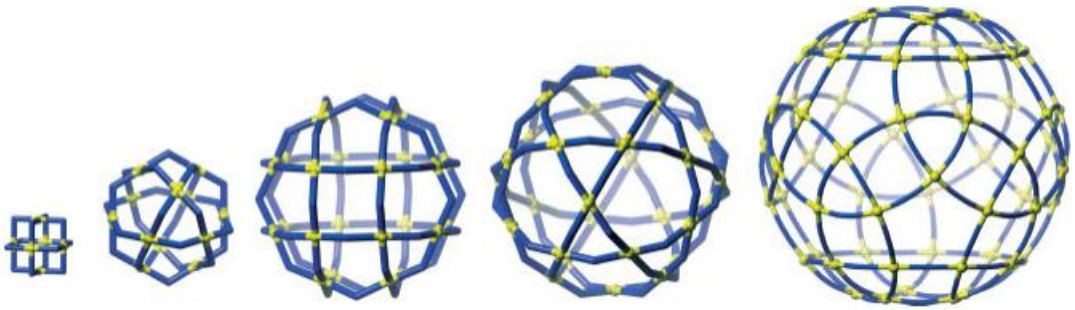

$M_6L_{12}$ $M_{12}L_{24}$ $M_{24}L_{48}$ $M_{30}L_{60}$ $M_{60}L_{120}$

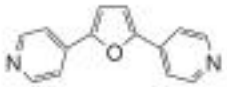


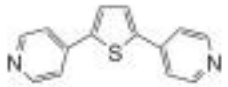


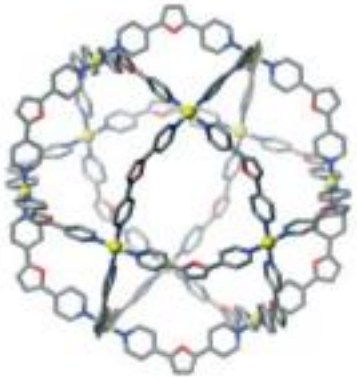

**15**

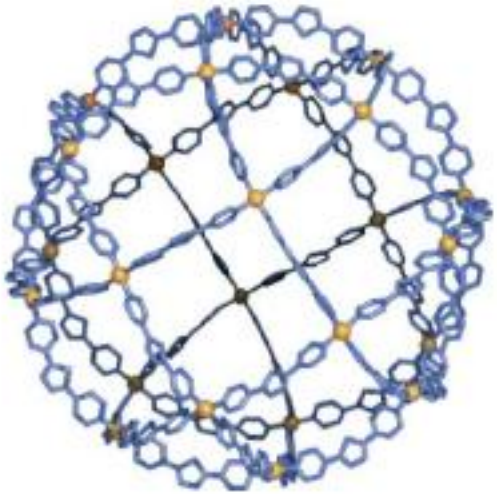

**16**